DEVELOPMENT OF SUSTAINABLE AND FUNCTIONAL JUTE-BASED FABRICS FOR INNOVATIVE AGRICULTURE APPLICATIONS

WANG XUE

PhD

The Hong Kong Polytechnic University

2026

The Hong Kong Polytechnic University

School of Fashion and Textiles

Development of Sustainable and Functional Jute-based Fabrics for Innovative Agriculture Applications

WANG Xue

A thesis submitted in partial fulfilment of the requirements for the degree of Doctor of Philosophy

April 2025

CERTIFICATE OF ORIGINALITY

I hereby declare that this thesis is my own work and that, to the best of my knowledge and belief, it reproduces no material previously published or written, nor material that has been accepted for the award of any other degree or diploma, except where due acknowledgement has been made in the text.

____________________ (Signed)

WANG Xue (Name of student)

Abstract

In modern agriculture, effective water-saving irrigation and weed management are crucial for ensuring the availability of water resources and maintaining soil health. However, current management strategies are deficient regarding sustainability and ecological impact. Agricultural plastic use is dominated by film and irrigation pipes, which account for more than 90% of total consumption. For example, water-saving irrigation methods faced challenges such as irrigation pipe recycling, waste of non-renewable resources, and soil pollution. Weed control strategies were challenged with issues like chemical resistance, soil microplastics, and non-targeted damage becoming increasingly prevalent. Therefore, there is an urgent need to develop multifunctional and fully biodegradable agricultural textiles that reduce plastic pollution and improve agricultural efficiency. Jute fabrics have emerged as a promising option for agricultural applications due to their durability, breathability, and biodegradability. However, research on environmentally friendly jute fiber-based multifunctional materials for agricultural applications remains limited. This study focuses on the development of multifunctional integrated agricultural textiles through the strategic design of materials, structures, and processing techniques in a simple and efficient manner.

Firstly, the basic characteristics of jute yarns before and after alkali treatment were systematically investigated. Mechanical strength and water absorption increased with longer treatment times. A sustainable composite seepage irrigation pipe based on eco-friendly and abundant jute fiber was proposed to explore its potential to replace the drip pipes. Jute fiber-reinforced polylactic acid (PLA) composites (JFPCs) and pipes were fabricated through an integrated knitting process and simple thermoforming technique. The adjustment of PLA content in JFPCs enhanced mechanical performance and allowed precise control of the seepage rate with tailored PLA film porosity. When increasing PLA content from 12.2 % to 40.8 %, JFPCs exhibited enhanced mechanical strength (3.1 MPa) and improved thermal decomposition temperature (376.9 °C), indicating better stability for maintaining material integrity or performance exposed to high temperature conditions. Seepage tests demonstrated JFPC pipes achieved controllable seepage rates ranging from 0 to 8.9 L/min with PLA film porosity adjusting. Sustainable analysis and degradation tests (showing a maximum 20.2 % weight loss after 3 months) confirmed the environmental suitability and biodegradability of JFPCs for sustainable agricultural applications. A potential weed control fabric based on jute fiber was also demonstrated that reduces weed growth and minimizes the level of water evaporation. Structural and density modifications were applied to jute weed control fabrics (JWCFs) to achieve different levels of porosity. The optimization of microporosity improved the performance of the fabric in suppressing weeds and retaining soil moisture. Field experiments with JWCFs revealed a reduction of 61 %~100 % in weed growth, an average decrease of 1.6~4.3 °C in soil heat accumulation, 6.0 %~68.5 % suppression of water evaporation, and a 47.5 % weight loss after 40 days of degradation. At last, a one-year field experiment successfully verified the functional effectiveness of JWCFs in weed control, soil enhancement and yield improvement. JWCF maintained 100 % weed suppression, improved soil conditions, and reduced nutrient loss. JWCF-4 retained significantly more soil moisture and minimized nutrient loss. Yield increased by 22.2 %, with a 102.7 % higher output than the uncovered area, along with improved fruit quality and market value. JWCFs exhibited durability for at least a year and biodegraded naturally, enriching the soil.

In summary, this work explored the feasibility of using jute-based fabrics as effective solutions for both controllable irrigation and weed control, providing a sustainable alternative to traditional irrigation and weed management methods. The work would also significantly contribute to the expansion of natural fiber applications, enhance the efficiency of agricultural production materials, and protect the soil environment.

List of Publications

Published Journal Paper:

1. **Wang X**, Zhao F, Cheung TW, Lee C, Li L. Enhancing hemp fiber performance: insights into chitosan treatment and structural evolution. *Textile Research Journal*. 2024;94(21-22), 2341-2350.
2. **Wang X**, Zhang Q, Li L. Biodegradable fabric with efficient thermal-wet management for eco-friendly weed control and water retention of soil. *Industrial Crops and Products*, 2025, 225: 120586.
3. **Wang X**, Tian X, Tao YF, Li L. Biodegradable jute fiber-based composites with controllable seepage for sustainable agricultural water-saving management. *Cellulose*, 2025.

In preparation:

1. **Wang X**, Tian X, Li L. Effect of alkali treatment on microstructure and mechanical properties of jute yarns.

Patent

1、Li L, WANG ZY, **Wang X**. Textile preparation method based on cross-linking, 2023. Chinese patent (application number: 2023115807135)

2、Li L **Wang X**, Zhang TH. The preparation method of agricultural management system for weed control and irrigation device.2024. Chinese patent (application number: 202410554719.3)

Conference Poster Presentation

Wang X, Zhang Q, Li L. Biodegradable fabric with efficient thermal-wet management for eco-friendly weed control and water retention. Conference Fiber 2025, Cologne, Germany.

Acknowledgements

Firstly, I would like to express my sincerest gratitude to my supervisors Prof. Li Li and Prof. Hong Hu for offering me such a precious chance to conduct my Ph.D. study in their group. I would like to thank Prof. Li Li for long-term support, patient instructions, and insightful enlightenment when I was lost. During the past three years, she taught me how to think broadly and critically in the research work. Her positive attitude and great enthusiasm toward scientific research inspire us for future study and work. I would like to thank her for providing the opportunity to participate in the project, from which I have gained a wealth of research experience, especially the planning of experiments, problem-solving skills, and self-regulation of mentality, all of which will benefit me a lot. I would also like to thank The Hong Kong Polytechnic University and School of Fashion and Textiles for the financial support and research platform.

I would also like to express my great appreciation to technicians of the School of Fashion and Textiles for the instrument operations: Dr. Samuel Lee, Mr. Calvin Tiu, Dr. Hui Kevin, Mr. Marco Sze, Mr. Shui-wing Ng, Mr. Kwan-on Choi. I would like to thank Dr. Xiao Tian, Dr. Fuwang Zhao for their valuable training, advice, and discussions during my daily research activities. I would also like to thank my classmates and friends, Ms. Yinshan Lau, Ms. Shuyang Li, Ms. Yanwing Tai, Ms. Poying Tam, Ms. Kwai Hing Tang, Dr. Jinli Piao, Ms. Zixin Ju and Ms. Shanshan Dong for their kind help during my research and life.

Finally, I would like to thank my boyfriend, Mr. Wei Liu, and my family members for their heir encouragement and love in supporting me through the many difficulties and disappointments over the past three years.

Table of Contents

List of Figures

panel: back effect of different JWCFs.

Figure 5-3 A photograph of the experimental setup for temperature change and water retention under sunlight. This setup is mainly consisted by a thermocouple data recorder, a temperature and humidity recorder, and a weather station. The chamber of the soil container is isolated from the surroundings by an Al film to reflect sunlight. The temperatures of soil and fabric surface are real-time measured by thermocouples recorder.

Figure 5-4 Photographs of the outdoor experiment condition to test the weed control of different covering materials. All fabrics of size 500 mm * 500 mm were laid in an outdoor experimental site with adequate sunlight in the campus of Hong Kong Polytechnic University, Hong Kong, China (114.1795 °E, 22.3051 °N).

Figure 5-5 Fabrication and characterizations of JWCFs for weed control. (a) Optical microscope photographs of JWCFs. Scale bar, 2mm. (b) Porosity of JWCFs, WCF-PE and WCF-PP. Compared the (c) water vapor and (d) air permeability of different fabrics. (e) Sunlight blocking by different covering materials in the wavelength range of 400-700nm.

Figure 5-6 The photographs of WCF-PE and WCF-PP are shown for comparison. Scale bar, 2mm.

Figure 5-7 Heat accumulation reduction and water conservation performance. (a) Absorptivity of different WCFs. (b) A schematic of the custom-made device for verifying the cooling effects of the JWCFs. (c) Surface temperature and (d) soil temperature recorded under covered of the JWCF and the three controls from 10:00 to 15:00. (e) Comparison of soil water evaporation loss under the JWCF application and the three control conditions. The JWCF can reduce heat accumulation after covering and achieve water-saving effect.

List of Tables

List of Abbreviations

PVC	polyvinyl chloride
PE	polyethylene
PP	polypropylene
PLA	polylactic acid
PET	polyethylene terephthalate
LDPE	low density polyethylene
PAEs	phthalates
DEHP	di（2-ethylhexyl）phthalate
BPA	bisphenol A
NB	Nile blue
PS	polystyrene

NBD-Cl	4-chloro-7-nitro-1,2,3-benzoxadiazole
PS-COOH	carboxyl-modified
PS-NH_2	amino modified
OH	hydroxyl groups
CHO	aldehyde groups
OCH_3	methoxy
C=O	carbonyl
UVB	ultraviolet radiation b
i-SCs	interfacial stereo complex crystallites
3D	three-dimensional
PCL	polycaprolactone

PHA	polyhydroxyalkanoates
PGA	polyglycolic acido
PA	polyamide
PHB	polyhydroxybutyrate
PBS	poly(butylene succinate)
PBAT	poly(butyleneadipate-co-terephthalate)
HDPE	high-density polyethylene
UV	ultraviolet
FAO	Food and agriculture organization
SEM	scanning electron microscopy
TGA	thermogravimetric analysis

TEM	Transmission Electron Microscopy
DSC	differential scanning calorimetry
NJATM	nonwoven jute agro-textile mulch
JHNF	jute-polyester hybrid nonwoven fabric
SOSA	bio-based hydrophobic liquid mulch film
CAGR	Compound Annual Growth Rate
Nano-G	nano-graphite
MC	mica clay
PAR	photosynthetically active radiation
TPS	thermoplastic starch
pH	potential hydrogen

SCP	stalk composite pipes
FTIR	Fourier-transform infrared spectroscopy
S. aureus	Staphylococcus aureus
E. coli	Escherichia coli
NaOH	sodium hydroxide
Na_2SO_3	sodium sulfite
JYs	jute yarns
JFPC	jute fiber-reinforced PLA composite
WCFs	weed control fabrics
WCF-PE	polyethylene weed control fabric
WCF-PP	polypropylene weed control fabric

JWCF	jute weed control fabric
N	nitrogen
P	phosphorus
K	potassium

Chapter 1 Introduction

1.1 Background

Agriculture serves as the foundation of the global economy and food security [1, 2], yet it faces pressing challenges, including inefficient resource utilization, low productivity, and environmental degradation [3-5]. With the global population expected to reach 9.7 billion by 2050 [6, 7], food demand is expected to rise by 70% [8], making agricultural innovation crucial—particularly in optimizing resource utilization, minimizing environmental impact, and enhancing production efficiency. Unsustainable agricultural practices have contributed to soil erosion, deforestation, habitat loss, and the acceleration of climate change [9, 10]. Moreover, stagnant agricultural productivity, the constraints of traditional practices, and increasing water shortages have intensified food security challenges, highlighting the urgent need for a transition to sustainable agriculture. As an important innovation in modern agriculture, agricultural textiles provide an effective solution to improve agricultural sustainability [11]. These materials, such as geotextiles, mulch films and shade nets, have the functions of regulating microclimate, reducing water evaporation, inhibiting weed growth and protecting crops from extreme weather [12, 13], thereby increasing crop yields and resource utilization efficiency. In the context of agricultural transformation, these materials are becoming an important tool to promote sustainable agricultural development, playing a key role in improving agricultural productivity and environmental friendliness.

Water scarcity in agriculture is becoming an increasingly critical issue, further exacerbated by climate change and population growth [14, 15]. In arid and semi-arid regions, limited water resources have emerged as a major constraint on agricultural production [16, 17]. In this context, drip irrigation technology has gained widespread recognition for its high efficiency and water-saving benefits [18, 19]. By precisely delivering water directly to plant roots, it minimizes evaporation and wastage, significantly enhancing irrigation efficiency and optimizing water resource utilization. However, the commonly used materials in current drip irrigation systems, such as plastics and polyvinyl chloride (PVC), while offering good durability, are often difficult to degrade and recycle after their service life, leading to significant environmental pollution. The release of plastic microparticles from these materials may pose potential risks to soil ecosystems and agricultural product safety [20]. Therefore, developing biodegradable, eco-friendly, and high-performance drip irrigation pipe materials has become an urgent challenge that needs to be addressed.

Weeds present a persistent and significant challenge in agriculture by competing with crops for important resources such as water, nutrients, and sunlight [21, 22]. The competition results in significant yield reductions and economic losses in agricultural production [23, 24]. Traditional weed control methods such as chemical herbicides, mechanical weeding, and biological control are widely used to control weed growth and protect crops. However, these methods have obvious limitations. For example, chemical herbicides can cause environmental pollution and herbicide resistance [25], while mechanical weeding and biological control may not provide lasting effects or damage crops. Many studies conducted around the world have reported the positive effects of mulches on weed control, demonstrating that they are superior to pesticides or manual weeding methods [26-28]. The use of polyethylene (PE) and polypropylene (PP) weed control fabrics, as well as black film materials, in agricultural mulches has increased dramatically worldwide due to their benefits, including effective weed control, soil moisture retention, and temperature regulation [29, 30]. However, the subsequent disposal of synthetic plastic materials, usually landfill or incineration, has caused serious pollution problems to the soil environment. Therefore, there is a growing demand for more sustainable and effective mulching materials.

Natural plant fibers are promising choices as agricultural textiles, offering high specific strength, sustainability, and biodegradability [31, 32]. Among various natural fibers such as straw fiber, bagasse, bamboo fiber, and jute fiber, jute stands out due to its affordability, widespread availability, excellent ductility, high modulus, and superior specific strength, making it a preferred choice for diverse agricultural applications [33]. Traditionally, jute fiber has been primarily used to make ropes, coarse cloth, and packaging materials [34]. In recent years, with growing emphasis on environmental sustainability, jute fiber has been further developed into geotextiles, seedling containers, and erosion control mats [35, 36], demonstrating both eco-friendliness and economic feasibility. Therefore, in order to address the challenges that are mentioned above, this study explored composite pipes and weed control based on jute fabrics as sustainable alternatives to conventional materials. By leveraging the inherent properties of jute fiber, the study aimed to develop agricultural materials that provide effective solutions for weed control and controlled irrigation while simultaneously minimizing environmental impact. The performance, environmental benefits, and practicality of these materials were evaluated through both laboratory tests and field experiments.

1.2 Research Objectives

The selection of weed-control mulching fabrics and controlled-irrigation pipes as the two focal applications is based on their dominant contribution to agricultural plastic consumption. Statistics indicate that plastic films and irrigation pipes together account for over 90% of total plastic use in the agricultural sector, making them the primary sources of waste accumulation and microplastic pollution. Addressing these two categories therefore offers the greatest potential environmental impact. Building on this rationale, this study aims to develop a fully biodegradable, multifunctional jute-based material system that integrates controllable targeted irrigation, weed suppression, and soil moisture regulation. By combining fiber modification, structural design, and textile processing, this study proposes a new framework for natural fiber-based agricultural materials with tunable performance and controllable degradation, which can significantly reduce soil pollution while enhancing the performance and resource use efficiency of agriculture materials. The specific objectives of this research are as follows:

(a) To study the basic characteristics of jute yarns before and after alkali treatment. The surface morphology, mechanical and thermal properties, and water absorption are systematically characterized.

(b) To develop appropriate jute fiber-based composite preparation techniques, optimizing porosity and pore distributions to enhance strength, durability, and functional performance. The physical and seepage controllable performance of composite pipes are demonstrated by mechanical and water seepage experiments.

(c) To design and fabricate jute weed control fabrics with varying porosity by adjusting the fabric structure and density. The functional effectiveness of jute-based fabrics is evaluated through lab tests and small-scale outdoor experiments and compared with commercial weed control fabrics to evaluate their suitability for agricultural applications.

(d) To demonstrate the field application of jute weed control fabrics. The long-term weed control performance, soil conditions, and fruit yield are evaluated.

1.3 Methodology

To achieve the above research objectives, the study is conducted using the following methodologies:

Exploration of the basic properties of jute yarn

The surface morphologies, thermal and mechanical properties, water absorption performance of jute yarn were evaluated before and after modification treatment. Specifically, scanning electron microscopy (SEM) was used to assess the surface morphologies, while thermogravimetric analysis (TGA) and differential scanning calorimetry (DSC) was conducted to investigate the thermal properties. Mechanical properties were determined through tensile testing to measure strength and elongation at break. Additionally, the water absorption performance was examined by immersing different yarns in water and measuring weight changes to evaluate their water absorption capacity.

Design and fabrication jute/PLA composites with excellent mechanical properties and controllable seepage performance

Sandwich-structured jute/ PLA composites were fabricated through simple knitting and molding techniques. The resulting fabric incorporated jute yarn on one side and polylactic acid (PLA) filament on the other. The jute layer provided enhanced protection for external use, while the PLA inner layer ensured effective seepage performance for the composite pipes. The content of PLA affected the porosities of composites. To investigate the effect of porosity on the seepage controllability of composite pipes, a variety of composites with different PLA contents were fabricated. Comprehensive analyses, including surface morphology, thermal stability, mechanical properties, water seepage behavior, and biodegradability, were conducted to evaluate the influence of material composition on overall performance and functional efficiency.

Design and fabrication jute weed control fabrics with excellent weed control and water retention

A multifunctional jute weed control fabric (JWCF) was designed and developed by adjusting fabric structures and densities. A systematic comparison was performed to evaluate the effectiveness of JWCF in comparison to two commercial weed control fabrics. Various lab tests and field experiments were conducted, including basic characterizations, temperature changes and water retention performance, weed control and biodegradation to assess their overall performance in agricultural applications.

Field experiment

To verify the long-term effectiveness of jute fabric, a one-year field experiment was conducted on an outdoor farm. The functionalities of jute-based fabric and commercial weed control fabrics were compared. The data on soil environment was monitored through sensors and final crop yield and durability were evaluated to evaluate their effectiveness for agricultural applications.

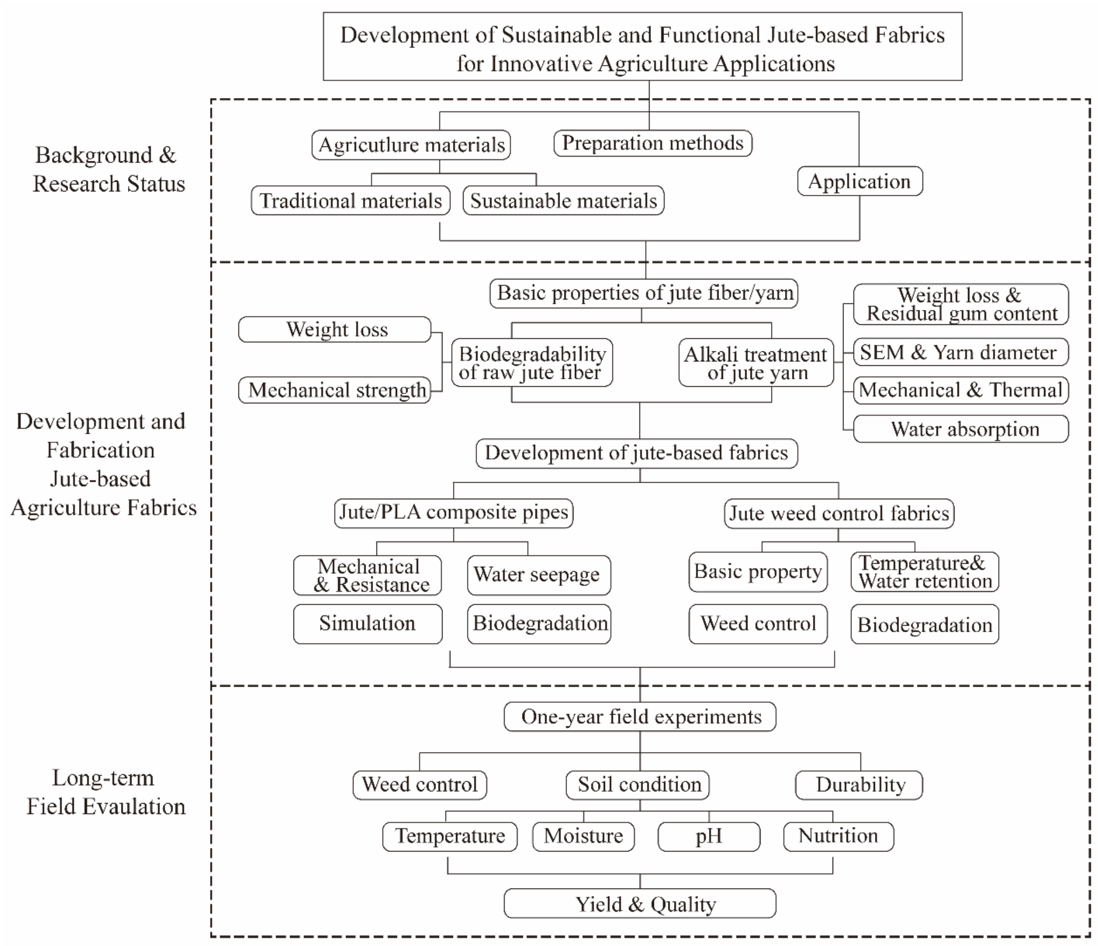

Figure 1-1 Flowchart of the research methodology.

1.4 Research Significance and Value

Although much research has been carried out on the use of jute fibers in different fields, the research for jute-based multifunctional agro-textiles is limited. Given superior performance and complete biodegradability, the jute-based agricultural materials proposed in this study show considerable promise as a viable alternative to traditional polymer-based materials in agriculture. The sustainability implications of these proposed materials are anticipated to be substantial. By using jute fiber to achieve controllable seepage irrigation and suppress weed growth while reducing soil environmental pollution, the proposed materials may advance the goal of promoting sustainable agricultural practices. Effective water saving and weed management can conserve vital resources and diminish the dependence on water-intensive irrigation and chemical herbicides, thereby fostering the long-term development of sustainable agriculture. This impact would contribute to protecting vulnerable ecosystems and fostering the sustainability of natural resource management. The work would lead to significant contributions to improving the efficiency of agricultural production materials and protecting the soil environment. Moreover, this work provides novel perspectives and innovative ideas for the application of cellulosic materials in agriculture and contributes to an important significance for expanding the application of natural fibers.

1.5 Outline of the work

This thesis is organized as follows:

Chapter 1 briefly introduces the research background of agricultural textiles and the current issues towards this field. Considering the challenges, the research objectives, methodologies and research significance and values of this study are described in detail.

Chapter 2 reviews the recent research progress of agricultural textiles, including traditional materials and their limitations, sustainable materials, fabrication methods, and applications.

Chapter 3 evaluates the basic characteristics of jute yarns before and after alkali treatment. Surface morphologies, thermal and mechanical properties, water absorption performance of jute yarn are systemically studied.

Chapter 4 develops a composite fabric based on jute yarn and PLA filament for controllable seepage irrigation. Based on structural design and rational materials configuration, composite seepage pipes are realized, including excellent mechanical properties and water seepage performance. The morphology, mechanical properties, and water seepage performance are studied.

Chapter 5 fabricates a multifunctional weed control fabric based on jute fiber. The properties of jute weed control fabrics (JWCFs) are systematically evaluated. The JWCFs not only has excellent weed control effects which are compatible with commercial weed control fabrics, but also reduces soil moisture evaporation.

Chapter 6 conducts the field experiment to verify the effectiveness of the proposed functional agricultural textile.

Chapter 7 summarizes the whole research project, states the existing limitations, and discusses the future work in the field of jute-based agriculture textiles.

Chapter 2 Literature Review

2.1 Agricultural Materials

Agricultural materials are designed using material science to help crops handle challenges such as pests, diseases, extreme weather, and limited resources [37]. Their primary goal is to tackle these agriculture challenges through physical, chemical, or biological methods, with applications including weed management, water scarcity, pest and disease control, and the optimization of crop growth environments. As essential tools driving the rapid advancement of modern agriculture, agricultural materials play a crucial role in enhancing crop yields, conserving resources, and reducing production costs for farmers [38-40].

2.1.1 Crop protection materials

Crop protection materials, as an essential component of modern agricultural system, are designed to shield crops from adverse environmental threats, thereby enhancing productivity and promoting sustainable cultivation through physical, chemical, or biological mechanisms [41, 42]. Mulches, weed control fabrics, and agricultural nets are widely used crop protection materials that help regulate soil microclimate and reduce environmental stress. Mulches retain soil moisture and minimize evaporation[43], while permeable weed control fabrics suppress weed growth without impairing soil aeration—particularly advantageous in organic farming [44]. Agricultural nets, including shade, insect-proof, and wind-proof types, further protect crops from adverse conditions [45]. Typically made from high-strength, UV-resistant plastic materials, these nets are known for their durability and resistance to aging.

2.1.2 Water management materials

Water management materials represent another important category of agricultural materials designed to optimize irrigation efficiency, enhance effective water use, and maintain soil structure. By controlling the flow and distribution of water, these materials effectively address the growing global issue of water scarcity, particularly in arid or semi-arid regions [46]. In modern irrigation systems, water management materials are tailored to different techniques, including drip drip, sprinkler, surface, and subsurface irrigation [19, 47]. Among them, drip irrigation is recognized as one of the most efficient methods, delivering water directly to plant roots while minimizing evaporation and runoff. Recently, advances in water management material science have been continuously developing to further improve irrigation efficiency and sustainability.

2.2 Traditional Agricultural Materials and Limitations

2.2.1 Traditional agricultural materials

In traditional agricultural production, a variety of materials are extensively utilized for crop cultivation, irrigation, and soil protection. Table 2-1 presents common agricultural production materials. Among these, plastics are among the most extensively utilized due to their affordability, ease of processing, and durability [48]. Plastics play a crucial role in agricultural applications, particularly in mulching films, irrigation systems, and packaging materials. According to FAO statistics, the global agricultural sector consumes approximately 12.5 million tons of plastic annually, with PE accounting for 67%, PP for 21%, and PVC for 9% [49]. Notably, plastic films and irrigation pipes constitute more than 90% of this total consumption.

Table 2-1 Common agriculture materials and their main applications [50].

Agricultural materials	Fiber type	Use in agriculture
Mulch mat	PP/PE	Weeding control; Preserve moisture
Crop cover	PP	Protect crop from adverse climatic
Weeding fabric	PP/PE	Weed control
Sunscreen	PE	Protect crop from UV radiation
Anti-bird net	PP/PE	Protect crop from bird
Irrigation pipe	PP/PE/PVC	Transport water
Soil protection fabric	Jute/Cotton/PP /Nylon	Prevent soil erosion

Agricultural coverings, particularly ground films, are among the most commonly used traditional agricultural materials. Plastic films, especially PE and PP films, are the most widely utilized due to their effectiveness in regulating the crop growth environment. These films help preserve soil moisture, suppress weed growth, retain soil heat, and accelerate crop development, ultimately enhancing overall agricultural productivity [51].

In agricultural irrigation, plastic pipes—particularly those made of PE and PVC—are extensively used due to their excellent corrosion resistance, pressure tolerance, and cost-effectiveness. PE pipes offer flexibility and durability, allowing them to withstand high water pressure over prolonged use while ensuring stable and uniform water distribution [52]. Most drip irrigation systems utilize plastic materials such as high-density polyethylene (HDPE) [53], which exhibit strong chemical resistance, adaptability to diverse soil conditions, and reliability in maintaining efficient irrigation performance.

In addition to mulches and irrigation systems, plastic materials are also extensively utilized in agriculture packaging, greenhouse construction, insect-proof nets, and other applications [54]. However, prolonged exposure to sunlight, moisture, and temperature fluctuations can induce material aging, degradation, and fragmentation, leading to environmental pollution and resource accumulation issues.

2.2.2 Limitations of traditional agricultural materials

Non-degradability of materials such as PE, PVC, and PP, commonly used in agricultural textiles, has led to significant soil pollution. Research indicates that plastic mulch films are one of the major sources of microplastics in agricultural soils [55]. The widespread use of plastics in the agriculture field, coupled with low recycling rates, results in the accumulation of plastic residues, which gradually degrade into micro-sized particles, releasing harmful substances and negatively impacting the environment.

Microplastic generation mechanism

The generation of soil microplastics is a complex environmental issue driven by multi-source inputs and multi-process interactions. Agricultural plastics are commonly in direct contact with or near soil environments. Exposure to environmental factors such as ultraviolet radiation, temperature fluctuations, and mechanical stress can cause the degradation of plastics, leading to the release of microplastic particles into the environment [56,57] (Figure 2-1). Ultraviolet radiation (UV) is a key factor in the decomposition of agricultural plastics into microplastic particles, primarily through the induction of peroxidation and molecular chain scission [58-60] (Figure 2-1a). During the early stages of degradation, plastic films with high molecular weight exhibit significant resistance to microbial degradation [61, 62]. UV radiation utilizes high-energy photons to break molecular bonds, initiating polymer chain scission and cross-linking [63], which renders the material photochemically brittle and leads to the in-situ degradation of bulk plastics [64, 65]. Carbonyl groups in PE can function as chromophores, initiating Norrish Type I and II reactions that cause main-chain scission [66]. The generated free radicals react with oxygen, forming peroxy radicals that break down into highly reactive species (Figure 2-1bi). PP is more susceptible to degradation than PE because its tertiary carbon is prone to oxygen attack [67]. Under UV exposure, impurities in PP form radicals, resulting in chain scission, cross-linking, and the production of lower molecular weight degradation products [68, 69] (Figure 2-1bii). PVC undergoes dehydrochlorination under UV radiation, forming conjugated double bonds that degrade further. Chromophores of PVC generate free radicals through UV radiation, which lead to hydroperoxides that break the backbone chain into smaller products [70, 71]. Photodegradation of PET breaks ester bonds, producing CO, CO_2, terephthalic acid, and other degradation products [63]. It also undergoes radical-induced degradation, where hydroperoxides form from CH_2 groups and react with aromatic rings, leading to hydroxyterephthalate groups and possible cross-linking [72, 73] (Figure 2-1biii).

In addition of UV radiation, mechanical abrasion is another significant factor contributing to plastic material degradation (Figure 2-1c). The shearing effect of farming machinery and the friction between soil particles work synergistically to accelerate the breakdown of materials [74]. Moreover, biological degradation mechanisms play a crucial role in the breakdown of plastics. Soil microorganisms, including bacteria and fungi, can colonize the material's surface and secrete enzymes that break down spolymer chains. White-rot fungi, for example, produce lignin-degrading enzymes like laccase, which can depolymerize plastics such as PE and PP (Figure 2-1d). Additionally, the activity of soil animals, such as earthworms, has a dual effect: it accelerates plastic fragmentation while their intestinal enzymes enhance biodegradation.

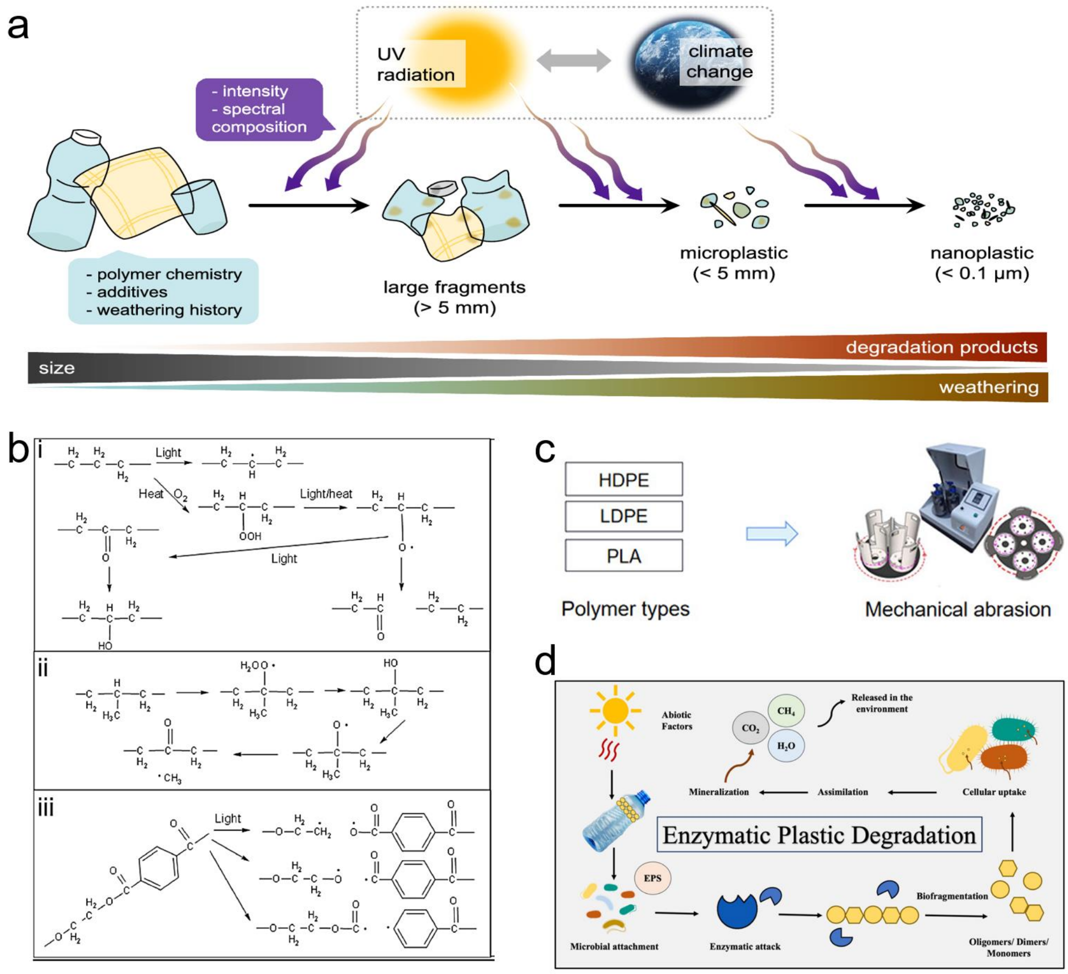

Figure 2-1 Conceptual diagram depicting the plastic degradation methods. (a) UV radiation of photodegradation [75]. (b)Photodegradation of (i) PE, (ii) PP and (iii) PET [59]. (c) Mechanical abrasion method of plastic degradation [74]. (d) Overview of enzymatic plastic degradation [76].

Mustafa Dogan [77]examined UV-induced degradation of LDPE using a fluorescence lamp and sunlight exposure. Results revealed progressive polymer breakdown, structural fragility, and slight color changes (Figure 2-2a). Edgars Kuka et al. [78] investigated UV-induced photodegradation in five recycled plastics, revealing that degradation varied more by waste source than polymer type. SEM confirmed microcracking in degraded samples, highlighting their potential for microplastic formation (Figure 2-2b). Ainali et al. [79]showed through UV aging experiments that prolonged exposure to UV-B radiation led to the formation of cracks and holes on the surface of plastic films (LDPE, HDPE, PP, PS), resulting in a significant reduction in both ductility and strength (Figure 2-2c). A simulation study by Da et al. [74] demonstrated that agricultural practices significantly accelerate the transformation of residual agricultural films into microplastics through mechanical wear, simultaneously releasing plasticizers such as phthalates (PAEs). The results revealed significant wear on the HDPE mulch film, with smaller fragments and an increase in submicron particles as abrasion time progressed (Figure 2-2d and Figure 2-2e), leading to exponential microplastic generation (Figure 2-2f) and the complete disintegration of the thinnest films (0.008 mm).

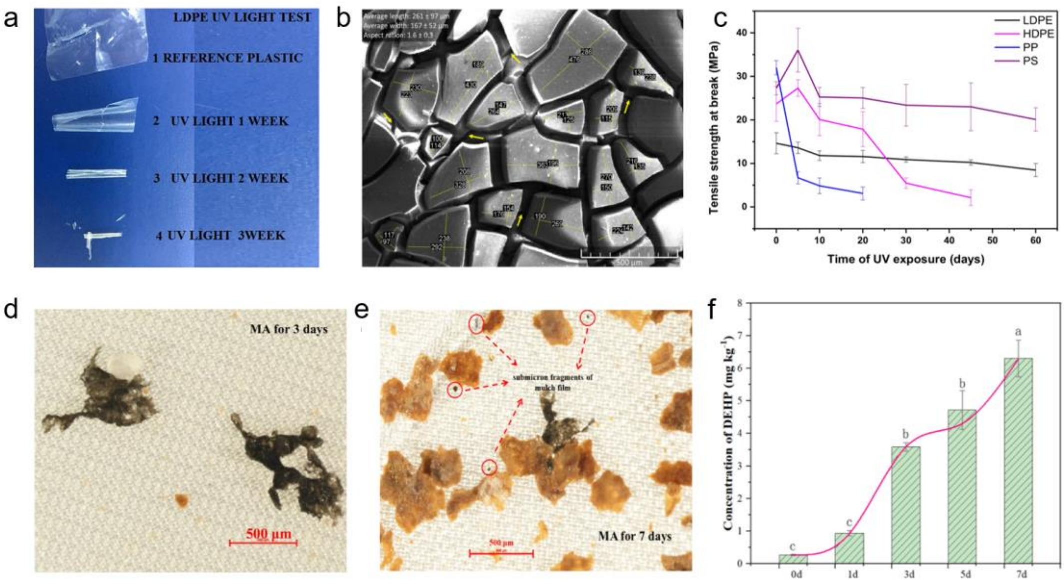

Figure 2-2 (a) Stages of LDPE plastic degradation under UV exposure. The LDPE plastic curls into a pipe shape within two weeks and eventually became brittle and

disintegrates by the end of the degradation experiment [77]. (b) SEM image of the shattered rPP1 pellet surface after 2000 hours of UV radiation, with measurements in µm of the resulting fragments; yellow arrows indicate crack formation beneath the surface layer [78]. (c) Tensile strength at break point of LDPE, HDPE, PP and PS during different days of UV exposure [79]. (d)–(e)The optical microscope images of HDPE mulch film degraded different time [74]. (f) The variation of DEHP concentrations [74].

Environmental impact

Agricultural plastic materials, such as ground film and drip irrigation pipes, are designed for long-term durability, often exceeding their actual usage needs and leading to persistent environmental pollution. While ground film is typically used for 3–6 months, LDPE as the common material of film, has a soil half-life of 10–30 years [80]. Similarly, PP drip irrigation pipes retain high tensile strength even after prolonged use [81]. Moreover, PVC greenhouse frames, when exposed to ultraviolet radiation and humid heat, release substantial amounts of DEHP, resulting in accumulated concentrations of hundreds of micrograms per kilogram in the surrounding soil [82]. These issues highlight the failure of traditional agricultural plastics to account for their long-term environmental impact, posing risks of soil and water contamination from residual substances after use.

Microplastics pose a threat to soil ecosystems through three main pathways: physical disturbance, biological toxicity, and chemical release [83]. These impacts further disrupt soil nutrient cycling, hinder plant growth, and alter overall soil properties, as illustrated in Figure 2-3a and Figure 2-3b. Microplastics can significantly impact soil physicochemical properties, such as porosity, bulk density, and water-holding capacity, thereby affecting soil aeration and nutrient cycling [84]. In addition, microplastics can serve as vectors for pollutants, adsorbing heavy metals, organic contaminants, and other hazardous substances, thereby posing a potential risk to soil microbial diversity and inhibiting plant root development and nutrient absorption [85, 86]. Wang et al. [87] reported a progressive decline in soil enzyme activity and microbial diversity with increasing plastic film residue, particularly when residual levels exceeded 450 kg/hm².The degradation of microplastics can lead to the release of plasticizers, monomers, and other additives, such as PAEs and bisphenol A (BPA) [88, 89], thereby facilitating the accumulation of organic pollutants and exacerbating their complex adverse effects on the environment [90].

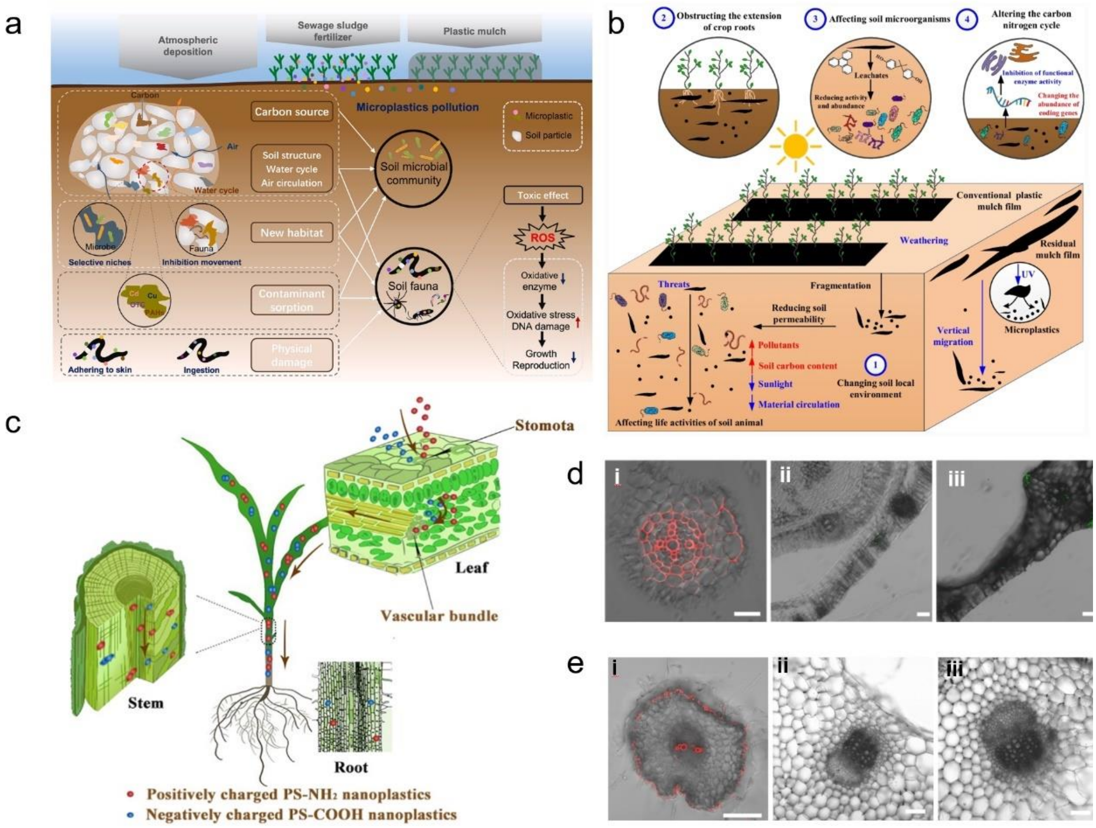

Figure 2-3 (a) Illustrative concept depicting the potential effects of micro- and nanoplastic pollution on soil organisms [91]. (b) Effects of residual traditional plastic films on the soil environment in agriculture [92]. (c) Diagram illustrating the uptake and transport of PS nanoplastics in maize plants [93]. (d) i-iii, Images of transverse

sections of a root (i), stem (ii) and leaf (iii) from a wheat plant treated with polystyrene beads labelled with Nile blue (NB) and polystyrene (PS) beads labelled with 4-chloro-7-nitro-1,2,3-benzoxadiazole (NBD-Cl).(e) i-iii , Images of transverse sections of the lettuce root (i), petiole (ii) and leaf (iii) treated with PS beads labelled with NB or PS beads labelled with NBD-Cl [94].

The spatial distribution of plastic residues in agricultural environments exhibits significant regional variation. An assessment of microplastic pollution in farmland ecosystems reveals serious contamination in many areas [95], as shown in Table 2-2. In southwestern Poland, 93% of cultivated soils contain microplastics, with loam soils exhibiting an abundance of 1,540 ± 912 particles per kilogram [96]. In Liaoning Province, China, the 0–10 cm soil layer contains 7,183–10,586 microplastic particles per kilogram. Farmland and riparian forest soils around Dianchi Lake in China show microplastic concentrations ranging from 7,100 to 42,960 particles per kilogram [97]. These minuscule plastic particles can be absorbed by plant roots and transported via cracks [94], increasing the risk of human exposure through the food chain and posing potential ecological and health hazards [98]. Sun et al. [93] investigated the foliar uptake and translocation of carboxyl-modified (PS-COOH) and amino-modified ($PS-NH_2$) polystyrene nanoplastics in maize seedlings. Results showed that vascular bundle was the main pathways for leaf-to-root translocation of nanoplastics (Figure 2-3c). Nanoplastics entered leaves through stomatal openings and were transported to roots, though aggregation limited root translocation, particularly for PS-NH2. Li et al. [94]demonstrated the uptake and translocation of 0.2 μm fluorescent polystyrene beads in wheat and lettuce using confocal microscopy. The beads accumulated in root intercellular spaces, vascular tissues in stems, and xylem in leaves, highlighting their systemic transport from roots to shoots (Figure 2-3d and Figure 2-3e). These findings together underscore the pervasive accumulation of agricultural plastic residues in both soil and organisms. This highlights the urgent need to develop biodegradable and environmentally friendly materials for agricultural applications to mitigate the long-term impact of microplastics on soil ecosystems, promote the sustainable use of soil resources, and safeguard ecological health.

Table 2-2 Prevalence of microplastics in agricultural soil ecosystems [95].

Area	Microplastic concentration (items kg^{-1})	Soil depth (cm)	Polymer type	Size range average (mm)
Spain	2 030 ± 1 310 5 190 ± 2 630	0-30	PP, PVC	0.15-0.25
Mauritius	420.0 ± 244.0	10-20	PP	/
Australia	2 800-2 900	/	/	/
Chile	600 ± 10400	0-25	LDPE, PVC	around 2
Germany	340 ± 360	0-5	PE, PS, PP	1-5
Switzerland	around 593	/	PS, PE, PVC	less than 0.5
Canada	4400-14900	/	/	less than 0.5
China Hangzhou	503 ± 2760	0-10	PE, PP	around 1
Xinjiang	308 ± 138.1	0-40	PE	5

Shanghai	78.00 ± 12.91 62.50 ± 12.97	0-3 3-6	PE, PP	around 1
Shaanxi	1430-3410	0-10	PP, PE	around 0.49
Wuhan	320-12560	0-5	PP, PA, PS	around 0.2

2.3 Sustainable Materials for Agricultural Applications

The widespread use of agricultural materials, particularly agricultural plastic films, has greatly enhanced productivity and output in densely populated countries. As technological advancements continue, agricultural inputs are evolving toward high-performance, low-pollution, and biodegradable alternatives, in response to the growing demand for sustainable agricultural practices. Biodegradable materials, seen as a sustainable alternative to traditional agricultural plastics, have the potential to reduce soil microplastic pollution. These materials are primarily categorized into natural fibers and biodegradable polymers.

2.3.1 Natural plant fibers

Natural plant fibers are renewable cellulose-based materials derived from various plant sources. Owing to biodegradability, abundance, and environmentally friendly, they are widely utilized in textiles, composites, construction, and agriculture [32, 99]. Based on their origin within the plant, these fibers are classified into leaf fibers (e.g., sisal and pineapple leaf fibers), seed fibers (e.g., cotton fibers), bast fibers (e.g., hemp, flax, ramie, and kenaf), and fruit fibers (e.g., coconut husk fibers), as shown in Figure 2-4.

Figure 2-4 Different natural plant fibers. (a) Leaf fibers, (b) seed fibers, (c) bast fibers, and (d) fruit fibers.

Natural plant fibers primarily consist of cellulose, hemicellulose, lignin, and pectin, among other components. The content of these components varies based on the fiber type, plant growth conditions, and extraction methods. Table 2-3 provides a detailed breakdown of the main chemical compositions of various natural plant fibers along with their respective content ranges.

Table 2-3 Main chemical components of common plant fibers [100].

Natural fiber	Cellulose (wt%)	Hemicellulose (wt%)	Lignin (wt%)	Pectin (wt%)	Wax (wt%)
Flax	71	18.6-20.6	2.2	2.3	1.7
Hemp	70.2-74.4	17.9-22.4	3.7-5.7	0.9	0.8

Jute	61-71.5	13.6-20.4	12-13	0.2	0.5
Ramie	68.6-76.2	13.1-16.7	0.6-0.7	1.9	0.3
Sisal	67-78	10.0-14.2	8-11	10	2
Bamboo	26-43	30	21.31	-	-
Coir	36-43	0.15-0.25	41-45	3-4	-

Cellulose

Cellulose serves as the predominant component in plant fibers, exerting significant influence on the physical and chemical properties of natural fibers. Variations in composition and structure arise in plant fibers due to differences in plant species, plant parts and growth conditions [101]. X-ray studies have demonstrated that in plant fibers, cellulose molecules are interconnected mainly by van der Waals forces and hydrogen bonds, forming two aggregation state structures, crystalline and amorphous regions [102], as shown in Figure 2-5. Many properties of cellulose are related to the ratio of crystalline and amorphous regions, for example, physical properties such as fiber strength and elasticity depend on the size of the crystalline region; whereas the swelling capacity, permeability, and reactivity of fibers depend on the size of the amorphous region [103]. Four crystalline variants of solid cellulose have been found, of which cellulose I is the natural crystalline form; and cellulose II, III, IV, and X are transformed from cellulose I under different conditions [104]. For example, cellulose II is a crystalline variant obtained by regeneration of cellulose I via alkali solution and this transformation is the main source of cellulose II [105]. In addition, the cellulose molecule cellulose IV is a high-temperature crystalline variant that is transformed from several other crystalline variants at different high-temperature conditions.

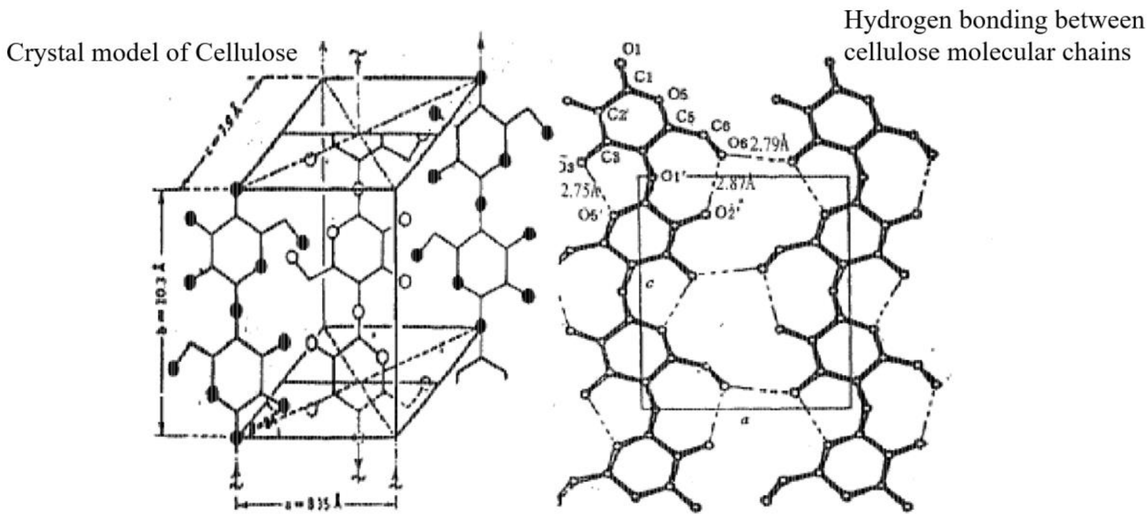

Figure 2-5 Structure model of cellulose molecule chain [106].

Hemicellulose

Hemicellulose is one of the associated components of cellulose and another major component of plant fibers. Compared to cellulose, hemicellulose is a much smaller polymer with significantly lower mechanical and chemical stability [107]. This is mainly due to the fact that hemicellulose contains a significantly higher content of reducible end groups, such as hydroxyl groups (OH) and aldehyde groups (CHO). Consequently, it displays chemically unstable characteristics, making it prone to hydrolysis, acid degradation, oxidation, and other chemical transformations. The content of hemicellulose has a significant impact on the properties of natural fibers, whereby higher hemicellulose content is associated with lower fiber strength [108].

Lignin and other impurities

Lignin is an amorphous polymer compound with aromatic properties. Lignin macromolecules contain methoxy (OCH_3), hydroxyl (OH) and carbonyl (C=O) groups. The methoxy group (OCH_3) contained in lignin is formed by phenolic hydroxyl group, which is difficult to decompose and remove. Pectin is a complex of acidic, highly polymerized, gelatinous carbohydrates, a substance consisting of a mixed chain containing glucuronic acid units. It is distributed between fibroblasts, between fibroblasts and non-fibroblasts, and also fills the voids of the primary wall, acting as a bond [109]. Pectin in general is easier to remove, but insoluble pectin binding between single fibers is stronger and not easily removed.

The application of natural plant fibers in agriculture offers both resource recycling and ecological benefits. It is estimated that 2.8 billion tons of crop residue production are generated globally each year [110, 111]. Improper disposal of this waste can lead to environmental pollution and carbon emissions. Converting natural plant fibers into functional materials, such as slope protection nets and biodegradable mulch films, helps reduce the ecological burden caused by open-air burning or landfilling, while simultaneously improving soil quality through material circulation. Research has shown that plant-fiber slope protection nets can increase soil porosity, reduce surface soil loss by over 90 %, and enhance soil structure through the humic acid released during fiber degradation, improving both water and air permeability [11, 112]. Moreover, the degradation of plant fibers does not produce toxic by-products. These fibers are rich in essential nutrients, including nitrogen, phosphorus, potassium, and minerals like calcium and magnesium [113]. Through microbial mineralization, they can replenish the soil's nutrient pool and mitigate soil compaction caused by prolonged fertilizer use. For instance, a rice straw return experiment showed that applying rice straw increased soil porosity by 8.8 %, reduced soil aggregate destruction rates by 34.3 %, and significantly improved the structure of the tillage layer [114]. Therefore, the use of natural plant fibers not only establishes a sustainable, closed-loop system but also provides an economically and ecologically resilient solution for the sustainable development of agriculture by regulating biogeochemical processes.

Natural properties of jute fiber

Jute fiber is a natural bast fiber extracted from jute plants (*Corchorus capsularis L.* and *Corchorus olitorius L.*) and represents a significant cellulose-based bioresource. Jute is considered a valuable crop in Asia, particularly in Bangladesh, Pakistan, and India [115]. As one of the most important long-fiber crops globally, jute ranks second only to cotton in terms of production and cultivation area, while being more cost-effective than cotton [116]. This economic advantage, combined with its high strength, excellent hygroscopicity, and biodegradability, has led to increasing interest in its use for sustainable and eco-friendly applications. Jute bundle fibers consist of multiple single-cell fibers bonded together by an intercellular matrix primarily composed of pectin. The fiber cross-section exhibits an irregular geometry [117], while the surface morphology is typically rough and characterized by randomly distributed micropores (Figure 2-6). Variations in fiber diameter and maturity across different parts of the jute plant contribute to surface morphology differences. A lower density of micropores generally indicates an immature fiber structure [118].

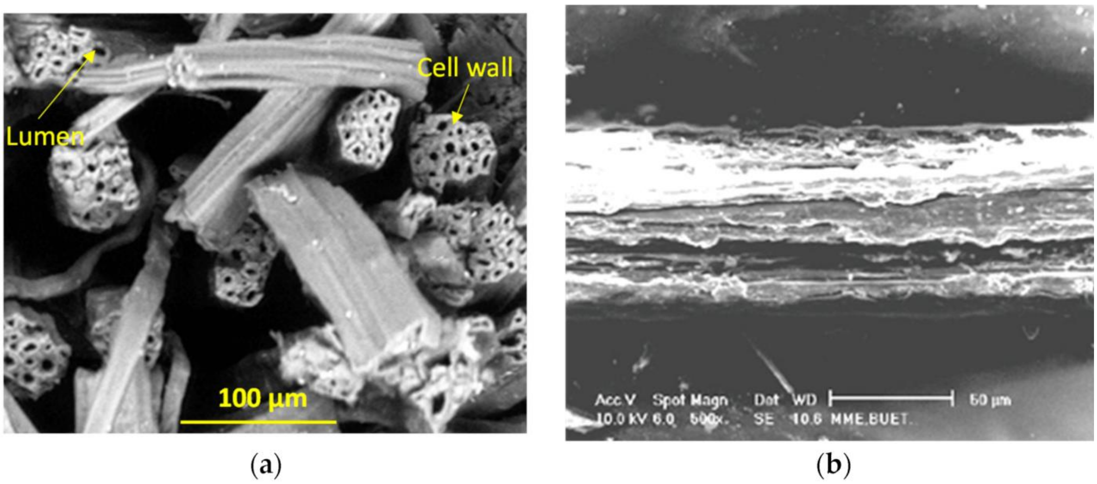

Figure 2-6 Jute fiber morphology (a) cross-section and (b) surface [117].

Hierarchical structure of jute fibers consists of cellulose microfibrils embedded within a hemicellulose-lignin matrix, providing an optimal balance of strength, flexibility, and durability [119]. As shown in Table 2-4, jute fibers, due to their low raw material cost and superior mechanical properties, make them widely utilized in industrial textiles, ropes, and environmentally friendly packaging materials. Cellulose is the predominant component of jute fiber, characterized by a structure comprising both amorphous and crystalline regions [120]. The amorphous regions exhibit high flexibility and strong interactions with water molecules, imparting jute fiber with excellent hygroscopic and desorption properties [121]. This allows it to effectively regulate soil moisture and temperature, making it particularly advantageous in agricultural applications. Conversely, the crystalline regions contribute to the mechanical strength and durability of jute fiber [122], reinforcing its suitability for agricultural mulch, geotextiles, and irrigation system components. Additionally, its biodegradability has garnered significant attention in agriculture and environmental protection, particularly as a sustainable alternative to petroleum-based plastics and synthetic materials. Compared to other natural fibers, jute requires lower energy consumption during production and generates minimal environmental pollution, further solidifying its potential as an ideal material for sustainable development.

Table 2-4 Comparison of the properties of natural plant fibers with synthetic fibers.

Fiber type	Density (g/cm^3)	Elongation at break (%)	Tensile strength (MPa)	Tensile modulus (GPa)	Specific strength ($MPa \cdot cm^3/g$)	Specific modulus ($GPa \cdot cm^3/g$)
Cotton	1.5	7.0~8.0	287~597	5.5~12.6	191~398	3.7~8.3
Hemp	1.5	1.6	690	/	460	/
Ramie	1.5	3.6~3.8	400~938	61.4~128	267~625	40.9~85.3
Sisal	1.5	2.0~2.5	511~635	9.4~22	341~623	6.3~14.7
Flax	1.5	2.7~3.2	345~1035	27.6	230~690	18.4
Jute	1.3	1.5~1.8	393~773	26.5	302~595	20.4
PET	1.38	25~40	370~571	9.8	268~421	7.1

2.3.2 Degradation polymers

Degradable polymers are materials that can be broken down into non-toxic substances through a series of physical, chemical, and biological processes mediated by microorganisms, fungi, or enzymes in the natural environment. Unlike traditional synthetic polymers, degradable polymers contain hydrolysable side groups such as ethers, esters, amides, and carbonates [123]. These groups enhance the flexibility of the polymer chain and facilitate interaction with the active sites of enzymes, thus imparting biodegradability to the polymer. This characteristic is crucial for reducing plastic pollution and improving resource utilization. With advancements in technology, a variety of biodegradable plastics with functional properties comparable to those of commercial-grade plastics have been developed, offering a promising alternative to non-degradable plastic materials, as detailed in Table 2-5.

Table 2-5 Main degradable polymer and their applications.

Type	Degradation	Issues	Industrialization	Fields of application
PLA	Hydrolysis + microbial degradation	Poor flexibility	High	Packaging, textile industry, agricultural films and biomedical polymers
PHA	Enzymatic degradation + Microbial degradation	Poor thermal stability; poor machinability; High cost;	Moderate Low	Medical field, food packaging and other high-value-added fields
PHB			Moderate Low	Medical field, food packaging and other high-value-added fields
PBS	Enzymatic degradation + Microbial degradation	Poor mechanical properties; High	Moderate high	Packaging films, tableware, foam packaging materials, bottles for daily

	+ Hydrolysis	cost;		necessities, medicine bottles, agricultural films, slow-release materials for pesticides and fertilizers
PBAT			High	Agricultural film, packaging, garbage bags
PBSA			Moderate	Agricultural film, packaging
PGA	Hydrolysis + microbial degradation	Extremely high cost	Low	High-value-added medical fields such as drug slow-release materials, tissue engineering materials, surgical sutures
PCL	Enzymatic degradation + microbial degradation + (weak) hydrolysis		Moderate	Medical field, food packaging and other high-value-added fields

Currently, degradable polymers can be broadly classified into three categories based on their primary degradation mechanisms: photodegradable polymers, biodegradable polymers, and dual-degradable polymers (photo-biodegradable polymers).

Photodegradable polymers

Photodegradable polymers are polymers that can undergo partial or complete degradation over time when exposed to light, oxygen, temperature, and other environmental conditions [124]. The two most common types of photodegradable polymers are synthetic and additive types. Typical synthetic photodegradable polymers include vinyl ketone copolymers, carbon monoxide and ethylene copolymers, among others [125]. These polymers achieve photodegradability through the incorporation of photosensitive groups, such as -C=O, during the copolymerization process. Research has demonstrated that the incorporation of appropriate photosensitizers into degradable polymers can significantly enhance the photodegradation process [126]. These polymers are classified as additive photodegradable polymers. The choice of photosensitizer can influence the photodegradation efficiency of the material.

Photodegradable polymers primarily undergo degradation under the influence of UV light (200nm–300nm), where UV-induced bond cleavage and free radical oxidation reactions lead to polymer degradation [127]. The specific degradation mechanism involves the reaction of molecular chains under controlled oxygen, temperature, and humidity conditions, causing the long polymer chains to break down into peroxides [128] (Figure 2-7). The degradation process of photodegradable polymers is highly dependent on adequate light exposure; however, most film materials cannot remain exposed to natural light for extended periods after use, limiting their ability to effectively interact with ultraviolet radiation and hindering photodegradation [129]. Furthermore, low-molecular-weight residual plastics and additives, such as photosensitizers, may persist in the environment after the degradation process, potentially exerting negative effects on subsequent crop growth.

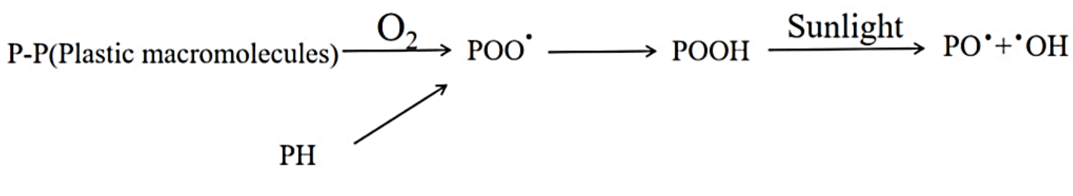

Figure 2-7 The mechanism of photodegradable [128].

Huang et al. [130] successfully designed cyclic acylsilane monomers for ring-opening metathesis polymerization, demonstrating efficient copolymerization and photodegradation under 390 nm irradiation (Figure 2-8a). Do et al. [131]developed a photodegradable vinylic polymer by incorporating a cyclic monomer (C3) via ring-opening polymerization. UVB exposure triggered cyclobutane cleavage, leading to polymer degradation, with sunlight inducing significant breakdown within 10 days (Figure 2-8b). Chae et al. [132] established a living cationic ring-opening polymerization of hetero Diels–Alder adducts using the reversible addition-fragmentation chain transfer method, resulting in polymers with unique thermal properties and enhanced photodegradation rates. Sunlight exposure caused a color change and increased hydrophilicity, confirmed by fluorescence contrast with methylene blue (Figure 2-8c). SEC analysis showed a molecular weight drop from 16.4 kDa to 2.2 kDa (Figure 2-8d), while nanoindentation indicated increased hardness and modulus (Figure 2-8e).

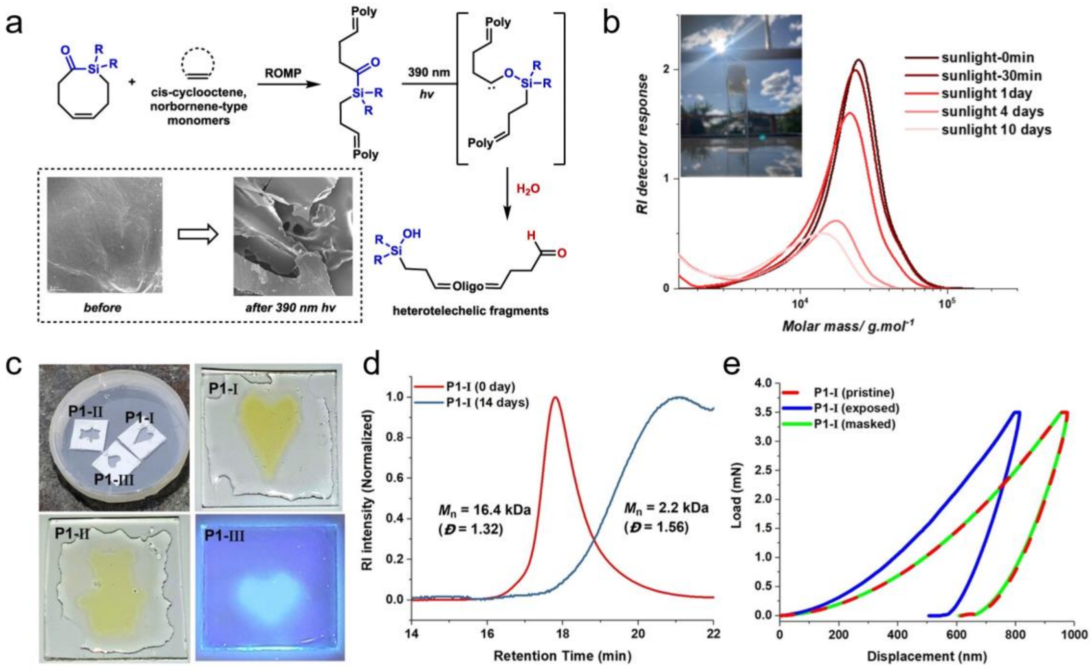

Figure 2-8 (a) Design of backbone-degradable polymers through ROMP and SEM image of the copolymer sample before and after 30min irradiation [130]. (b) SEC chromatograms depicting copolymer mass distribution after solar irradiation for 0 min, 30 min, 1 day, 4 days and 10 days [131]. (c) Masked P1 films under natural sunlight (upper left) and the resulting P1 films (others). A fluorescence image of P1-III was captured after sunlight exposure and subsequent treatment with an aqueous methylene blue solution. (d) SEC traces of P1-I before and after 14 days of sunlight exposure. (e) Load-displacement curves from nanoindentation, comparing the profiles of pristine P1-I and masked P1-I [132].

Biodegradable polymers

Biodegradable polymers encompass natural polymers, synthetic polymers, and their blends. Natural polymers originate from biomass resources, including starch, cellulose, and lignin, whereas synthetic biodegradable polymers are chemically synthesized, such as polylactic acid (PLA), polycaprolactone (PCL), polycarbonate, and polyphenolic compounds. Owing to their environmentally favorable characteristics, these polymers hold significant potential for applications in sustainable materials.

The degradation of biodegradable polymers involves microbial and enzymatic activity, breaking them down and integrating them into natural biogeochemical cycles, reducing environmental impact [133]. This process occurs in two stages (Figure 2-9): extracellular enzymes and abiotic factors depolymerize long-chain polymers into oligomers, often accompanied by the hydrolysis of readily degradable components like starch, forming a porous structure that facilitates further degradation [134, 135]. In the next stage, bacterial and enzymatic catalysis induce hydrolysis or oxidative cleavage of the polymer backbone, producing low-molecular-weight fragments that undergo microbial assimilation and biomineralization, ultimately converting into mineralized end products under aerobic or anaerobic conditions.

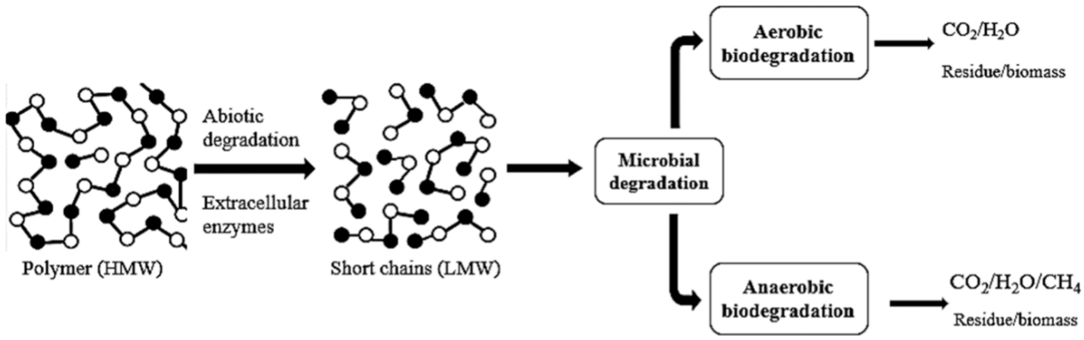

Figure 2-9 Biodegradation steps of polymers [136].

PLA is a representative bio-based degradable polymer, synthesized through the fermentation of starch from plant-derived resources such as corn and wheat, followed by polymerization of lactic acid [137]. It exhibits excellent biodegradability, biocompatibility, and non-toxicity, making it widely applicable in agriculture, horticulture, biomedicine, and other fields [138-140]. Studies indicate that under composting conditions, PLA can undergo substantial degradation within approximately

30 days, with the degradation rate influenced by environmental factors and microbial activity [141]. As a degradable polymer, PLA holds significant potential in supporting sustainable development and environmental conservation. Chen et al. [142]developed a biodegradable polymer blend of PLA and PBAT with a stable co-continuous morphology at an asymmetric 70/30 ratio (Figure 2-10a), achieved through interfacial stereo complex crystallites (i-SCs) via reactive blending. The incorporation of i-SCs significantly enhanced the material's mechanical properties, including tensile strength, ductility, and impact resistance, as shown in Figure 2-10b and Figure 2-10c. Wu and Zhang [143]developed highly toughened PLA/PBAT multicomponent blends through reactive melt-blending with EMA-GMA. The optimized blend exhibited a remarkable notched impact strength of 61.9 kJ/m² (Figure 2-10d) and an elongation at break of 278% (Figure 2-10e), demonstrating exceptional toughness. These results underscore the potential of PLA/PBAT/EMA-GMA blends for applications in packaging and agricultural films.

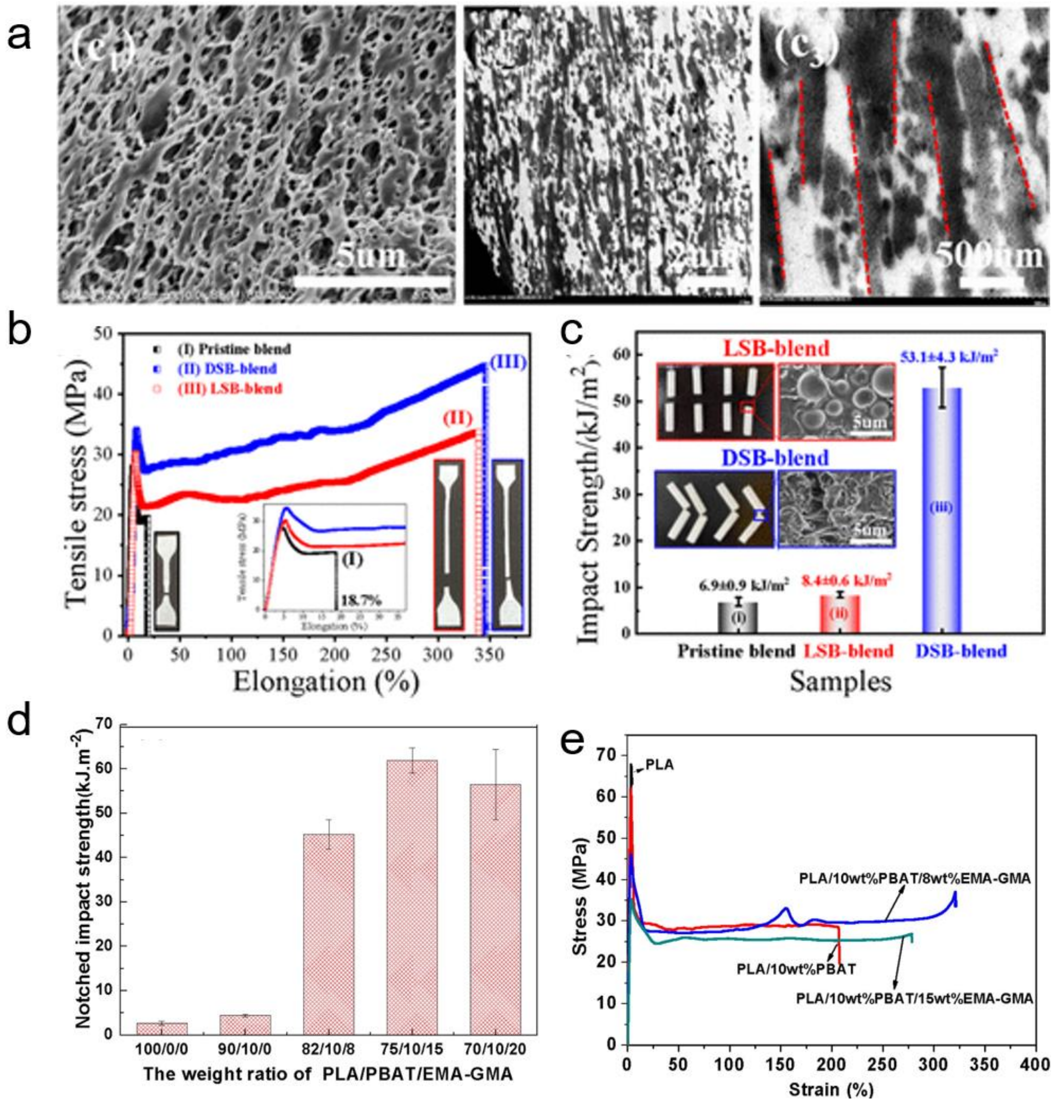

Figure 2-10 (a) SEM and TEM images of the stable co-continuous PLA/PBAT (70/30) blend with and without compatibilizers. (b) Stress–strain curves and (c) notch impact strength of the PLLA/PBAT (70/30) blends with and without compatibilizers [142]. (d) Notched impact strengths and (e) stress-strain curves of PLA, PLA/PBAT and PLA/PBAT/EMA-GMA blends [143].

Photo-biodegradable polymers

Photo-biodegradable polymers are composite materials created by incorporating photosensitizers into biodegradable polymers, enabling both photodegradation and biodegradation [144]. The degradation process is typically initiated by the absorption of UV light, which breaks the chemical bonds within the polymer, leading to a reduction in molecular weight and the formation of reactive sites. These changes enhance the polymer's susceptibility to microbial degradation. Matson et al. [145] synthesized a bio- and photodegradable. The resulting films exhibited tunable mechanical properties and thermal stability up to 273 °C. UV exposure induced photodegradation via Norrish photocleavage, leading to complete mechanical loss.

2.4 Preparation Methods of Agricultural Materials

The preparation methods of agricultural materials vary significantly based on their type and intended function. Depending on the chemical composition and functional requirements, the preparation methods of agricultural materials can be broadly categorized into two main groups: the preparation methods of agricultural plastics and the preparation methods of agricultural textiles.

2.4.1 Preparation of agricultural plastics

Agricultural plastics are typically derived from synthetic or bio-based polymers, such as polyethylene and polylactic acid, and rely on thermoplastic processing techniques, including extrusion, blow molding, and injection molding, to achieve morphological transformation in the molten state. These methods are primarily used for producing materials like biodegradable films and irrigation systems.

The extrusion molding method is a fundamental preparation technology, which is typically used as a preparatory step before injection molding [146]. The process relies on a single or two-screw extruder as the core equipment, where polymer particles such as PE, PP, or biodegradable materials (e.g., PLA/PBAT) are heated and melted [147]. The molten material is then extruded through a mold, cooled, and solidified (Figure 2-11a). This mature and well-established process ensures stable, long-term production while maintaining product consistency and quality.

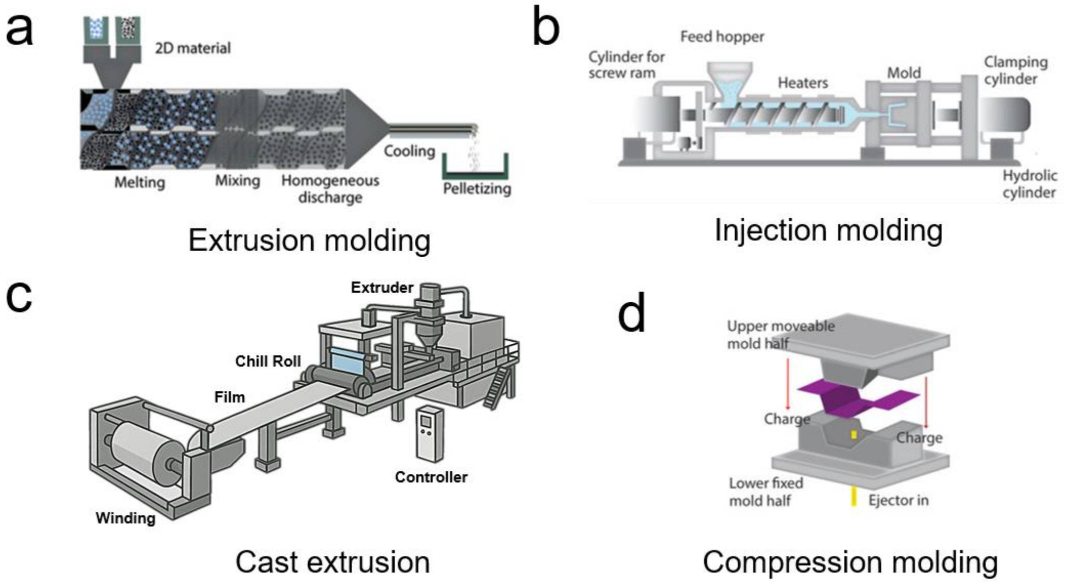

Figure 2-11 Schematics of common plastic manufacturing techniques. (a) Extrusion molding, (b) injection molding, (c) cast extrusion, and (d) compression molding [148].

The injection molding method for agricultural plastics is an efficient process in which molten polymer is injected into a closed mold under controlled pressure, then cooled and solidified to form the final shape [149, 150]. It is widely utilized for the mass production of complex structural components such as seedling trays, irrigation pipes, and biodegradable flowerpots. This process employs an injection molding machine as the core equipment, where polymers are heated to a molten state and injected into the mold cavity under high pressure, driven by the advancement of a screw. The molded product is then demolded after pressure maintenance and cooling (Figure 2-11b). The high production efficiency and precision of this method allow for precise control over product details and performance, meeting the specific needs of various agricultural applications. However, the process entails high investment in molds and equipment, as well as high-energy consumption [151], which makes it less suitable for small-scale production of agricultural plastic products.

The cast film extraction method is a prevalent technique in which molten polymer is extruded onto the surface of a cooling roller through a flat-slot die, and gravity or mechanical stretching is used to form a film [152]. This method is primarily employed in the production of film-type agricultural plastic products, such as agricultural covering films, greenhouse films, and packaging materials. By controlling the flow rate, cooling rate, and pulling speed of the melt, this process enables the production of films with uniform thickness, high transparency, and a smooth surface, effectively meeting the requirements for film materials in the agricultural sector [153] (Figure 2-11c). However, the high equipment investment, stringent process requirements, and limited scope of application mean that this method is primarily used for the production of film products.

Compression molding is a closed-forming technology that enables precise control over product dimensions and surface quality through mold design and applied pressure (Figure 2-11d). This method offers distinct advantages in the manufacturing of agricultural plastic products, particularly for high-strength components with complex geometries. However, its relatively long production cycle and stringent mold quality requirements limit its suitability for high-efficiency, large-scale production.

2.4.2 Preparation of agricultural textiles

Agricultural textiles use natural fibers or synthetic fibers as structural units, forming porous networks through physical processes such as knitting, weaving, or needle punching. These textiles are primarily used in applications such as weed control, moisture retention, and other related agricultural functions, with woven, knitted, and non-woven fabrics being commonly used.

The weaving method involves interlacing warp and weft yarns at right angles, creating a structured and repetitive pattern in the fabric construction [154]. During the weaving process, warp yarns are typically kept in a straight alignment, while weft yarns interlace over and under them at right angles. This interwoven structure provides excellent dimensional stability in both directions, ensuring durability and strength [155]. Additionally, woven fabrics exhibit low shear stiffness, enhancing their adaptability to various applications. Due to these characteristics, woven fabric technology is widely utilized in agricultural textiles, including weed control fabrics, shade nets, windbreak barriers, and high-strength greenhouse coverings. These textiles are designed to offer superior mechanical performance, resistance to environmental conditions, and functional properties such as tensile strength, weather resistance, and breathability, making them well-suited for modern agricultural applications.

The knitting method involves creating a unique interlocking loop structure, which offers excellent stretchability and drape, allowing fabrics to conform to complex shapes [156]. The exceptional formability of the fabric enables the creation of precise shapes, including intricate and curved geometries. These advantages make them highly adaptable for various applications, such as plant support nets, shading fabrics, and protective covers. Additionally, knitted fabrics offer several key benefits, including superior flexibility, high impact resistance, enhanced interlayer bonding, efficient molding capabilities, and the ability to achieve high production efficiency with short processing cycles [156].

The nonwoven method involves bonding fibers together through mechanical, thermal, or chemical processes, and the resulting fabrics are commonly used in agricultural applications, particularly in mulch fabrics, geotextiles, and biodegradable crop covers. The two primary methods for producing these nonwoven fabrics are needle punching and hydroentanglement. Nonwoven fabrics, while cost-effective and versatile in applications, typically exhibit lower strength and durability due to their random fiber orientation and bonding methods. This often limits their performance in applications requiring high tensile strength and long-term reliability.

2.5 Applications of Degradable Material in Agriculture Field

The application of degradable materials in agriculture has gained significant attention as a sustainable alternative to conventional synthetic materials. The global biodegradable materials market was valued at approximately US$5.732 billion in 2023 and is projected to reach US$27.703 billion by 2030, reflecting a compound annual growth rate of 21.73% [157]. This rapid expansion highlights the transition of green agriculture from technical exploration to large-scale implementation. By replacing conventional plastics and enhancing resource efficiency, biodegradable materials have demonstrated remarkable advantages.

2.5.1 Mulching

As the global use of plastic mulches continues to rise, the market for degradable soil mulches is also expanding [158]. The global market for soil degradable mulches was valued at $62.7 million in 2022 and is projected to grow at a CAGR of 7.6%, reaching $83.6 million by 2026 [159]. Unlike traditional plastic mulches, which must be removed after use, degradable soil mulches are designed to be incorporated into the soil at the end of the planting season [160, 161]. Once tilled into the soil, these mulches break down through microbial activity under both aerobic and anaerobic conditions, converting into microbial biomass, carbon dioxide, and water [61]. Therefore, soil degradable mulches present a more sustainable and cost-effective alternative to polyethylene mulches.

Photodegradable mulch materials

Zhang et al. [162] explored the development of a photodegradable Nano-G/TiO_2/PVC composite film by incorporating nano-graphite (Nano-G) and TiO_2 photocatalysts into PVC. The resulting composite film demonstrated significantly enhanced photodegradability, with a weight loss of 17.24% after 30 hours of UV irradiation, in contrast to only 2.12% for pure PVC. The optimal nano-graphite doping level was determined to be 1 wt%. Nano-graphite facilitated the migration and separation of TiO_2 photogenerated electrons, thereby improving the photodegradation rate of PVC (Figure 2-12a and Figure 2-12b). Zheng et al. [163] developed photodegradable plastics by incorporating a photocatalyst into LDPE. The results showed that after 120 hours of light exposure, the weight loss rate was 1.0 μg/h and the carbonyl index increased significantly (from 0 to 0.47). This approach provides an efficient and sustainable solution to plastic pollution by achieving controlled photodegradation only after exposure to light (Figure 2-12c and Figure 2-12d).

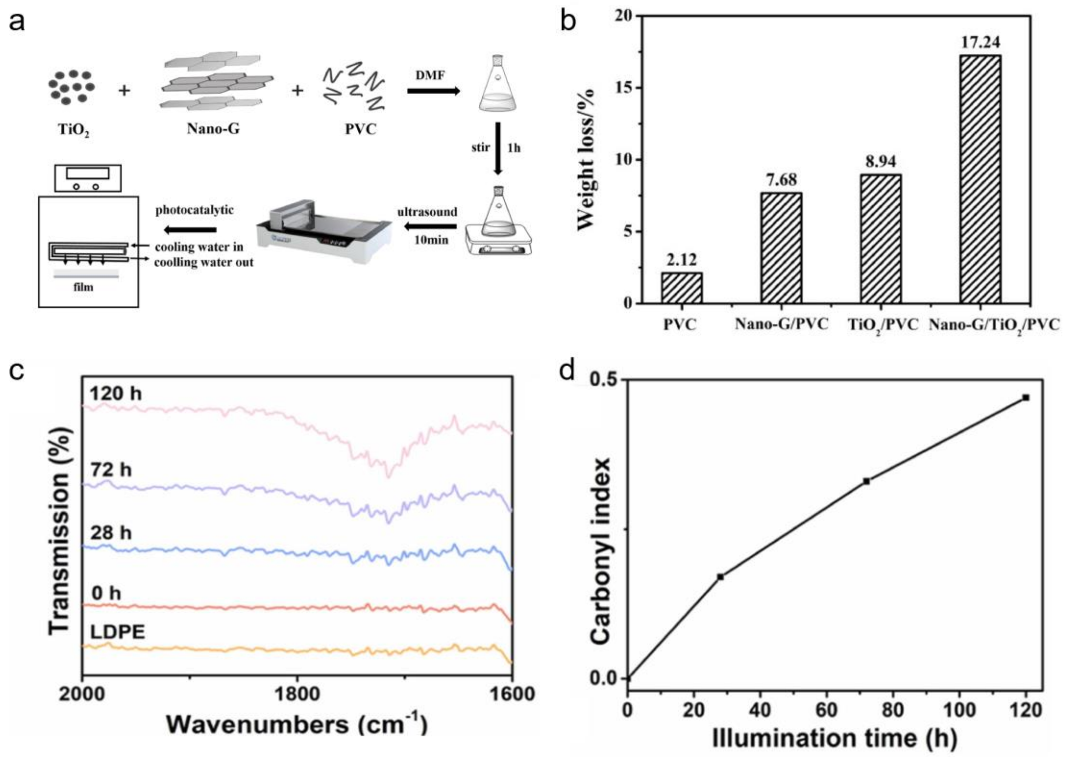

Figure 2-12 (a) Preparation and photocatalytic process diagram of the Nano-G/TiO_2/PVC composite film and (b) weight loss after 30-hour UV exposure [162]. (c) FTIR spectra of LDPE and LDPE-T@CDIH before and after exposure to different durations. (d) Carbonyl index of LDPE-T@CDIH before and after different illumination time [163].

Biodegradable mulch materials

Biodegradable mulch is typically composed of natural polymers, such as starch, PLA, PHA, or their composite materials. It undergoes decomposition into harmless byproducts, offering significant environmental benefits. Li et al. [164] developed a bio-based hydrophobic liquid mulch film (SOSA) made from waste soybean oil, starch and acrylate monomers. The soybean oil was oxidized into epoxy groups, then reacted with acrylic acid to increase the reactivity, followed by free radical polymerization with acrylate monomers to form a three-dimensional polymer network (Figure 2-13a). Studies have shown that the SOSA film effectively reduces soil erosion, enhances moisture retention and promotes crop growth, with soil loss reduced by 80.6 % and yield increased by 57.4 % (Figure 2-13b). SOSA exhibited excellent biodegradability, showcasing a biodegradation rate of 81.7 %, notably surpassing that of LDPE film (8.1%) (Figure 2-13c). Passaretti et al. [165] prepared the biodegradable mulching film derived from thermoplastic starch (TPS) reinforced with mica clay (MC) particles. The incorporation of MC into the TPS matrix results in a significant reduction in the transmission of photosynthetically active radiation (PAR), which is effective in inhibiting weed growth (Figure 2-13d). The inclusion of mineral particles enhances mechanical integrity of the TPS films, thereby improving durability throughout the crop cycle. Preliminary agronomic assessments demonstrated favorable crop growth (Figure 2-13f), suggesting that these composite films offer a promising, environmentally sustainable alternative to conventional non-degradable mulching materials.

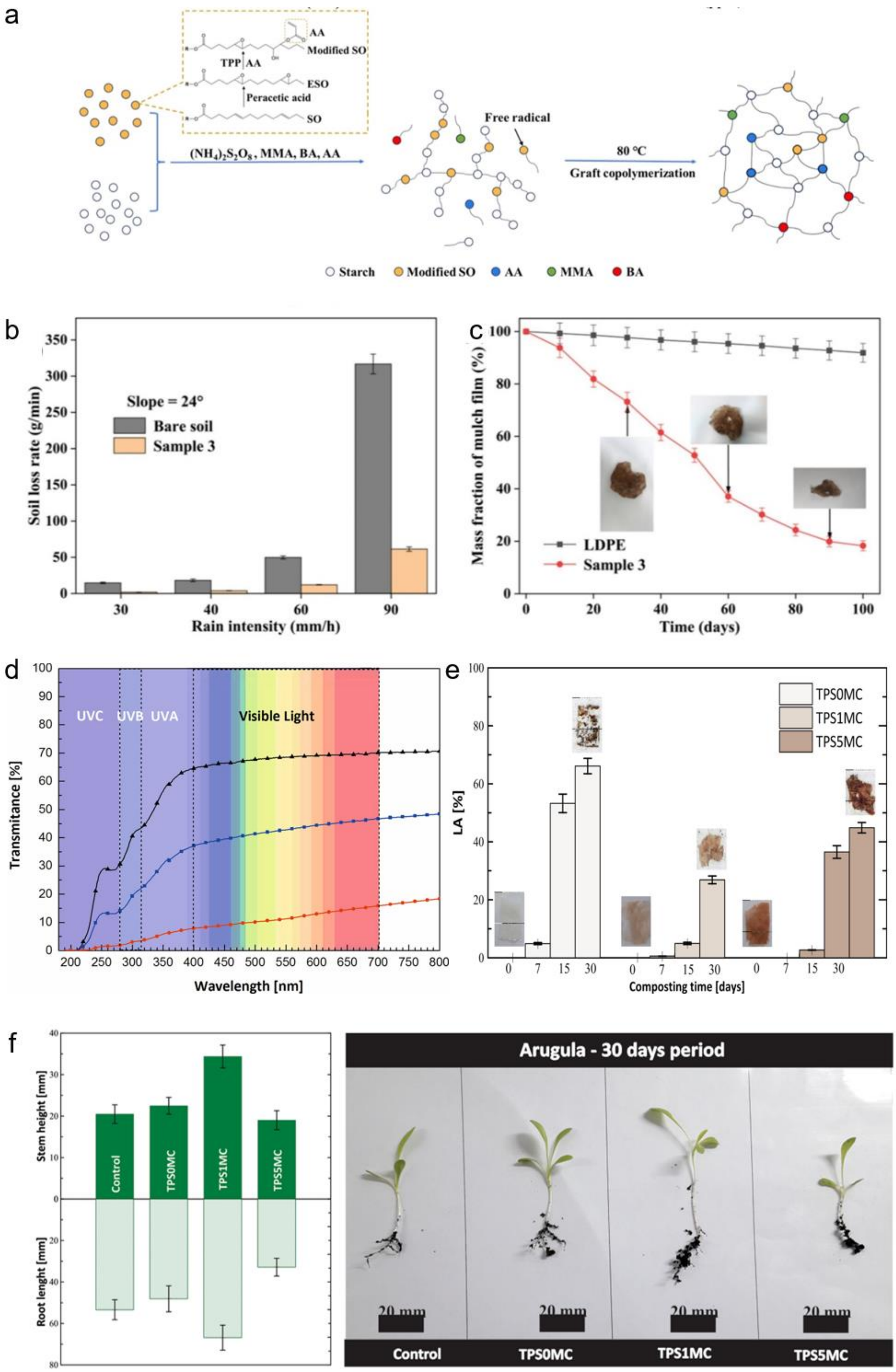
a
AA
Modified SO
TPP AA
ESO
Peracetic acid
SO
$(NH_4)_2S_2O_8$, MMA, BA, AA
Free radical
80 °C
Graft copolymerization
Starch
Modified SO
AA
MMA
BA
b
Slope = 24°
Bare soil
Sample 3
Soil loss rate (g/min)
Rain intensity (mm/h)
c
Mass fraction of mulch film (%)
LDPE
Sample 3
Time (days)
d
UVC
UVB
UVA
Visible Light
Transmitance [%]
Wavelength [nm]
e
TPS0MC
TPS1MC
TPS5MC
LA [%]
Composting time [days]
f
Stem height [mm]
Root lenght [mm]
Control
TPS0MC
TPS1MC
TPS5MC
Arugula - 30 days period
20 mm
Control
TPS0MC
TPS1MC
TPS5MC

Figure 2-13 (a) Grafting reaction mechanism involving BA, MMA, modified SO, and starch. (b) Soil loss at different rainfall intensities on a terrace slope of 24°. (c) Mass fraction of SOSA and LDPE films after degradation [164]. (d) UV–vis spectra of thermoplastic starch films. Symbols: (black filled triangle) TPS0MC, (blue colored square) TPS1MC, and (red colored circle) TPS5MC. (e) Loss area observed during composting assays of TPS and TPS composites. (f) Roots and stems growth during agronomic assay [165].

Additionally, PLA and/or PBAT, along with their composite biodegradable films, have demonstrated comparable effects to traditional plastic films in the cultivation of tomatoes [166], lettuce [167], strawberries [168], and corn [169]. Several studies have explored the use of kelp, sodium alginate, and chitin to produce environmentally friendly mulch films, further confirming that biodegradable films can serve as effective substitutes for plastic mulch in agriculture[170, 171]. However, the degradation rate of these biodegradable films is influenced by environmental factors such as temperature, humidity, and pH, as well as material composition, making it challenging to precisely control the rate of degradation. Furthermore, improvements in the physical properties of biodegradable films, including strength, moisture resistance, and weather durability, are necessary to enhance their performance in mechanized mulching practices.

Cellulose fiber-based mulch materials

The mulches mentioned above contain non-biodegradable components, which may result in the persistence of fragments during the degradation process. To address this issue, researchers have proposed fully biodegradable cellulose-based mulches, designed to ensure more complete degradation and prevent the formation of residual waste. Common types of cellulose-based mulches include cellulose-based mulch fabrics, fibers, papers, and sprayable cellulose-based mulches.

Cellulose fiber-based mulches have a positive impact on soil health and moisture retention and can increase crop yields while improving crop quality [12]. Another essential application of these covers is weed control, achieved by blocking light transmission and inhibiting photosynthesis. This method reduces the reliance on chemical herbicides, decreases labor requirements for weed management, and enhances the growing environment for crops. Hemp canvas produced plant yields comparable to plastic mulch while promoting soil health through its homogeneity and biodegradability properties [172]. Tan et al. [173] used waste plant fibers (ramie and cotton fibers) and biodegradable polymer PVOH to prepare composites of agricultural mulch film. The physical properties and degradability tests showed that the mulch film had good physical properties and biodegradability. Tan et al. [174]employed the solution casting method to prepare PVOH/kenaf fiber composite materials for biodegradable mulch films with the additional function as fertilizer carriers. The composites exhibited good water solubility and controlled release properties. Baheti and Militky [175]utilizied jute fibers at different scales to reinforce biodegradable composites and evaluates their effects on the mechanical properties of the composite films. The results showed that the composite films containing nanofibrils exhibited the highest increase in elastic modulus (65.21 %), followed by microfibrils (25.40 %) and millifibers (13.04 %) compared to neat PLA film. Cao et al. [176] developed biodegradable nonwoven mulch mats from end-of-use cotton garments, which effectively suppressed weeds, improved water infiltration, and biodegraded faster than plastic mulches. The mats performed well in controlling soil temperature and moisture retention, depending on soil texture, and offered a sustainable solution to textile waste in agriculture. Liu et al. [177] exploited recyclable natural fibers to develop a biodegradable mulch film with crop yields similar to those of plastic mulch, while providing better insulation and weed suppression. The film degrades after 90 days, highlighting its potential for sustainable agricultural use.

Jute fiber, a natural and abundant plant fiber material, is renowned for its environmental benefits. It is widely utilized across various industries due to its biodegradability, air permeability, and high mechanical strength. Initially, jute fiber was predominantly used in traditional products such as ropes, twine, sacks, and burlap [12]. However, with the growing emphasis on sustainable agriculture and eco-friendly materials, its application in agriculture has expanded. Leveraging its inherent physical properties, jute fiber is now used in the production of agricultural mulches, geotextiles, irrigation systems, and plant protect nets. These applications contribute to enhancing crop growth environments, facilitating complete degradation post-use, and preventing residual waste. Furthermore, during its degradation process, jute fiber can enrich soil organic matter and improve soil structure. The effectiveness of jute agro-textiles has been demonstrated in soil protection and slope stabilization.

A field experiment in Eastern India showed that nonwoven jute agrotextile mulch significantly improved broccoli productivity, soil moisture retention, microbial population, and nutrient content, while effectively suppressing weeds [178]. Manna et al. [179]found that residual 400 gsm nonwoven jute agro-textile mulch (NJATM) outperformed rice straw and black polythene in enhancing maize yield, soil fertility, moisture retention, and microbial activity in lateritic soil. It achieved the highest grain yield (6.90 t ha^{-1}), improved microbial populations, and significantly suppressed weeds. Additionally, 400 gsm NJATM maximized soil moisture and nutrient content, making it the most effective option for sustainable maize cultivation. Shahid et al. [180] explored the development of jute-polyester hybrid nonwoven fabric (JHNF) for packaging applications (Figure 2-14a). The JHNF exhibited strong antibacterial activity (Figure 2-14b), high mechanical strength, water repellency, and low thermal conductivity, demonstrating it to be a promising thermally insulative and eco-friendly packaging. Mridha et al. [181] demonstrated that jute-based nonwoven mulch, particularly 650 gsm pure jute, significantly improved soil moisture retention, temperature regulation, microbial growth, nutrient uptake, and water use efficiency compared to no mulch and plastic mulch in summer tomato cultivation (Figure 2-14c and Figure 2-14d). The 650 gsm jute mulch increased tomato yield by 84 % over no mulch and 28 % over plastic mulch, highlighting its potential as a sustainable alternative for eco-friendly tomato production. Chattopadhyay et al. [182] demonstrated that jute geotextiles offer a cost-effective and practical drainage solution, enhancing construction safety and efficiency (Figure 2-14e). Behera et al. [183]developed modified soy-based nonwoven jute composites for sapling pots, which effectively promoted plant growth. Degradation analysis revealed an 80% mass loss after 90 days (Figure 2-14f), demonstrating the high biodegradability of the pots and highlighting their potential as a sustainable alternative to plastic pots.

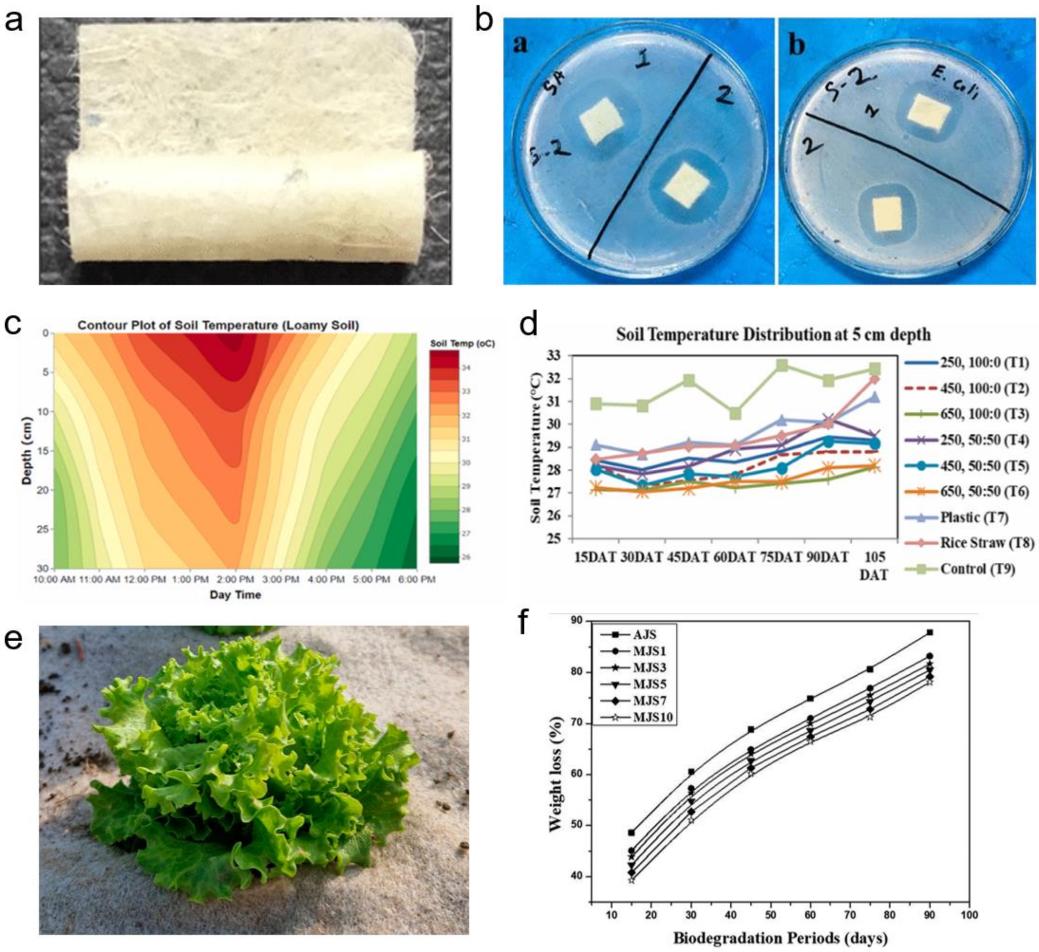

Figure 2-14 (a) Actual image of proposed jute-based hybrid nonwoven fabric. (b) Antibacterial tests of jute-based hybrid nonwoven fabric against *S.aureus* and *E.coli.* [180]. Diurnal soil temperature and temporal variation of (c) soil temperature and (d) 5 cm soil temperature [181]. (e) Laying actual situation. (f) Weight loss of modified soy-based nonwoven jute composites after different biodegradation periods [183].

2.5.2 Water management

The application of degradable materials in agricultural water management provides innovative solutions for sustainable resource utilization, effectively reducing plastic pollution while improving water resource efficiency. Zai et al. [184] conducted field tests to study seepage rate and uniformity of stalk composite pipes (SCP) in subsurface irrigation (Figure 2-15a and Figure 2-15b). Seepage rate decreased with pipeline length but increased with diameter, while irrigation volume had no clear effect. Uniformity declined with length, showing ambiguous trends for other factors. Das et al. [185] developed a biodegradable hydrogel using NaCMC and HEC crosslinked with citric acid to enhance soil water retention. The hydrogel-modified soil improved porosity and reduced density (Figure 2-15c), and increased water use efficiency by 25.25 %–45.52 % (Figure 2-15d). Growth studies on cucumber, tomato, and mung bean showed enhanced seedling viability, plant growth, and photosynthetic ability. The findings suggest that hydrogel modification optimizes water and nutrient absorption, promoting plant growth in water-limited conditions. Hiskakis et al.[186] investigated the feasibility of biodegradable rigid pipes made from Mater-Bi materials for drip irrigation systems. Biodegradation assessments revealed that Mater-Bi materials decomposed within 6 to 12 months in soil. The study highlighted the potential of biodegradable drip irrigation systems as a sustainable alternative to conventional plastic-based systems, while also identifying technical challenges and proposing future research directions for optimization.

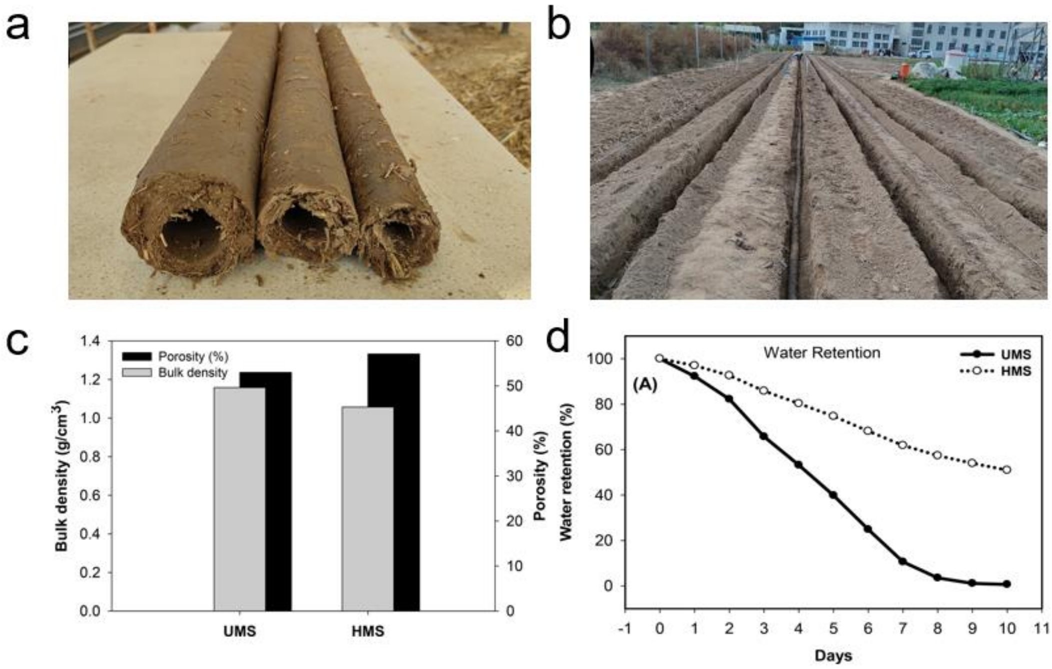

Figure 2-15 (a) SCPs with three cross-sectional sizes and (b) their field laying of SCPs [184]. (c)Bulk density and porosity of the HMS and UMS soil property. (d) Water retention capacity of unmodified soil and soil modified with hydrogel [185].

Other agricultural applications of biodegradable materials, such as seedling containers, have also shown potential in reducing plastic waste and improving root growth. represent an innovative solution aimed at fostering sustainable gardening and agriculture. Constructed from degradable materials, including plant fibers, starch-based polymers, and other environmentally friendly composites, the degradable seedling containers offer substantial benefits over conventional plastic containers[187-189]. By addressing the environmental concerns associated with traditional seedling pots, providing an optimal environment for root development while mitigating the waste and ecological impact typically linked to plastic products[190]. As plants mature, these pots gradually degrade in the soil, eliminating the need for post-harvest removal and reducing plastic waste in landfills.

2.6 Conclusion

This chapter provides a comprehensive overview of the current status of agricultural materials, the environmental impact of traditional materials and the need for sustainable alternatives. From a materials perspective, the extensive use of traditional materials (especially plastics) in agricultural practices is a growing problem in terms of the microplastic pollution they generate. Therefore, there is an urgent need to explore and develop sustainable and degradation materials for agriculture. The preparation methods of agricultural materials and the application of degradable materials in agriculture are discussed. To maximize their applicability and effectiveness, appropriate fabrication techniques should be selected based on the specific functional properties required. Degradable polymeric materials have been widely used in agriculture; however, the problems of their complex degradation process, uncertainty of degradation rate and stability under different environmental conditions still exist. In particular, the degradation performance of polymeric materials is often not as good as expected under some extreme conditions such as high humidity, low temperature or strong light, which poses a challenge for their long-term application in agriculture. In contrast, natural fibers, especially jute fibers, can effectively contribute to green and sustainable agricultural production due to their good inherent properties. The use of natural fibers in agricultural applications such as erosion control and crop protection has received much attention. However, research on its application in areas such as water-saving irrigation and weed management is still relatively limited compared to other areas of application. With the increasing demand for sustainable agricultural development, the potential of natural fibers in water-saving irrigation systems and weed management needs to be further explored. In addition, the performance of these materials in practical agricultural applications, including weed control, moisture and temperature management, and crop protection, requires further investigation to fully evaluate their long-term effectiveness and impact on crops and soil health. Through in-depth research on the physical and chemical properties of natural fibers, combined with advanced preparation and processing technologies, natural fibers are expected to become a key material in future agricultural production, driving agriculture in a more environmentally friendly and efficient direction.

Chapter 3 Characterization of the Basic Properties of Jute Yarns

3.1 Introduction

Jute fiber, derived from the bast of *Corchorus capsularis L.* and *Corchorus olitorius L.*, is a significant cellulose-based bioresource with widespread agricultural and industrial importance[191]. Predominantly cultivated in South Asia, particularly in Bangladesh, India, and Pakistan[192], jute is one of the most extensively grown long-fiber crops worldwide, ranking second only to cotton in terms of production and cultivation area[193, 194]. Notably, jute offers a more cost-effective alternative to flax and other comparable natural fibers, enhancing its economic viability for various applications. The physical properties of jute fibers, characterized by high tensile strength due to their high cellulose content and low microfibrillar angle[195, 196], along with moderate stiffness, excellent moisture absorption, biodegradability, and environmental sustainability, make them highly suitable for applications in textiles, agriculture, construction, and composite materials[12, 197, 198].

Similar to other cellulosic fibers, jute fiber consists of approximately 50 %~70 % cellulose, along with non-cellulosic components such as hemicellulose, lignin, and pectin[119, 199]. The distinctive physical and mechanical properties of jute fibers to the composition and relative proportions of cellulose, hemicellulose, and lignin, which facilitate stress transfer by linking cellulosic microfibrils[200, 201]. However, excessive proportion of non-cellulosic components also affects their interfacial adhesion, moisture absorption, and overall performance in various applications[202, 203]. The removal of non-cellulose components is a crucial step in enhancing performance and broadening application potential, which could enhance the surface properties of fibers and strengthens their interaction. Surface modification treatment of jute fibers through various chemical[204, 205] and physical[206] methods is necessary to use to properly remove impurities. Among the various surface modification techniques, alkali treatment is recognized as one of the most effective methods for enhancing the properties of natural fibers[207, 208]. This treatment removes hemicellulose, lignin, and surface impurities, leading to improvements in fineness, flexibility, and mechanical strength, which in turn enhances the suitability of the fibers for a wide range of industrial applications[209, 210]. Kaysar et al.[194] treated jute fibers from Corchorus olitorius (tossa) and Corchorus capsularis (white) with different sodium hydroxide (NaOH) concentrations (1–6 wt%) and found that a 5% NaOH treatment enhanced cellulose content, crystallinity, and fiber strength. Ghosh et al. [211] explored alkali-treated jute fibers for quilt thermal insulation. The treatment improved fiber crimp and reduced thermal conductivity, with the highest crimp and lowest conductivity achieved under specific conditions. SEM images revealed the removal of lignin, resulting in individualized, bulky, and porous fiber morphology. Tiwari et al. [212] studied alkali-treated Grewia Flavescens fibers, finding that 5 % NaOH treatment for 45 minutes significantly improved cellulose content, tensile strength, crystallinity, and thermal stability. SEM revealed a rougher fiber surface after treatment, indicating impurity removal. It is well established that the deformation of natural fibers depends to a large extent on the relationship of the elementary fibers in the yarn. Yarn, composed of fibers, is the primary determinant of functional behavior in textile applications. The structure of yarn influences not only the processability but also the properties and performance of the final textile product. Therefore, understanding the basic characteristics of jute yarn, as well as the properties of alkali-treated jute yarn, is essential to evaluate the practice performances in fabrics.

In this study, the basic characteristics of jute yarn (JY) were investigated, and alkali treatment was applied to JYs. The effects of different treatment durations on the properties of JYs were then evaluated. Morphological and structural changes induced by alkali treatment were analyzed to understand fiber surface modification and compositional alterations. Additionally, the influence of treatment time on the tensile strength, thermal stability, and moisture absorption behavior of JYs was systematically evaluated. The findings from this study provide insights into understanding the basic properties of JYs and the effects of alkali treatment conditions on the performance of JYs.

3.2 Experiment Section

Surface treatment experiments on JYs were conducted to investigate the effect of alkali solution treatment duration on the properties of JYs, as shown in Figure 3-1. Firstly, JYs were treated different times to obtain experimental samples using mixture solution ($NaOH$ & Na_2SO_3). The morphology, mechanical properties, thermal stability, and water absorption of the yarns under different conditions were then carried out, thereby the effects of alkali solution treatment times on the properties of JYs were evaluated.

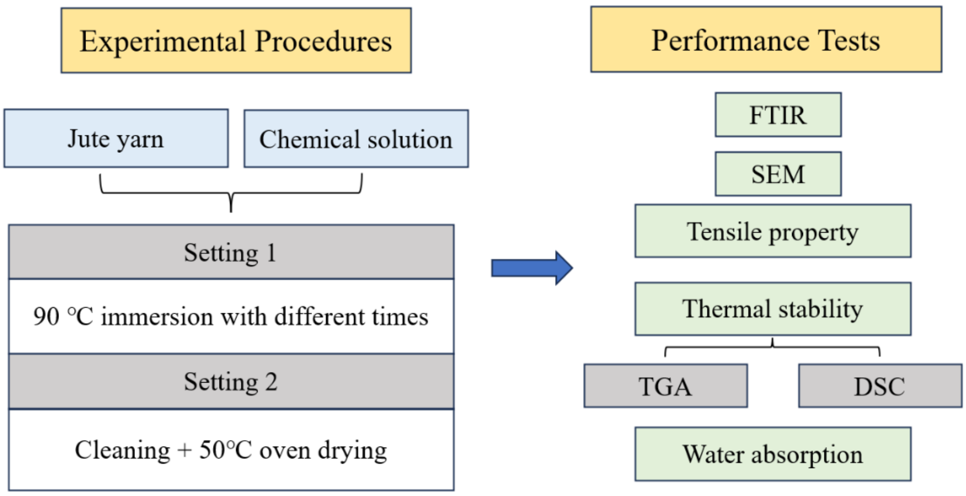

Figure 3-1 Experimental procedures and performance tests.

3.2.1 Material

JYs were purchased from Taobao commercial recourses. All chemicals, including $NaOH$ (Dieckmann, China) and Na_2SO_3 (Dieckmann, China) used in this study and obtained from commercial sources, were of analytical grade and were used without additional purification.

3.2.2 Alkali treatment of JYs

The chemical treatment procedure for JY follows the work route as shown in Figure 3-2. JYs were treated with a 2.0 wt% NaOH solution and a 0.25 wt% sodium bisulfite solution at a 1:30 fiber-to-solution ratio, heated to 90 °C to enhance the removal of non-cellulosic components. The alkali treatment was carried out for varying durations—0.5, 1.0, 1.5, and 2.0 hours—to evaluate the effect of treatment time on the degumming process of JYs. After treatment, the yarns were thoroughly washed with distilled water to neutralize the residual chemical and remove dissolved impurities, then dried in an oven at 50 °C for 6 hours and stored under controlled conditions at 25 °C and a relative humidity of 60 %.

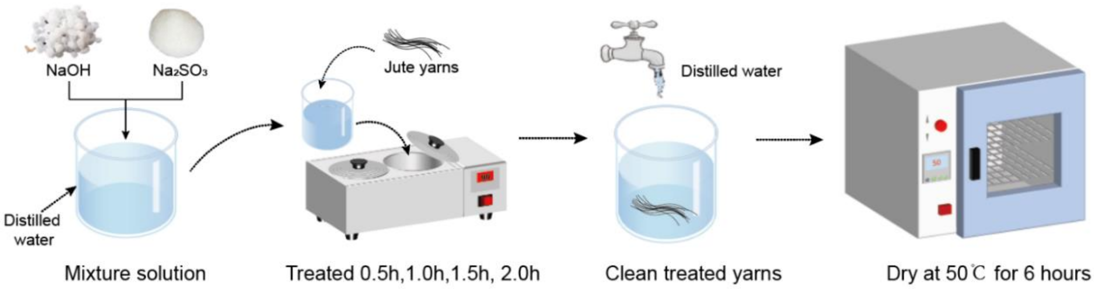

Figure 3-2 Schematic diagram of the chemical treatment of JYs.

Table 3-1 Different JYs before and after chemical treatment.

	Treated time (h)
JY (jute yarn)	0

JY-0.5h	0.5
JY-1.0h	1.0
JY-1.5h	1.5
JY-2.0h	2.0

3.2.3 Characterization

Dry samples of JYs, both untreated and treated, were mounted on SEM stubs and gold-coated with platinum before being examined using a ZEISS Sigma 300 SEM (Carl Zeiss AG, Germany). Surface characteristic photographs of the samples were captured randomly.

FTIR spectra of JY and alkali-treated JY with varying treatment times were recorded using a Vertex 70 FTIR spectrometer, with a resolution of 4 cm^{-1}. The measurements were taken within the wavenumber range of 650 ~ 4000 cm^{-1}.

The weight loss of dry samples before and after treatment were measured and calculated using the formula (3-1):

$$w = \frac{w_0 - w_1}{w_0} \times 100\% \tag{3-1}$$

Where, w_0 is the initial weight of JY, g. w_1 is the weight of JY after treatment, g.

The residual gum content of JYs was tested according to GB/T 18147.2-2008. The degreased sample was treated with 150 mL of a 20 g/L sodium hydroxide solution for 3 hours. The sample was then reacted with 30 mL of a 72 % sulfuric acid solution for 24 hours, followed by repeated washing and filtration until the filtrate was free of sulfate ions. Finally, the sample was dried to a constant weight and reweighed. The residual gum content was then calculated using the formula (3-2)：

$$G = G_1 + G_2 \tag{3-2}$$

$$G_1 = \frac{m_1 - m_2}{m_0} \times 100 \tag{3-3}$$

$$G_2 = \frac{m_4 - m_3}{m_0} \times 100 \tag{3-4}$$

Where, G is residual gum content of samples, %. G_1 is the weight of pectin and hemicellulose, %. G_2 is the weight of lignin, %. m_0 is the weight after extraction of waxes, g. m_1 is the weight of the sample after extraction of waxes and weighing bottle, g. m_2 is the weight after extraction of waxes, hemicellulose, pectin and weighing bottle, g. m_3 is the dried weight of glass core crucible, g; m_4 is the total dried weight of the sample lignin and glass core crucible, g.

The yarns were conditioned in a constant temperature and humidity chamber for at least 24 hours before testing. For each sample, yarns with length of 20.0 cm were selected and their tensile properties were measured using an Instron 5566 Universal Testing Machine (Instron, United States) according to ASTM D2256. The results are presented as the average of the five measurements for each sample to minimize uncertainties.

Thermal stability of JY was analyzed using differential scanning calorimetry (DSC) and thermogravimetric analysis (TGA). TGA measurements were performed on a TGA4000, (PerkinElmer, United States) by heating the samples from 30 °C to 600 °C at a rate of 15 °C/min under a nitrogen flow of 20 ml/min. DSC analyses were conducted using a DSC8000 thermal analyzer (PerkinElmer, United States) with approximately 4 mg samples sealed in aluminum pans and tested under constant nitrogen flow of 50 ml/min. The temperature program was set in the range of 30 °C to 500 °C at a heating rate of 15 °C/min.

The water absorption rate of JY was evaluated after water exposure. Initially, the sample was dried in an oven at 50 °C for 24 hours and then cooled to room temperature in a desiccator. After recorded the dry weight of the sample(M_1), the sample was then immersed in distilled water at 23 °C for 24 hours. The sample was removed, and excess surface water was gently blotted off with filter paper. The weight of the sample (M_2) was measured within one minute of removal. The water absorption rate was then calculated using the formula:

$$L = (M_2/M_1)/M_1 \times 100\% \tag{3-5}$$

where M_1 was the weight of the original dried JY and M_2 was the wet weight of JY after immersion. The measurement was carried out in three parts each time, and the average value was taken.

3.3 Result and Discussion

3.3.1 Surface morphology of JYs

Figure 3-3 shows optical and SEM images of untreated and treated JYs. Untreated JY shows a loose appearance with more hairiness. However, after chemical treatment for varying durations, the fiber packing of JYs became significantly tighter, likely due to the removal of impurities. This alteration in packing density led to a noticeable reduction in yarn diameter shown in Figure 3-4. Yarn diameters were slightly reduced from 0.9 mm to 0.6 mm, which is in agreement with the results obtained in previous studies [213, 214]. Significant differences in the surface morphologies of JY were observed in SEM images after alkali treatment with different duration. SEM images show that there were visible impurities on the fiber surface of JY which related to the presence of natural waxes, lignin, and hemicellulose. Alkali surface treatment removed above impurities and improved the fiber surface smoothness [209]. In addition, the surface of jute fiber exhibited grooved and folded appearances after alkali treatment, as similarly observed by other researchers [215]. Impurities (hemicellulose, lignin, glue, etc) are sensitive to alkali solutions and could be readily removed during alkali treatment, which caused fibrillation of individual fibers within the yarn. These changes in morphology indicated that chemical solution can effectively improve the surface properties of JYs.

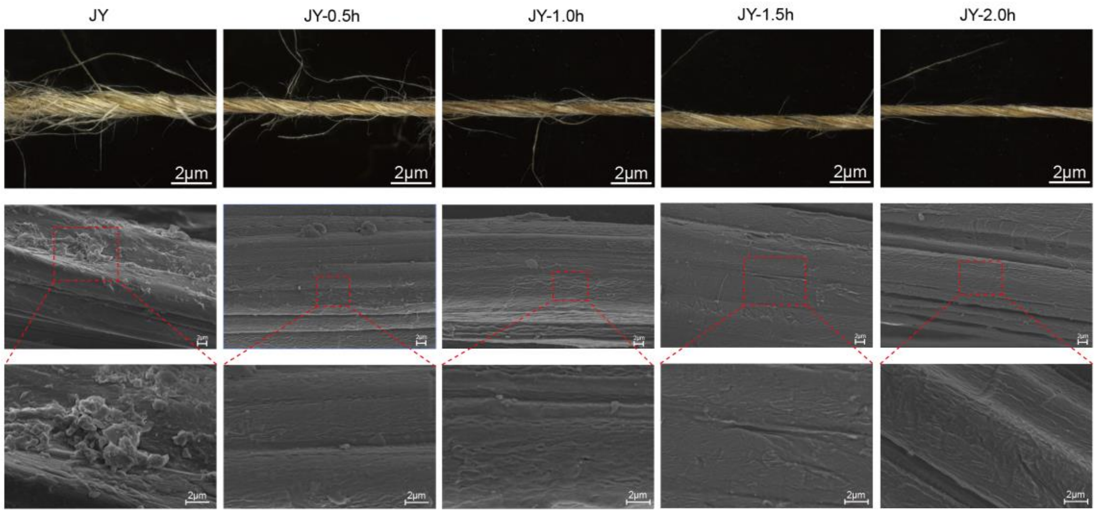

Figure 3-3 Optical and SEM micrograph of untreated and treated JY.

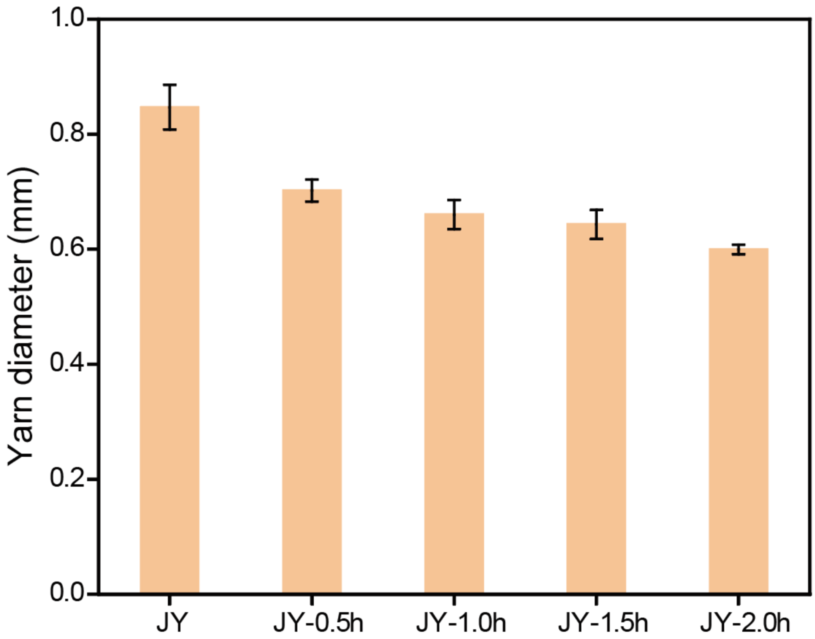

Figure 3-4 Yarn diameter of untreated and treated JYs.

3.3.2 FTIR analyses of JYs

FTIR spectra confirm the functional groups and chemical structure changes of JYs treated with alkali solution. Figure 3-5 shows the FTIR spectra of JYs both before and after treatment with different durations. All the JYs exhibited a similar pattern with key absorption bands corresponding to the primary components of jute fibers, including cellulose, hemicellulose, and lignin. The peak observed at 3430 cm^{-1} corresponds to O-H stretching vibration of cellulose and hemicellulose [216]. Similar broad double bands at 2922 and 2850 cm^{-1}, primarily attributed to stretching of $-CH_3$ and $-CH_2$ groups in cellulose [217, 218]. The peak at around 1742 cm^{-1} corresponds to the C=O stretching associated with pectin, waxes, and hemicellulose [219]. The peak observed at 1593 cm^{-1} represents the C=C stretching vibrations in lignin [220], which contribute to the structural rigidity of plant cell walls. The absorption band at 1156 cm^{-1} is attributed to the C–O–C asymmetric stretching of glycosidic linkages in cellulose and hemicellulose, indicating the presence of polysaccharide structures [221]. Meanwhile, the peak at 1027

cm^{-1} corresponds to the C–O stretching vibrations in cellulose, hemicellulose, and lignin, reflecting the complex network of oxygen-containing functional groups in jute fibers.

Comparing the FTIR spectra of untreated and treated JYs, the intensity of the double peaks at 2922 cm^{-1} and 2850 cm^{-1} significantly increased in the treated JYs, indicating more cellulose structure exposed in the JYs after treatment due to effectiveness of degumming process in impurities removal. Similarly, the peak intensity at 1156 cm^{-1} increased, reflecting the increased presence of cellulose as lignin and hemicellulose were removed. Conversely, with the alkali treatment time increased, the peak intensity at 1593 cm^{-1} gradually decreased, indicating the progressive degradation or removal of lignin [222]. The above changes of spectral confirm the effectiveness of chemical treatment in selectively eliminating impurities while preserving and exposing more of the cellulose framework in jute fibers.

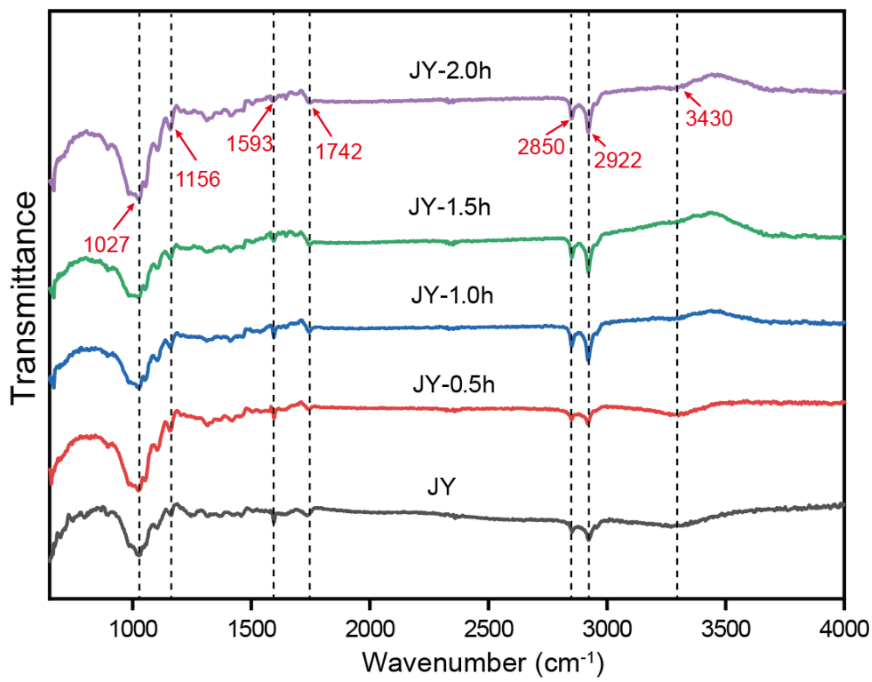

Figure 3-5 FTIR spectra of JYs before and after alkali treatment.

3.3.3 Weight loss and residual gum content of JYs

The weight loss and residual gum content of JYs were measured to assess the effectiveness of alkali degumming. Figure 3-6a shows the weight loss of JYs subjected to alkali treatment for varying durations. As the alkali treatment duration increased, a significant reduction in yarn mass was observed. JY-2.0h exhibited a 16.7 % weight loss compared with JY, indicating the effective removal of impurities such as pectin, hemicellulose, and lignin, which contribute to the overall mass of the yarn. Meanwhile, the experiment analysis of residual gum content further demonstrated the gradual removal of non-cellulose components, as shown in Figure 3-6b. Specifically, the gum content of JY was 32.8 %, and after alkali treatment, it significantly decreased to 22.3 % in JY-2.0h. This reduction highlights the effectiveness of the degumming process in removing non-cellulosic components, contributing to improved fiber purity and structure.

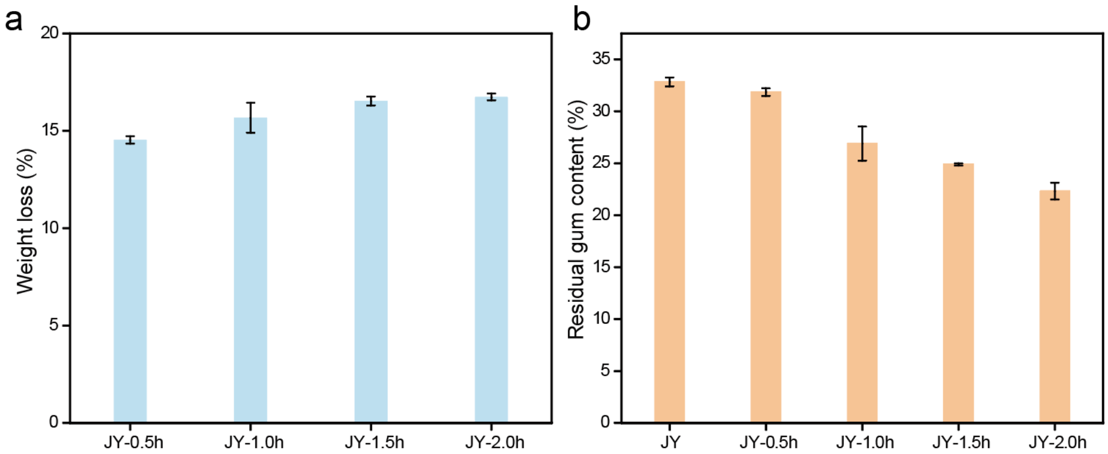

Figure 3-6 (a)Weight loss and (b) residual gum content of JYs after treatment with different durations.

3.3.4 Thermal and mechanical analysis of JYs

The discernible influence of JYs with distinct alkali treatment durations can be evident in the thermogram. This thermogram, recorded at a heating rate of 15 °C/min, is illustrated in Figure 3-7. The initial mass loss of all samples occurred around 100 °C (Figure 3-7a), primarily attributed to the evaporation loss of water content [223]. The degradation weight loss of JYs both before and after treatment was observed around 296.5 °C and 311.6 °C, respectively. primarily due to the decomposition of hemicellulose, the breaking of cellulosic glycosidic bonds, and the cleavage of α and β ether bonds in lignin [224, 225]. The DSC results shown in Figure 3-7b align well with the TGA findings. The small endothermal peaks appeared in the temperature range of 100 – 150 °C, mainly due to the dehydration of absorbed water from the intercellular region of the fibers [226]. The thermal decomposition temperature of JYs increased from 349.4 ℃ to 368.7 ℃ after alkali treatment with duration ranged from 0 h to 2.0 h. The increased degradation temperature was attributed to the removal of non-cellulosic components, such as hemicellulose and a portion of lignin, which further enhanced the thermal stability of JYs. Compared to non-cellulosic components, the thermal degradation of cellulose, which is more exposed after treatment, is influenced by its crystallinity and typically occurs at higher temperatures. These results together confirm that alkali treatment is an effective method of removal easily hydrolysable substances including hemicellulose and lignin to improve the thermal stability of JYs.

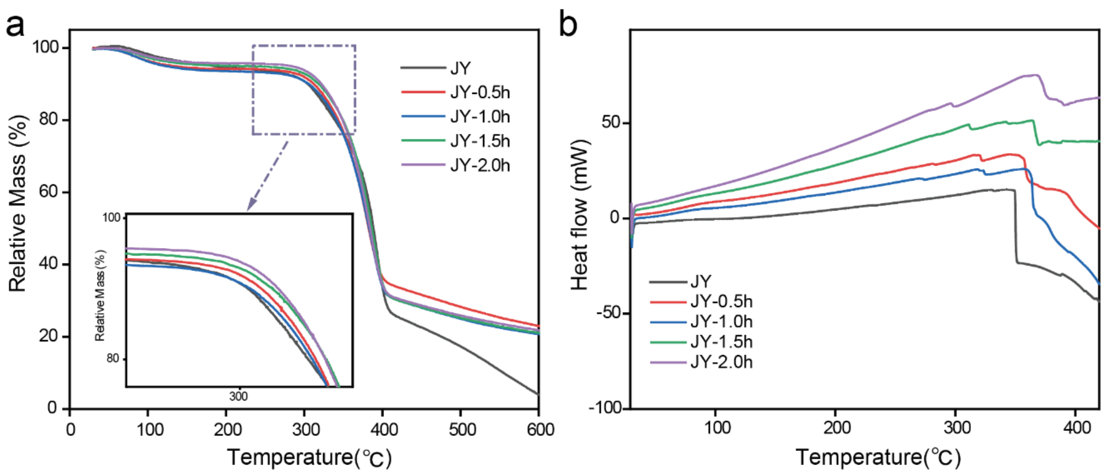

Figure 3-7 TGA (a) and DSC (b) curves of JY both before and after treatment.

To analyze the tensile behavior of JYs before and after treatments, yarn tensile test was conducted using Instron machine. Figure 3-8 illustrates stress-strain curves, the tensile strength of JYs treatment with alkali solution in varying times. From Figure 3-8a, an increase in tensile stress and strain of JYs was observed after alkali treatment. JY exhibited a relatively lower tensile strength of 69.5 MPa and a tensile strain of 2.2 %, which is similar with previous studies [227, 228]. These lower mechanical properties are primarily attributed to the inherent brittleness of jute fibers, the presence of non-cellulosic components such as hemicellulose and lignin, and the natural irregularities in fiber structure. Compared with JY, JY-2.0h showed a 25.4 % increase of tensile strength with an increase of strain at ultimate strength of 17.1 %, which may be due to the improvement in the packing order of cellulose chains. Alkali solutions are commonly used to remove impurities from fiber surfaces and eliminate hemicellulose from the interfibrillar region, resulting in excessive fibrillation and improved fiber packing order. It can be seen from Figure 3-8b that the tensile strength of JY samples increased as the treatment time increased. Among them, JY-2.0h sample presented superior tensile strength with values around 95.4 MPa. Under tensile loading, the elementary fibers within the JYs realign and orient themselves parallel to the yarn's length. Alkali treatment reduced the spiral structure of cellulose microfibrils, promoting the rearrangement of cellulose chains and enhancing fiber packing. This structural modification alleviated internal stress, ultimately improving both strength and elongation.

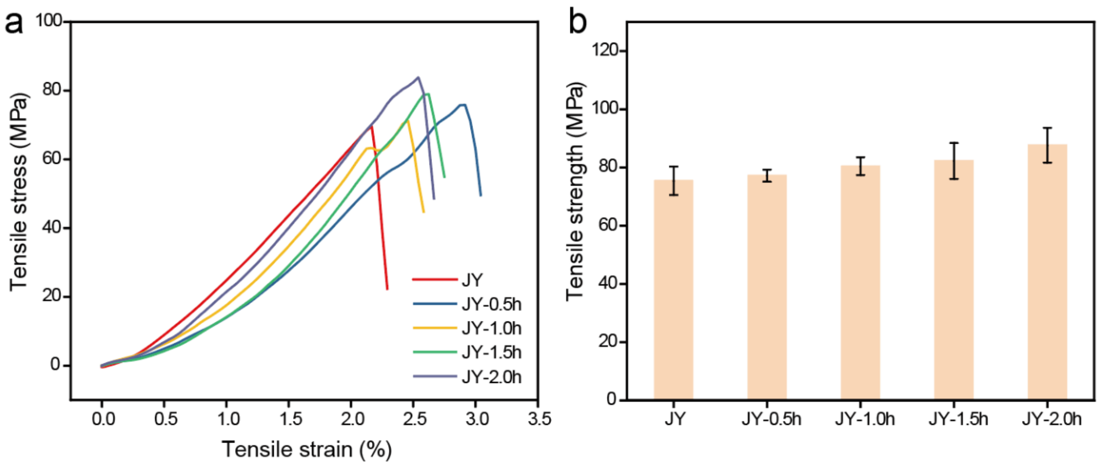

Figure 3-8 Stress-strain curve (a) and tensile strength (b) of JY both before and after treatment.

3.3.5 Water absorption performance of JYs

The interaction between alkali-treated JYs and water can be explained as a competition between the hydroxyl groups (mainly from cellulose and non-cellulosic components such as hemicellulose and lignin) for hydrogen bonds formation with the water molecules or water clusters [207]. Water penetrates into the fiber, disrupting secondary interactions between cellulose macromolecules, which are then adsorbed into the fiber via hydrogen bonding, resulting in fiber swelling [229], as shown in Figure 3-9.

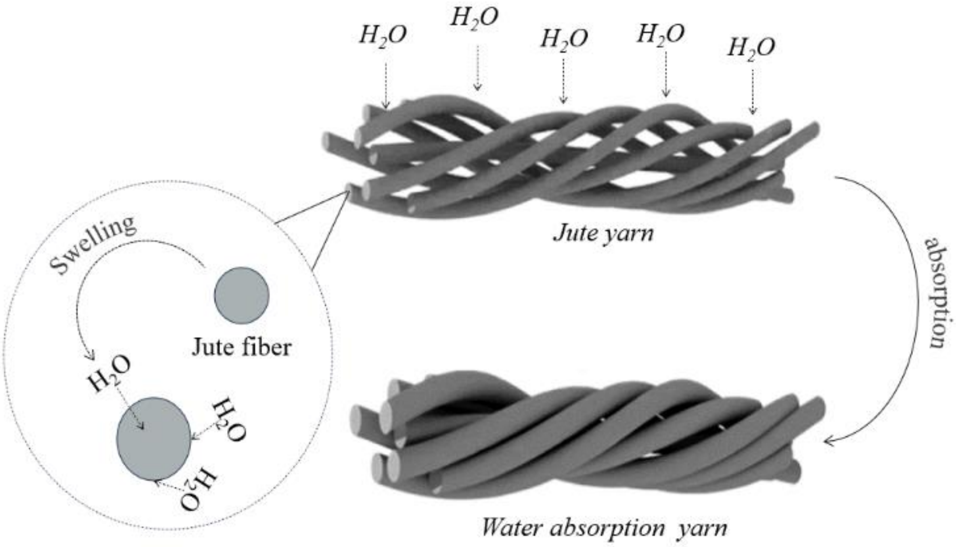

Figure 3-9 Water absorption behavior of JYs.

Figure 3-10 shows the water absorption of different JYs. JY sample exhibited the absorption rate of 79.5 %. The alkali treatment considerably increased the water absorption rate of JYs. It can be observed that the water absorption of alkali-treated JYs increased with longer treatment times. Notably, the JY-2.0h sample exhibited the highest water absorption with a value of 131.3%, which represents a 65.2% increase compared to the JY absorption rate. This significant increase in water absorption can be attributed to the enhanced hydrophilicity of the fibers after alkali treatment. The treatment promotes the removal of non-cellulosic components and disrupts the crystalline structure of cellulose, allowing more water to be absorbed into the fiber. The improved fiber structure and higher surface area facilitate greater interaction between the hydroxyl groups of cellulose and water molecules, leading to the observed swelling and increased water uptake.

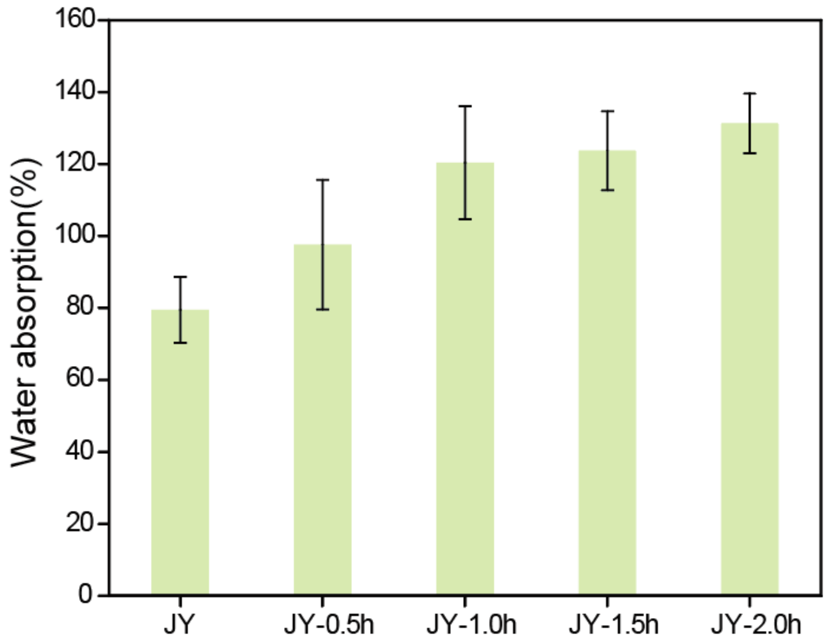

Figure 3-10 Effect of alkali treatment time on water absorption of JYs.

3.4 Conclusion

This study investigated the basic characteristics of jute yarn and examined the effects of alkali treatments with varying durations on the properties of JYs. SEM analysis revealed the removal of impurities, with grooved and folded surface features observed, accompanied by a 30.6 % reduction in yarn diameter. As the treatment duration increased, JY-2.0h showed a 16.7% weight loss and a reduction in gum content from 32.8 % to 22.3 %, enhancing fiber purity and structure. The results of the mechanical performance testing indicate that the JY-2.0h sample achieved the maximum tensile strength of 95.4 MPa, exhibiting a relative increase of 17.1 % compared to JY. The TGA and DSC analyses showed that the thermal stability of alkali-treated jute fibers was improved. The water absorption of jute fibers was improved after alkali solution treatment. Among them, JY-2.0h showed a 65.2 % increase in absorption rate compared to JY.

Chapter 4 Development and Fabrication of Jute/PLA Composites for Sustainable Agricultural Irrigation

4.1 Introduction

Water is fundamental to human development, agricultural production and ecosystem sustainability[230, 231]. However, water scarcity has emerged as a global challenge, particularly in arid and semi-arid regions[232, 233]. Agriculture is a major contributor to water consumption, and the efficient use of water resources is crucial for ensuring food security and fostering sustainable development[234, 235]. Therefore, the implementation of comprehensive and effective water-saving irrigation strategies is essential for the sustainable management of water resources and the enhancement of crop yields. Drip irrigation technology is currently regarded as one of the most effective water-saving methods and has gained widespread adoption worldwide[236-238]. The global agricultural drip irrigation pipe market was valued at USD 63 million in 2023 and is projected to grow at an annual rate of 11.8% by 2030 [239]. Drip irrigation technologies significantly enhance the efficiency of water usage in irrigation, leading to notable improvements in crop yields [240, 241]. However, traditional materials used in drip irrigation systems, such as rubber, plastic and PVC, contribute to significant environmental pollution due to their difficulty in being recycled at the end of their lifespan[242, 243]. Consequently, there is an urgent need to develop and implement sustainable, water-saving irrigation strategies that not only conserve water but also minimize environmental impact.

Natural fiber reinforced composites, as a new type of environmentally friendly material, have attracted much attention as a substitute for traditional metal and plastic materials due to their good biodegradability, renewability and low cost [244, 245]. Chatterjee et al.[246] investigated the tensile properties and thermal behavior of the jute fiber-reinforced PP composites. Results showed that the mechanical properties of the composites improve up to two plies and then deteriorate. Jute/PP composites show potential for applications in the automotive industry and building components. Zolfakkar et al.[247] investigated the mechanical properties and erosion resistance of natural fiber-reinforced epoxy composites with natural fibers (flax, jute, and luffa). The results show that jute-epoxy composites exhibited superior tensile and flexural strength, as well as erosion resistance, highlighting the potential for various applications due to their high strength and durability. You et al.[248] presented a method for making wood fiber/polyamide composites by removing hemicellulose from wood fibers through hydrothermal pretreatment. This process enhanced the mechanical strength and thermal stability of the composites without the need for chemical additives. The resulting composites exhibited high flexural strength and thermal stability while maintaining low density, making them suitable for a range of lightweight, high-strength engineering applications. The main applications of natural fiber-reinforced composites are focused on the automotive industry, as well as their use in construction and consumer products[249, 250].

To date, reports on the use of natural fiber-reinforced composites in sustainable agricultural applications have remained relatively limited. Additionally, the non-degradability of polyolefins (e.g., PP and PE), PVC, and polyamides, which are commonly used in natural fiber composites[251], limits their potential as sustainable agricultural materials. Therefore, the development of green fiber-reinforced composites with good mechanical properties, controlled leakage, degradability and sustainability for agricultural irrigation through the use of innovative structural designs, environmentally friendly materials and sustainable manufacturing techniques is clearly not yet fulfilled.

Herein, a kind of green jute fiber-reinforced PLA composite (JFPC) pipes based on abundant and eco-friendly jute fiber and PLA was proposed. The JFPC is tailored for water-saving seepage irrigation without chemical use, achieving sustainable agricultural irrigation management (Figure 4-1a). Jute fiber and PLA are chosen to construct the JFPCs with sandwich structure as they are eco-friendly and abundant availability [252] (Figure 4-1b). Raw jute fiber is derived from cellulosic material found in plant stems, while PLA is a biodegradable polymer derived from renewable plant starches. Both materials can biodegrade after use without causing pollution [253-255]. Through optimizing the porosity through the adjustment of PLA content, JFPC not only exhibits enhanced mechanical properties and thermal stability but also effectively regulates water seepage rate. In addition, traditional drip irrigation typically follows a single circular diffusion pattern[256, 257], whereas the proposed irrigation design generates multi-sector circular diffusion, enhancing water resource utilization efficiency by increasing horizontal spread and reducing deep water leakage (Figure 4-1c). The synergistic effect of these properties of JFPCs has led to significant results in sustainable irrigation management, further enhancing their potential for agricultural applications.

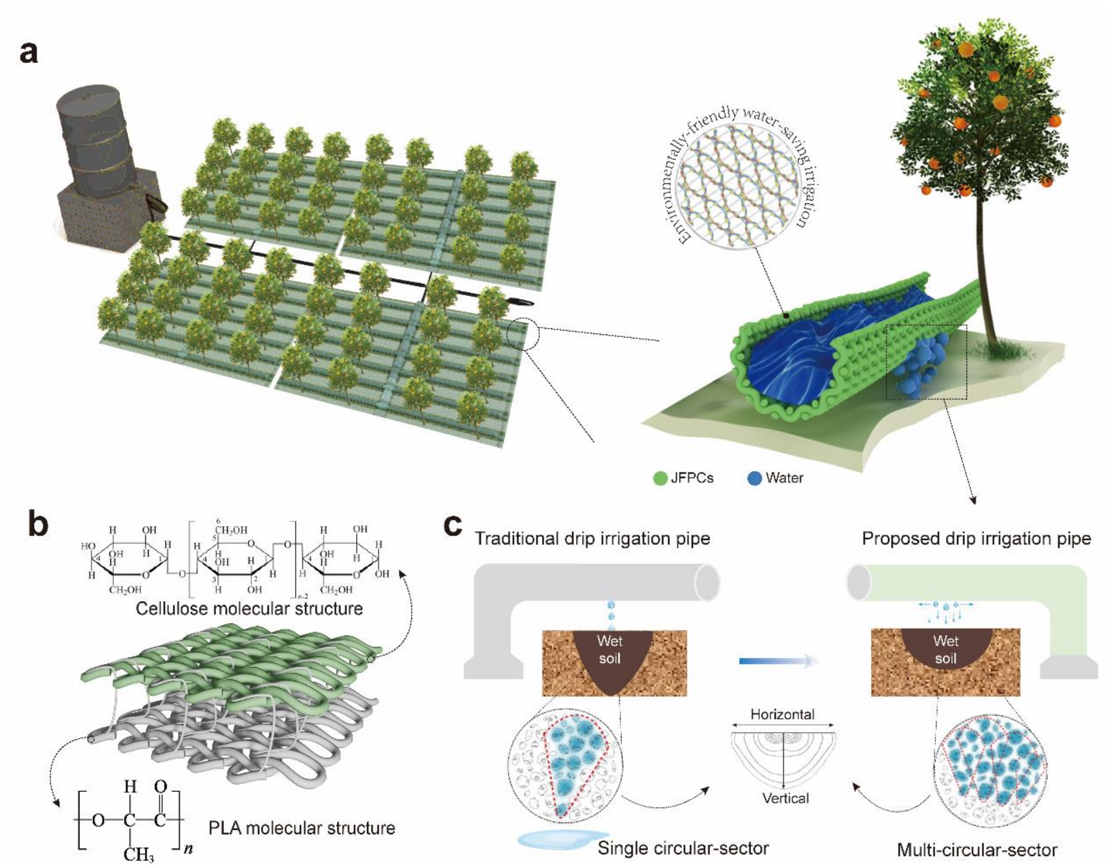

Figure 4-1 Schematic and working mechanism of the JFPC for sustainable water-saving management. (a) Schematic illustration of the JFPC pipe application. (b) Raw materials used to fabricate JFPCs with sandwich structure. (c) Comparison of soil moisture movement patterns under traditional drip irrigation pipe or proposed drip irrigation pipe.

4.2 Experimental Section

4.2.1 Material

PLA filament (150D, 1.25 g/cm^3) was supplied by HI-TECH Fiber Group Corporation. Jute yarn (8lbs, 1.45 g/cm^3) was obtained from Anji Zhenxing Lianma Spinning and Weaving Co., Ltd. These materials were directly used to prepare the composites without undergoing any additional processing.

4.2.2 Preparation of JFPCs and the JFPC pipes

JFPCs were developed using PLA filaments and jute yarns due to their inherent durability and biodegradability (Figure 4-2a). Different finenesses of PLA yarns obtained using the pre-doubling technique (Figure 4-2b) were used to optimize the structural integrity and porosity of JFPCs. A sandwich structure was selected for the fabric fabrication shown in Figure 4-2c on CMS530 automatic flat knitting machine from STOLL (Reutlingen, Germany). The knitting density of fabrics was adjusted through pre-tests and finalized at 12.5G to ensure a uniform and compact yarn arrangement which is essential for the performance of the final composite. The distinct surface functionalities were achieved through a sandwich structure comprising jute on one side and PLA on the other (Figure 4-2d). The jute layer provides mechanical reinforcement and surface protection, while the PLA film enables controllable water seepage by regulating its porosity. This bilayer design allows precise tuning of water-seepage performance without compromising the overall strength and flexibility of the composite.

After knitting the composite fabric, JFPCs were oven-dried to remove moisture and then hot-pressed between Polytetrafluoroethylene (PTFE) films to prevent impurities and facilitate demolding (Figure 4-2e). Based on preliminary optimization trials, the hot-pressing parameters were set at 190 °C under 3 MPa for 2 minutes (Table 4-1), which provided adequate consolidation without thermal degradation. After hot pressing, the composites were allowed to cool naturally before removal in the equipment to room temperature with a cooling duration of 1h. The fabricated JFPCs (Figure 4-2f and detailed parameters shown in Table 4-1) were cut into required dimensions for different mechanical and other related tests.

Additionally, the pipe samples were fabricated for seepage rate testing (Figure 4-2g).

Steel tubes used mandrels to fabricate the JFPC pipes, with the hot-pressed fabric swiftly removed from the mold and tightly wrapped around the tube. The application of mold release agents significantly facilitated the removal of the JFPC pipes from the mandrel. The fabric wale orientation relative to the pipe axis was set at θ = 90°. The joints were bonded using PLA material to form a continuous tubular structure. The specimens were then consolidated by curing at room temperature for 10 days, after which the pipes were easily demolded.

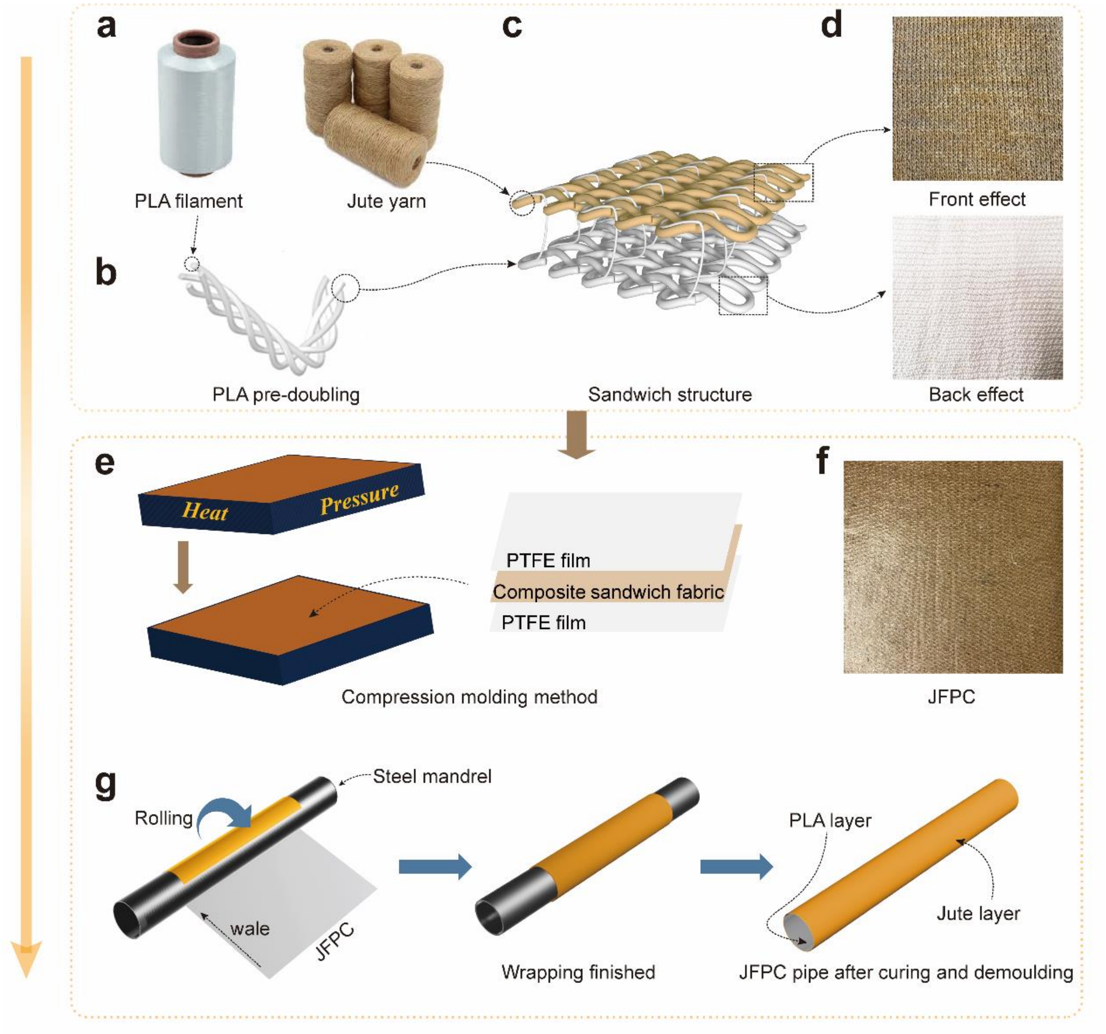

Figure 4-2 Fabrication process of JFPCs and JFPC pipes. (a) Fabrication materials. Jute yarn, a low-cost natural yarn with good mechanical properties, was used as a protective

layer. PLA filaments, with excellent water repellency and biodegradable properties, were used as the water-blocking layer of the composites. (b) Pre-doubling technique for PLA yarn. (c) Sandwich structure. (d) Front and back effect of composite fabric. (e) Compression molding method used to prepare JFPCs. (f) An actual photograph of JFPCs. (g) Manufacturing process of JFPC pipe specimens.

Table 4-1 The parameters of different samples.

Code	Material	Yarn count (Tex)		Weight ratio of PLA (%)	Weight (g/m^2)	Thickness (mm)
		Jute yarn	PLA			
JF	Jute yarn		-	-	408.25	2.36
JFPC -2	Jute yarn & PLA	280.72	33.14	12.18	414.75	1.90
JFPC -4			67.86	21.99	523.25	1.93
JFPC -6			102.95	27.18	560.75	2.05
JFPC -8			138.78	34.39	622.25	2.12
JFPC-10			171.10	40.77	689.25	2.24

JF: jute fabric; JFPC: jute fabric-reinforced PLA composite. JFPC-X refers to JFPCs with varying PLA content, where X indicates the number of PLA yarns used in the pre-doubling process before hot pressing (JFPC-2, JFPC-4, JFPC-6, etc.).

4.2.3 Characterization

The surface morphologies of jute fabric and JFPCs were observed under a Leica DM2500 light-emitting diode optical microscope.

The pore size distribution and maximum pore diameter of fabrics were measured using a capillary flow porometer (CFP 1500, PMI, USA). Before testing, the samples were fully saturated with isopropanol to ensure complete filling of the pores. During the measurement, the sample was placed in the test chamber, and a controlled air pressure was gradually applied to displace the liquid from the pores. The pore diameter (D) was measured three times for each sample, which was calculated using the equation (4-1):

$$D = 4\gamma cos\theta / P \tag{4-1}$$

Where γ is the surface tension of isopropanol, θ is the contact angle, and P is the pressure required to expel the liquid from the pore.

FTIR spectra of JF and JFPCs were conducted by a Vertex 70 FTIR spectrometer (Bruker, United States) with a resolution of 4 cm^{-1}, covering the wavenumber range of 600–4000 cm^{-1}. Each sample was conducted three times to ensure consistency.

Thermogravimetric analysis (TGA) and differential scanning calorimetry (DSC) was employed to examine thermal properties of JFs and JFPCs, which is essential for materials durability under fluctuating outdoor temperatures. A TGA4000 instrument (PerkinElmer, United States) was using to measure the weight change of various samples within temperature increased from 30 °C to 600 °C at a heating rate of

20 °C/min and a nitrogen flush rate of 20 ml/min. DSC analyses were conducted by a DSC8000 thermal analyzer (PerkinElmer, United States) within temperature increased from 30 °C to 500 °C at a heating rate of 20 °C/min and a nitrogen flow rate of 50 ml/min. Each characterization test was conducted three times to guarantee the reliability of the results.

Mechanical property tests were conducted to evaluate the structure strength to ensure suitability for agricultural use. The tensile performances of JFPCs were tested using an electronic universal testing machine (Instron 5566, United States) according to ASTM D3039 standard. The three-point flexural test was performed following the GBT1449-2005 standard using the same machine at a testing speed of 2 mm/min. Standard sample strips measuring 50 mm * 25 mm were prepared for testing. The ball bursting experiment was conducted in compliance with the GB/T19976-2005 standard. The bursting strength test was carried out using the Instron 5566 (Instron, United States) with a 25 mm diameter spherical plunger at a speed of 300 mm/min. The tearing test was performed using the Instron 5566, with the initial jaw separation of the upper and lower grippers set to 100 mm in accordance with the HG/T2581.1-2009 standard. Prior to the experimental tests, the specimens were humidified under standard atmospheric conditions. Each property was measured five times, and the mean value of these measurements was taken.

Seepage performance tests assessed the controlled water seepage behavior, which is essential for efficient seepage irrigation systems. A water flow control and measurement system was designed to test the seepage performance of the JFPC pipe (Figure 4-3). The system was divided into four parts, including water supply system, flow stabilization system, water collection system and water level height test system. The water flow passed through a horizontally placed composite pipe at a fixed velocity, and then the water leakage volume was recorded and measured by a vertically placed water level height sensor inside the test container. The pipe sample with a length of 20 cm was installed in the container. The seepage rate of JFPC pipes was measured and recorded for two-minute after stabilizing the water flow at a constant rate of 1.2 L/min.

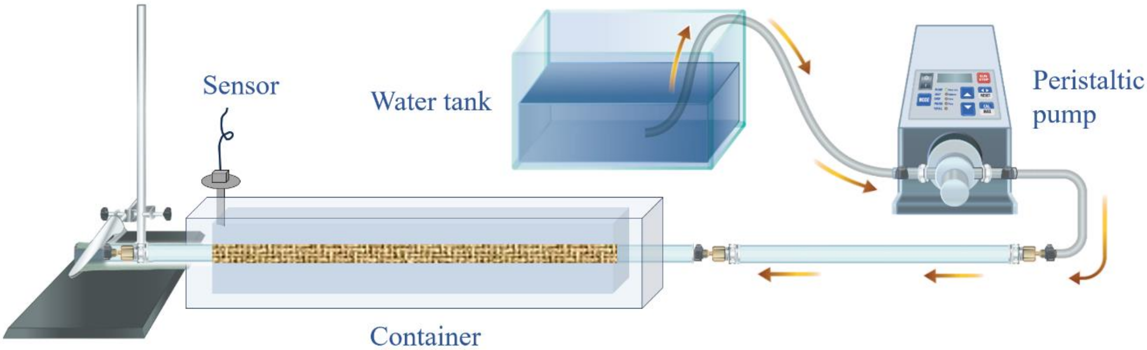

Figure 4-3 Schematic of water control and measurement system of JFPC pipes.

Biodegradation tests were conducted to verify the environmental compatibility of the materials after their service life, aligning with the goal of reducing plastic waste in agriculture. Biodegradation tests on JFPCs were conducted through outdoor soil burial in the Hong Kong Polytechnic University, Hong Kong, China (114.1795° E, 22.3051° N), where was loamy soil with a pH of 6.2. Rectangular specimens (5 cm * 5 cm) were placed in yarn nets (6 cm * 6 cm) for ease of sampling and buried approximately 15 cm below the soil surface. Samples were collected from the soil every 30 days, gently cleaned using distilled water, and then dried at 50 °C to a constant weight. Dry samples were photographed and measured the weight loss to evaluate the biodegradability of JFPCs. The experiment was conducted three times, and the average value of the measurements was calculated. Weight loss is calculated using the equation (4-2):

$$W_l = \frac{W_i - W_e}{W_i} \times 100\% \quad (4\text{-}2)$$

Where, W_l is the weight loss of JFPCs after degradation (%); W_i is the initial weight and W_e refers to the final fabric weight after degradation, g.

4.3 Result and Discussion

4.3.1 Design, fabrication and characterizations of JFPCs

The schematic diagrams of JFPCs and pipes fabrication are shown in Figure 4-2. JFPCs were developed using coarser jute yarns and PLA. The sandwich structure was selected for the fabric fabrication to design with a distinct functional surface effect. The outer jute layer provided reinforcement and surface protection, enhancing durability under agricultural conditions, while the inner PLA layer allowed for porosity adjustment to control water seepage behavior. This design enabled a balance between durability and controllable seepage performance, meeting the practical demands of agricultural irrigation systems.

The surface morphology and pore size of the JFPCs were observed using an optical microscope. Figure 4-4a shows that there are obvious surface differences in the composites with different PLA contents. The surface of the JF exhibited numerous fabric and yarn pores, along with abundant fine pores and surface hairiness. After heat treatment, a PLA film was observed on the surface of the JFPC. As the PLA mass proportion increased, the surface of the composite became smoother and more uniform, with a gradual reduction in pore size, eventually leading to the complete disappearance of pores. The change in surface morphology, particularly the reduction in pore size, is evidenced by the measurements of pore diameter. As depicted in Figure 4-4b, JF exhibited the largest average pore diameter of 162.8 μm. With increasing PLA content, the pore structure of JFPCs changed significantly. The average pore size progressively decreased from 135.4 μm in JFPC-2 to 32.1 μm in JFPC-10, indicating that the PLA matrix effectively filled the fabric pores. Moreover, the minimum standard deviation of pore size decreased by 88.4% compared with that of JF, suggesting improved uniformity in pore distribution. These results together confirmed that the higher PLA matrix contributed to the formation of smaller and more uniform pores of composite fabric.

As shown in the FTIR spectra (Figure 4-4c), the characteristic peaks corresponding to main components in jute fibers (cellulose, hemicellulose, and lignin) were observed, including O-H stretching vibration at 3,200~3,600 cm^{-1} [258], C-H stretching at around 2893 cm^{-1} [259]. The FTIR spectra of the JFPC samples exhibited characteristic features confirming the incorporation of PLA. A broad peak appeared around 2800-3000 cm^{-1} corresponding to the C-H stretching vibrations from CH_3 and CH_2 groups from PLA [166, 260]. C=O stretching vibration in hemicelluloses, pectin and waxes were shown at 1738 cm^{-1} [261]. The C=O band became more pronounced and shifted to slightly higher wavenumbers at 1784 cm^{-1} with increasing PLA content, indicating enhanced carbonyl presence. The distinct peak at 1263 cm^{-1} could be assigned to O-C stretching of carboxylic acid groups and their derivatives [262]. Additionally, the presence of PLA was also confirmed by the bands at around 1142 cm^{-1} (C-O-C stretching vibration) [263]. These bands were completely absent in the FTIR spectra of pure jute fibers. No additional chemical interaction occurred during composite formation, which is in correspondence with the literature.

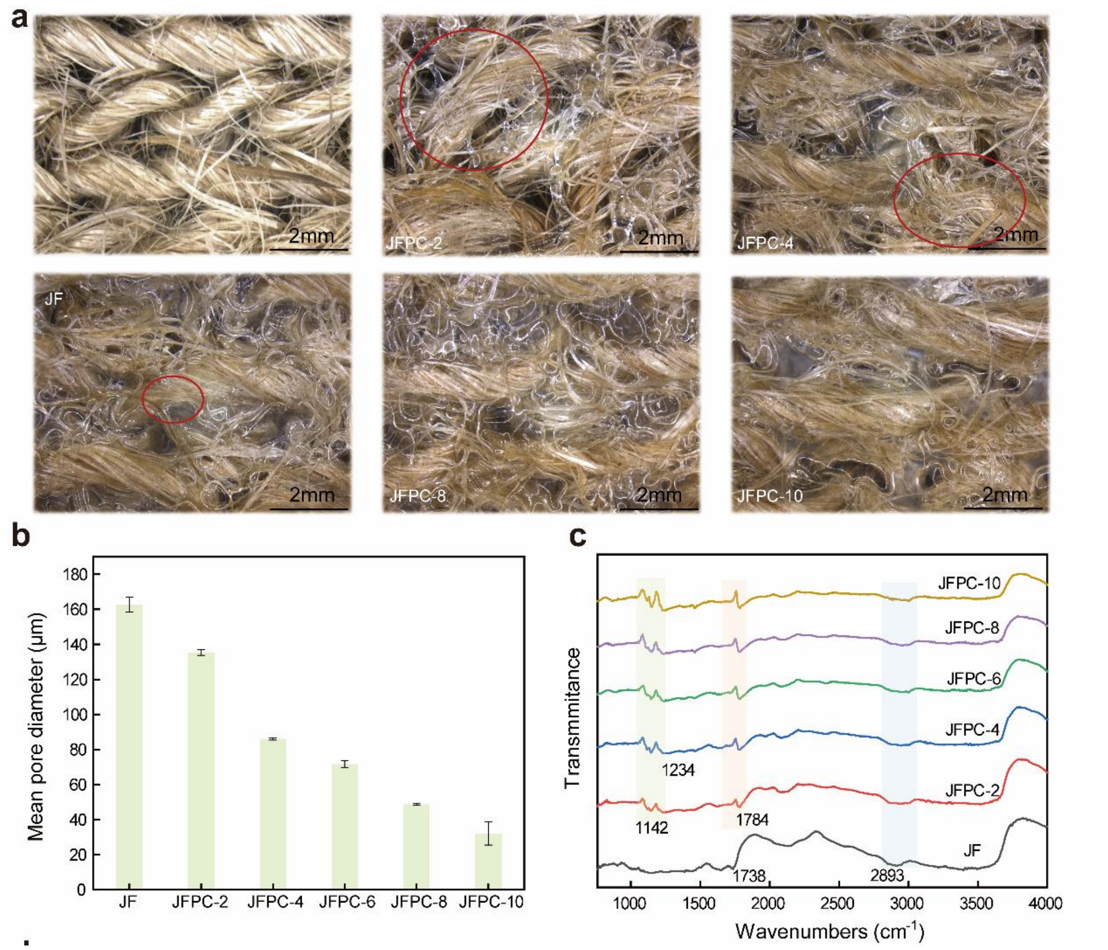

Figure 4-4 Basic morphological and chemical characterizations. (a)Surface images of jute fabric (JF) and jute fiber-reinforced PLA composites (JFPCs). Scale bar: 2 mm. (b) Pore diameter. (c) FTIR spectra of different samples.

4.3.2 Thermal stability analysis of JFPCs

The thermal behavior of JFPCs with varying PLA contents is illustrated by the thermograms (Figure 4-5). All samples exhibited an initial mass loss around 100 °C, primarily due to the moisture evaporation associated with the hydrophilic nature of jute fibers [264]. The main decomposition occurred between 300 °C and 380 °C (Figure 4-5a), corresponding to the thermal depolymerization of cellulose glycosidic bonds and the decomposition of the PLA molecules [265]. Pure PLA showed a degradation onset at

334.4 °C, followed by a rapid thermal decomposition resulting in negligible residue. The degradation temperature of JFPCs increased progressively with the higher PLA content, indicating improved thermal stability consistent with the study conducted by Sang et al [266]. The improved thermal stability can positively affect durability of pipes under fluctuating environmental temperatures and prolonged exposure to sunlight, which may induce localized heating.

The DSC results showed a shift in the melting temperature of JFPCs (Figure 4-5b). This is primarily attributed to the improved crystallization behavior of PLA due to the incorporation of jute fibers [267, 268]. Pure PLA showed two distinct melting peaks at 172.81 °C and 178.18 °C, related to crystallization and recrystallization processes [269, 270]. In contrast, JFPCs exhibited a single, broadened melting peak between 170~180 °C, with intensity increasing with PLA content. This shift indicates a more uniform crystalline morphology within the composites, which is beneficial for enhancing the thermal resistance and dimensional stability of the pipes under agricultural field conditions.

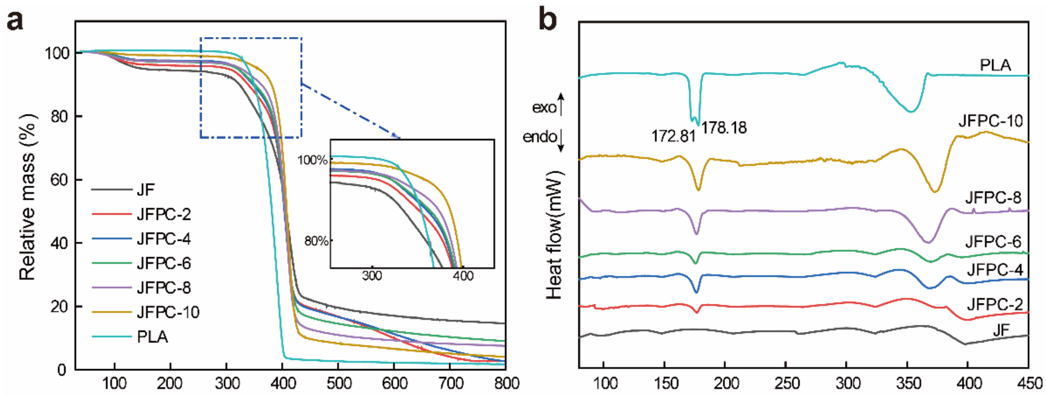

Figure 4-5 Thermal properties (a) TGA and (b) DSC curves of JF and JFPCs with different content of PLA.

4.3.3 Mechanical analysis of JFPCs

The mechanical fracture processes are shown in Figure 4-6. The JFPCs shown in Figure 4-6I initially exhibited elastic deformation under tensile loading. However, as tensile loading continued, the PLA matrix in the composites experienced crack initiation due to the brittleness of JFPCs, as illustrated in Figure 4-6II. With further tensile loading, these cracks propagated along the tensile direction (Figure 4-6III), leading to progressive debonding at the interface and the fracture of the most vulnerable jute fibers. At the sites of major cracks, the JF acted as the primary load-bearing structure. As depicted in Figure 4-6IV and Figure 4-6V, the jute yarn was stretched along the direction of the knitted coil, ultimately resulting in complete fracture failure under continued tensile stress. This behavior followed a typical fiber damage pattern, where weaker fibers fractured randomly, and the load initially borne by these broken fibers was transferred to the remaining intact fibers.

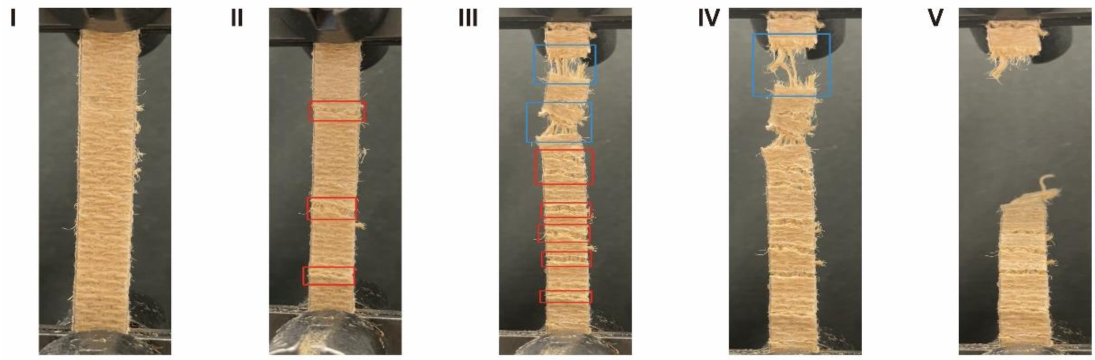

Figure 4-6 Tensile fracture process of JFPCs.

Figure 4-7 presents the mechanical performance of JFPCs with different PLA content, including tensile, flexural, bursting and tear strength and the modulus was calculated based on the tensile strength to characterize the stiffness and load-bearing capacity of the composites. The significance differences between PLA content and mechanical strengths were evaluated using one-way analysis of variance (ANOVA), with Tukey's test applied post-hoc to identify specific differences at a 5% significance level. The ANOVA results revealed that the PLA content had a significant effect on the mechanical strength of the composites ($p < 0.05$), including tensile strength, flexural strength, bursting strength and tearing strength. Post-hoc analysis further revealed the specific pairwise differences among the groups, with letter groupings above the bars to clarify the significance of differences.

Tensile strength of JFPCs with higher PLA content exhibited a significant increase compared with that of lower PLA content (Figure 4-7a). JFPC-10 exhibited highest tensile strength and modulus of 3.1 MPa and 11.3 MPa, respectively. This significant enhancement ($p < 0.05$) can be attributed to the formation of a continuous PLA matrix that effectively facilitated stress transfer between the jute fibers and the polymer matrix, thereby reinforcing the overall mechanical performance of the composite.

Flexural strength (Figure 4-7b) exhibited a more consistent and linear improvement with increasing PLA content. with JFPC-8 reaching a bending strength of 6.7 MPa. Further increases in PLA content led to a decline in the flexural performance of the JFPCs. This reduction is attributed to the increasingly matrix-dominated nature of the composite, wherein the brittleness of PLA reduced the overall flexural resistance.

The bursting strength of fabrics exhibited initially increased before decreasing trend (Figure 4-7c), with a significant increase was observed in JFPC-6 compared to JF. Similarly, tearing strength showed a pattern of initial increase followed by a subsequent decrease with the rise in PLA content as shown in Figure 4-7d. JFPC-4 demonstrated the maximum tearing strength, with a 69.1% improvement over JF, which primarily due to the additional structural reinforcement provided by PLA matrix. Moreover, the tearing failure mode of JFPCs evolved with varying PLA content. Jute fabric-dominated tearing failure manifested as tensile fracture in the wale direction of knitted structure at lower PLA content. With PLA content increasing, improved interfacial adhesion and matrix continuity led to a transition toward a tearing-dominated failure mode.

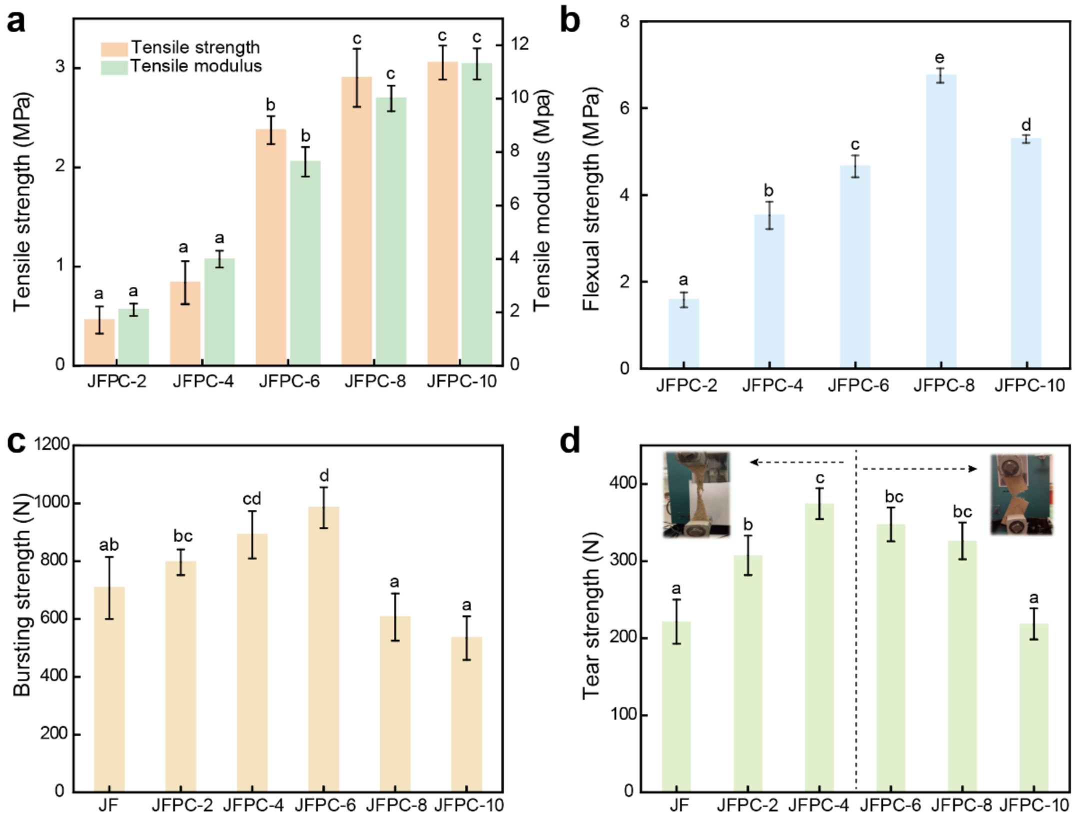

Figure 4-7 Mechanical performance (a) tensile, (b) flexural, (c) bursting and (d) tearing strength of JF and JFPCs with different PLA content. The same letter was used to indicate statistically similar.

4.3.4 Water seepage performance of JFPC pipes

The seepage performance of the JFPC pipes was evaluated by direct seepage measurements through the designed water flow system (Figure 4-3). JFPC pipes of 20 cm length with different PLA contents were placed in the water measurement system and the results were compared with pure jute fabric pipe as a control. The photographs in Figure 4-8a showed the seepage behavior of JF and JFPC pipes. JF pipe, characterized by their abundant porosity, facilitated continuous water penetration through the tube walls, forming a water column under pressure that fully entered the test container. In contrast, the addition of PLA resulted in a reduction of the seepage volume in the JFPC pipes. The water seepage behavior transitioned from an initial columnar flow to droplet leakage, ultimately leading to complete seepage inhibition.

Statistical analysis demonstrated a strong correlation between fabric porosity and seepage rate ($P<0.05$), which explained the significant variation in seepage controllable performance among different fabrics. which explained the significant variation in seepage controllable performance among different fabrics. Variation in PLA loading induced corresponding changes in the porosity of the composite pipes. JFPC pipes with higher porosity (lower PLA content), such as JFPC-2 and JFPC-4, exhibited higher seepage rates. In contrast, JFPC pipes with lower porosity (higher PLA content), as seen in JFPC-6, JFPC-8, and JFPC-10, significantly reduced water seepage and even achieved complete cessation of seepage (100% non-seepage). These results indicated that adjusting PLA content provided a simple and effective means to precisely tune the porosity of pipes and thereby tailor their water seepage performance. This flexibility offered a promising strategy for developing customizable irrigation materials capable of meeting diverse water delivery requirements in agricultural applications.

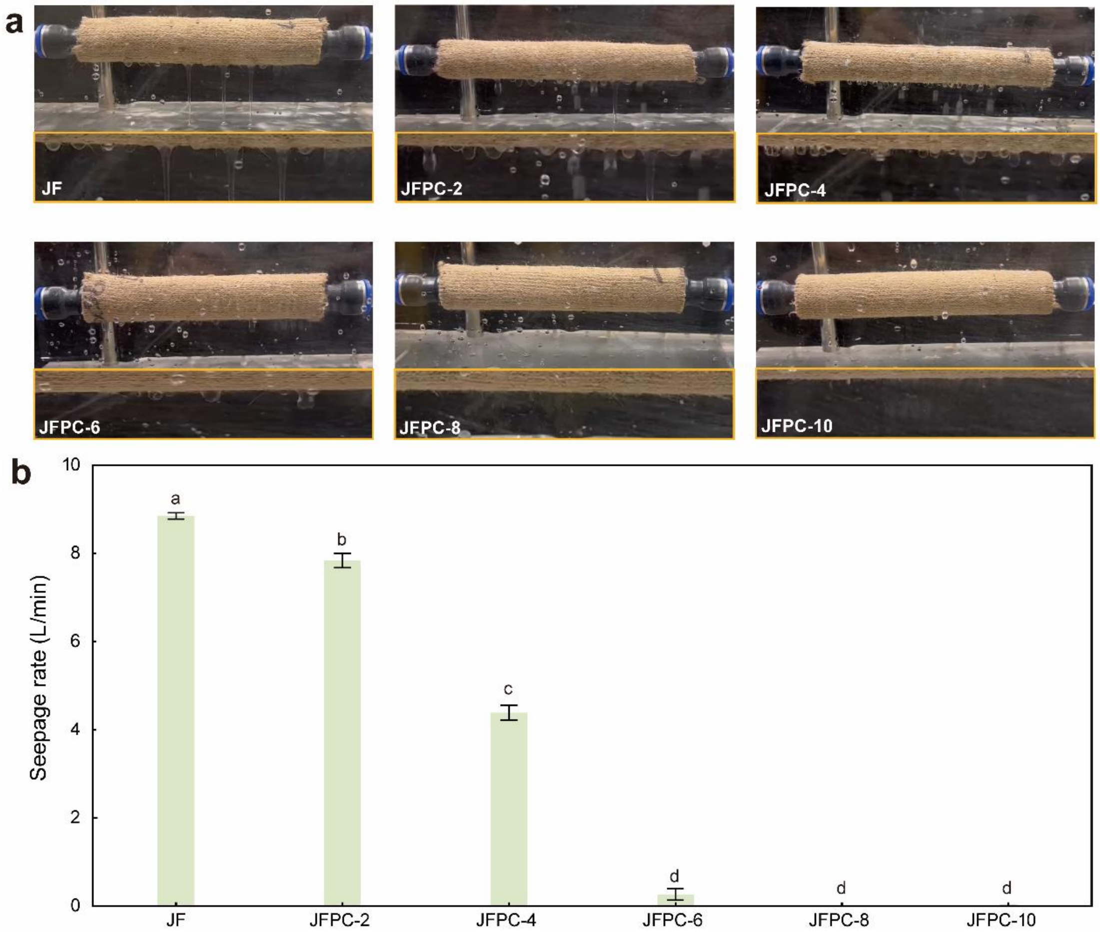

Figure 4-8 Water seepage performance of jute fabric pipe and JFPC pipes. (a) Photographs presenting the water seepage behavior of different fabric pipes. The length of fabric pipes is 20 cm. (b)Water seepage rate of jute fabric and JFPC pipes.

4.3.5 Sustainable and biodegradation of JFPCs

While the characteristics and water seepage of JFPCs have been demonstrated, their environmental impact at the end of life remains an important factor that requires thorough consideration. Figure 4-9a illustrates the production and application stages of JFPCs, beginning with the cultivation of renewable biological sources such as corn/straw and Corchorus plants. Raw materials are often extracted from these renewable resources and spun into filaments and yarns. Composite fabrics are fabricated through knitting or weaving and subsequently processed into pipes via heat molding, curing, and demolding. At the end of their use phase, disposal pathways include landfilling, incineration, mechanical or chemical recycling, composting, or reuse, underscoring efforts toward environmental sustainability [271, 272]. Some previous studies indicated that PLA exhibits a substantially lower carbon footprint as low as 0.5 $kgCO_2/kg$, representing a remarkable 75% reduction compared to most traditional plastics [273, 274]. Therefore, PLA and jute fibers hold potential as sustainable alternatives for fossil-based materials.

The biodegradability of JFPC-2, JFPC-6 and JFPC-10, which represented three different levels of PLA content, was measured in an outdoor soil environment. JFPCs showed noticeable surface discoloration over time caused by mould and mildew growth [117, 275](Figure 4-9b). JFPCs experienced a significant mass reduction after degradation, especially JFPC-2 with 20.2 % weight loss after three months of soil buried (Figure 4-9c). Comparison of the degradation of different JFPCs revealed that increasing PLA content decreased the overall degradation rate. This is primarily attributed to the relative lower biodegradability of PLA compared to jute fibers. As PLA content increased, more jute yarns became encapsulated within the PLA matrix, limiting microbial access to more jute fibers and thereby relatively slowing down the overall degradation process of composites.

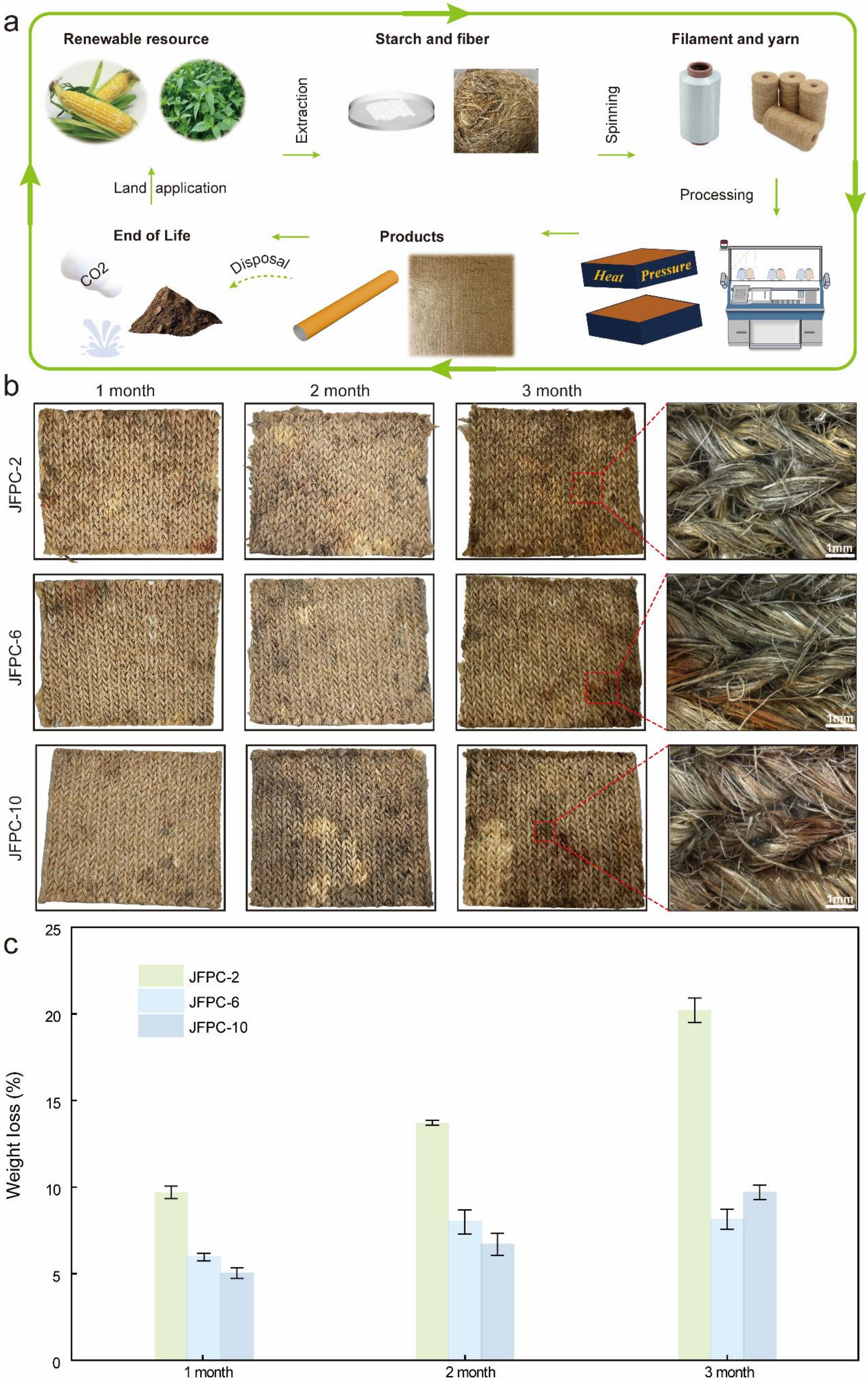
a
Renewable resource
Starch and fiber
Filament and yarn
Extraction
Spinning
Land application
Processing
End of Life
Products
CO2
Disposal
Heat
Pressure
b
1 month
2 month
3 month
JFPC-2
JFPC-6
JFPC-10
1mm
c
JFPC-2
JFPC-6
JFPC-10
Weight loss (%)
0
5
10
15
20
25
1 month
2 month
3 month

Figure 4-9 The sustainable and biodegradability performance of JFPCs. (a) Schematic overview of the raw material sourcing, fabrication, and possible end-of-life pathways of JFPCs. (b) Photographs of JFPCs degradation at different burial durations with discoloration or mildew. (c) Weight loss of the JFPCs after three months degradation..

4.4 Conclusion

In this work, a green jute fiber-reinforced composite was proposed for sustainable controllable irrigation while reducing soil pollution. The key findings include:

- Increasing the PLA content in JFPCs enabled effective pore regulation, significantly reducing average pore size and enhancing the uniformity of the internal structure.
- The thermal analysis demonstrated that increasing PLA content in JFPCs progressively enhanced thermal stability.
- The incorporation of PLA significantly influenced the mechanical behavior of JFPCs, with moderate PLA content enhancing tensile, flexural, bursting, and tearing strengths. However, excessive PLA led to a decline in mechanical resistance owing to matrix brittleness and poor interfacial bonding.
- The seepage experimental results demonstrated that the seepage rate of JFPCs could be precisely adjusted by varying the PLA content.
- JFPCs exhibited a maximum weight loss of 20.2 % after 3 months of soil burial.

Therefore, these results together demonstrated that JFPC pipes hold promise for advancing sustainable agricultural practices by enabling efficient, water-saving seepage irrigation. Given the current experimental limitations, future research will focus on further enhancing the composite mechanical properties to expand their application in high water pressure environments without compromising biodegradability. Moreover, long-term field evaluations will be conducted to fully assess the durability, environmental impact, and practical performance of JFPCs in diverse agricultural applications. These biodegradable natural composites not only reduce reliance on non-renewable materials and water-intensive irrigation methods but also mitigate end-of-life issues associated with conventional plastics. Moreover, this work offers approaches for integrating natural fiber-reinforced composites into agriculture, supporting the wider adoption of sustainable materials.

Chapter 5 Development and Fabrication of Jute Fabrics for Eco-friendly Weed Control and Soil Water Retention

5.1 Introduction

Weeds compete with cultivated plants for essential resources such as nutrients, water, light, and space, and also serve as hosts for plant pathogens that may led to diseases in cultivated crops [276, 277]. Weeds cause huge losses in global crop production [278-280]. Therefore, implementing comprehensive and effective weed control strategies is essential to maintaining healthy crops and ensuring sustainable agricultural practices. Currently, various weed control methods, such as chemical herbicides [281], mechanical weeding [282-284] and biological control [285-287] are widely used to manage weed growth and protect crops [281]. However, these methods have significant limitations [288, 289]. For instance, chemical herbicides can lead to environmental contamination and herbicide resistance [290-294], while mechanical weeding and biological control may not provide long-lasting effect or damage crops [284].

Weed control fabrics (WCFs)—which spontaneously inhibit weed growth by blocking sunlight transmission while simultaneously keeping soil moisture—have opened an important avenue for weed management [295, 296]. Over the past few years, petroleum-based WCFs, such as polyethylene weed control fabric (WCF-PE) and polypropylene weed control fabric (WCF-PP), have been rapidly developed in weed management due to the significant effects in controlling weeds [297, 298]. However, their extensive use has also posed challenges such as microplastic contamination, reduced soil permeability, heat accumulation and difficulties in disposal and recycling [242, 299]. Weed control management should not conflict with the basic needs of environmental protection. Therefore, there is an urgent need to develop sustainable weed control strategies that can significantly control weed cover while minimizing the impact on the soil environment.

The primary mechanism by which WCFs suppress weeds is through physical barrier to blocking weeds upward growth and sunlight deprivation to disrupt weeds photosynthesis [300, 301]. Therefore, the proposed covering material, while providing a basic physical cover, must block almost all sunlight (400-700 nm) that facilities weed photosynthesis. In addition, moderately air permeability of the coverings is needed to transfer heat flow to the surroundings and outer space [302]. This prevents excessive heat accumulation after covering, thereby reducing the risk of soil overheating and potential damage to plant roots [303]. Water permeability ability is also required to prevent root suffocation and waterlogging, ensuring adequate oxygen supply and drainage, which are essential for healthy plant growth and nutrient uptake [299]. In addition, the appropriate porosity design can reduce the evaporation of soil moisture while meeting the above-mentioned water permeability and air permeability functions [304]. Hence, the above primary mulch material properties design enables weed control and water saving, thereby reducing competition for nutrients and ensuring a favorable soil environment for healthy plant growth.

Herein, a kind of WCF based on abundant and eco-friendly jute fiber was demonstrated. The jute weed control fabric (JWCF) is tailored to reduce weed cover and water evaporation without energy consumption, achieving sustainable weed control management. Jute fiber is chosen to construct the WCF as it is eco-friendly and abundant availability. Raw jute fiber is derived from natural lignocellulosic material that exists extensively within plant stems, which can biodegrade after use without any pollution (Figure 5-1a) [253, 254]. Through the coverage and the optimal adjustment of porosity, JWCF not only reduces the transmission of sunlight for inhibiting weed growth, but also effectively regulates water evaporation, thereby enhancing soil moisture retention (Figure 5-1b). In addition, the JWCF, due to its excellent hygroscopic properties [305, 306], absorbs water from the environment and release it into the soil to maintain the stability of soil moisture. The porosity adjustment allows JWCF to control water evaporation while retaining the necessary air permeability [307, 308], thus providing a suitable growing environment for plants in the soil. The synergistic effect of these properties of JWCF has led to significant results in weed control and moisture management (Figure 5-1c), further enhancing their potential for agricultural applications. Therefore, the JWCF shows promise as viable, scalable and eco-friendly substitute for traditional weed control and water conservation methods, contributing to worldwide carbon neutrality objectives.

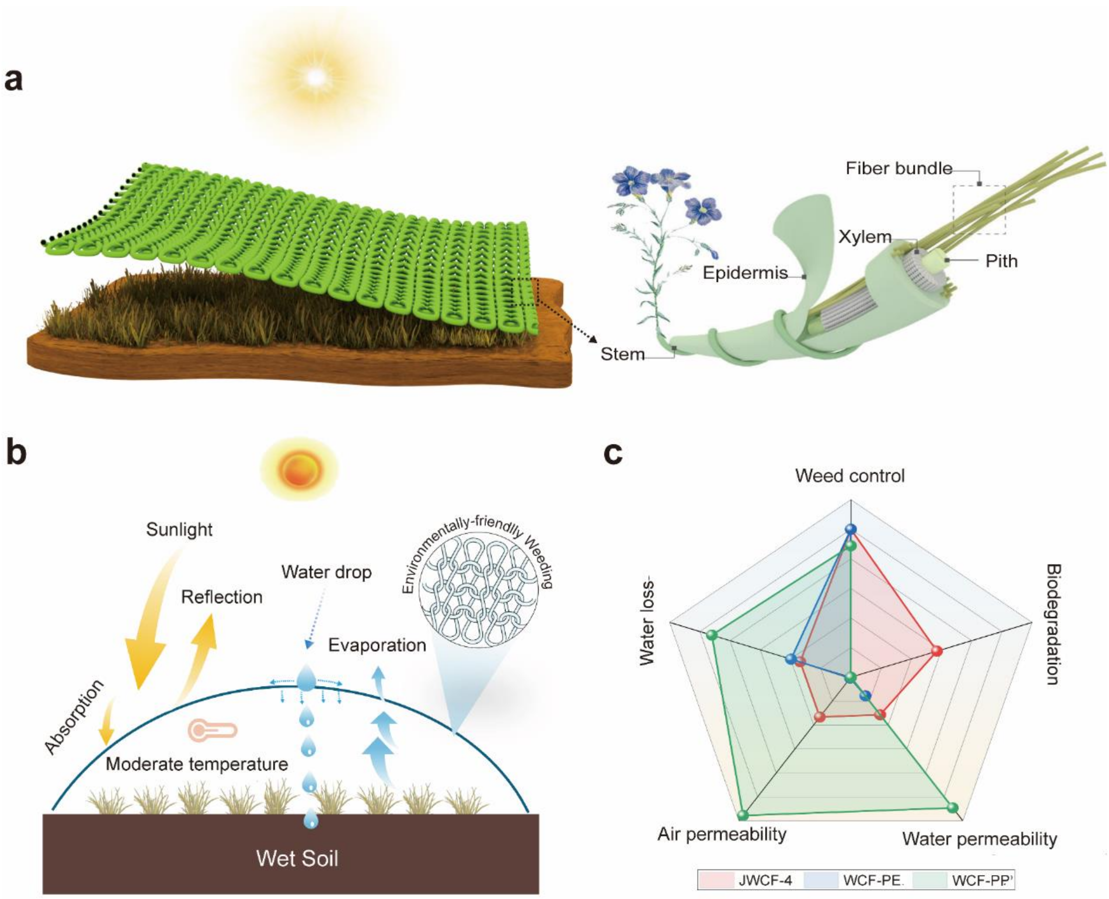

Figure 5-1 Schematic of the JWCF for sustainable weed control and water retention management under sunlight and its working mechanism. (a) Schematic illustration of the JWCF application and the abundant raw materials of JWCFs can be derived from the stem of natural Corchorus plants. (b) Schematic illustration of the working mechanism of JWCF for weed control management and evaporation control. (c) A comparative analysis of JWCF-4 with the main performance characteristics of current commercial WCFs.

5.2 Experimental Section

5.2.1 Materials

Jute yarn used in the study was purchased from Anji Zhenxing Lianma Spinning and Weaving Co., Ltd., China. Two conventional WCFs made from polyethylene (WCF-PE) and polypropylene (WCF-PP) were purchased from Taobao commercial sources.

5.2.2 Fabrication of jute weed control fabric (JWCF)

The sustainable JWCFs were fabricated using different knitting structures on a STOLL CMS530 computerized flat knitting machine (Stoll Machine, Germany), with a machine gauge of 7, constant machine settings, and uniform tension. The materials and photographs of JWCFs are presented in Figure 5-2 and Table 5-1 for further details.

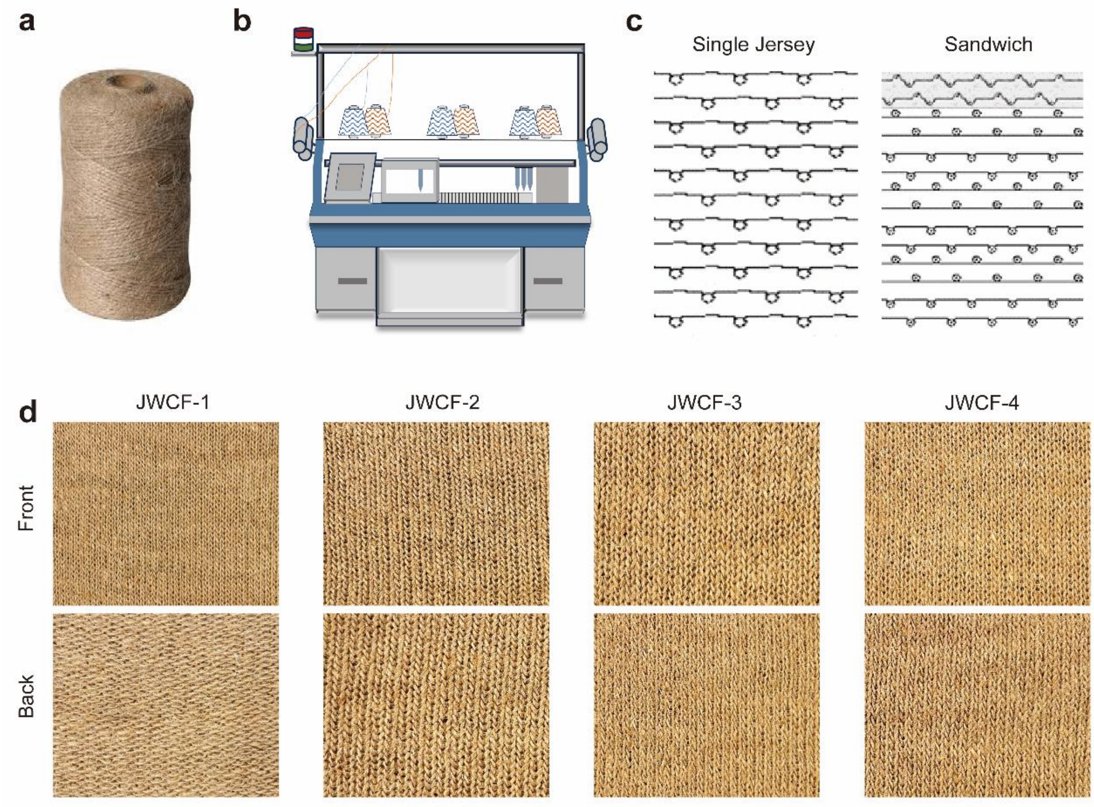

Figure 5-2 (a) Coarse jute yarns were used as raw materials to prepare the JWCF. (b) Schematic diagram of Stoll flat knitting machine. (c) Two knit structures (Single jersey and Sandwich) were used to change the porosity of JWCFs. (d) The photographs of different jute weed control fabrics.Top panel: front effect of different JWCFs. Bottom panel: back effect of different JWCFs.

Table 5-1 Detail parameters of JWCFs

Fabric Code	Material	Structure	Fabric Density (G)	Yarn Count (Tex)	Thickness (mm)

JWCF-1	100% jute yarn	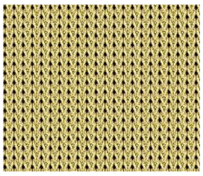 Single jersey	12.25	235	2.832
JWCF-2			12.25		5.764
JWCF-3		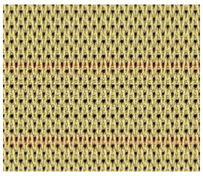 Sandwich	12.25 & 13.5		5.932
JWCF-4			12.25	235 & 368	6.016

5.2.3 Characterizations

WCF-PE and WCF-PP were used as performance comparators to assess the effectiveness of JWCF. Both fabrics (WCF-PE and WCF-PP) were black in color, primarily functioning to absorb sunlight, thereby reducing light penetration to the soil and effectively suppressing weed growth. All fabrics were placed in a controlled room at (20.0±2.0) °C and (65.0±4.0) % relative humidity for 24h prior to testing.

The microscopic picture was captured by optical microscope (Leica DM2500 LED). The fabric surface image was binarized using MATLAB software, where black pixels represent the areas occupied by yarns, and white pixels indicate the pore regions. Surface porosity was then calculated using equation (5-1):

$$P = \frac{\Phi_{\mu}}{\Phi_{a}} \times 100\% \quad (5\text{-}1)$$

Where, P represents the fabric surface porosity (%); Φ_{μ} denotes the number of white pixel pointes on the fabric surface; and Φ_{a} indicates the total number of pixel points on the fabric surface.

The moisture permeability test of the fabric was performed according to ASTM E96 standard. Circular samples with diameter of 9.3cm were prepared. Water vapor permeability is calculated according to equation (5-2):

$$\mathrm{WVT} = \frac{24\Delta m_c}{A \times t} \quad (5\text{-}2)$$

Where, WVT represents the water vapor permeability per square meter per day $g/(m^2 \cdot 24h)$; Δm_c is the difference between two weighing's of the same test combination(g); A denotes the effective test area(m^2).; and t is the test duration(h).

Air permeability measurements of WCF fabrics were conducted by using an YG(B) 461G automatic air permeability tester. Light blocking effect of fabrics was evaluated according to AATCC TM203-2021. The transmissivity and reflectivity within the UV, visible (Vis), and near-infrared (NIR) spectrums were conducted by a UV-Vis-NIR spectrometer (Lambda 1050+, PerkinElmer) with a 150 mm integrating sphere (InGaAs). Barium sulfate was used as a reference for the UV-Vis-NIR measurement.

Both pots covered with different WCFs and uncovered pots were exposed under sunlight for 4 hours, as shown in Figure 5-3. The weather conditions were monitored and documented by an automatic weather station (TOLAISI, TS-G1). K-type thermocouples (FLUKE,1586A Super-DAQ) were used to measure and record the temperatures of fabric surface and soil in real time. Water loss was measured by an electronic balance (LICHEN, JA3003). Each container initially contained 80 g of dry soil and 80 g of water (m_{wi}). The masses of the containers were measured before and after exposure, providing the initial (mi) and final (m_e) masses for calculating the water loss rate as $(m_i - m_e)/m_{wi}*100\%$.

Figure 5-3 A photograph of the experimental setup for temperature change and water retention under sunlight. This setup is mainly consisted by a thermocouple data recorder, a temperature and humidity recorder, and a weather station. The chamber of the soil container is isolated from the surroundings by an Al film to reflect sunlight. The temperatures of soil and fabric surface are real-time measured by thermocouples recorder.

All WCFs of size 500mm * 500mm were laid in an outdoor experimental site with adequate sunlight in the campus of Hong Kong Polytechnic University, Hong Kong, China (114.1795° E, 22.3051° N). The positionings of different WCFs are shown in Figure 5-4. Two groups, the non-irrigation group and the irrigation group

(1000ml/piece/day), were set up to investigate the impact of moisture on the weeding effect of fabrics. Both groups were covered continuously for 70 days, with weed growth in the experimental areas photographed every 7 days to compare the weed control performance of each fabric. The proportion of green pixels (Pg) in images of the same size was calculated using a MATLAB program combined with a clustering algorithm. The weed control efficiency was then determined as 100%-Pg.

Figure 5-4 Photographs of the outdoor experiment condition to test the weed control of different covering materials. All fabrics of size 500 mm * 500 mm were laid in an outdoor experimental site with adequate sunlight in the campus of Hong Kong Polytechnic University, Hong Kong, China (114.1795 °E, 22.3051 °N).

Biodegradation tests on WCFs were carried out by soil burial tests. Rectangular specimens of size 10 cm*10 cm were prepared and fixed in yarn nets of 12 cm*12 cm (convenient for sampling). The samples were buried about 20cm below the soil surface, exposing to the indigenous microorganisms presented in the natural soil. The samples were taken from the soil at regular 10-day intervals and were gently cleaned with distilled water. The samples were then dried at temperature 50 °C in an oven to a constant weight, photographed and weighted to determine the mass loss of WCFs.

Weight loss is calculated according to equation (5-3):

$$W_l = \frac{W_e - W_i}{W_i} \times 100\% \quad (5\text{-}3)$$

Where, W_l represents the weight loss of WCFs after degradation (%); W_i is the initial weight of the fabrics(g); and W_e indicates the final weight of the fabrics after degradation.

5.2.4. Statistical analysis

Statistical analyses were performed to evaluate the significance of the factors on the differences in weed control efficiency. One-way analysis of variance (ANOVA) was used to assess significant difference, with Duncan's multiple range test applied post-hoc to identify specific differences at a 5 % significance level. The same letter was used to indicate statistically similar. Spearman's correlation coefficient was used to evaluate the correlation between variables. All statistical analyses were performed using SPSS Statistics 25.0 (IBM Corp., USA) software, with statistical significance set at $p < 0.05$.

5.3 Result and Discussion

5.3.1 Design, fabrication and characterizations of JWCFs

The schematic diagrams of the development of JWCFs are shown in Figure 5-2. JWCFs were developed using coarser jute yarns with lower energy consumption, mainly because of the relatively low precision required for the processing of soil cover materials. Two fabric structures, single jersey and sandwich structure, were selected for the fabric fabrication. Single jersey structure, known for its simplicity [309], demonstrated excellent moisture permeability and breathability, promoting soil aeration and plant growth while covering the soil. The multilayer sandwich structure demonstrated enhanced durability, making it suitable for areas with varying soil conditions and extreme climates.

The optical microscope pictures of JWCFs are presented in Figure 5-5a. It shows that JWCFs had porous structures with abundant hairiness on the jute yarn [310]. This feature was attributed to the use of relatively coarse jute yarns, which tend to have more exposed fibers due to larger fiber bundles, lower twist and the inherent roughness of jute fibers. WCF-PE exhibited a tight fabric structure with no discernible fabric pores, whereas WCF-PP displayed a porous structure with multiscale pores throughout its surface and interior (Figure 5-6). As depicted in Figure 5-5b, WCF-PP demonstrated the highest porosity at 56.3%. Through the variation of fabric structure and density, four JWCFs presented different porosity levels, which were 126.2%, 76.0%, 79.5%, and 45.5% more porous than WCF-PE, respectively. The differences in porosity directly influence the functional properties of the fabrics, particularly in their capacity for water and air permeability. WCF-PP, with its highest porosity, exhibited the highest water vapor transmission rate of 800 g/m^2/day and air permeability of 1541.8 mm/s (Figure 5-5c and Figure 5-5d). WCF-PE showed the poorest water-vapor transmission rates and air permeability due to the compactness of the fabric structure. Gradual decreases in moisture permeability and air permeability of JWCFs were observed with reducing fabric porosity, consistent with findings from other research studies[311, 312]. The inherent hollow structure of jute fibers, along with the porous nature of fabrics, provided adequate water vapor permeability and breathability [313]. The measured light-blocking rates of different JWCFs, WCF-PE and WCF-PP are presented in Figure 5-5e, respectively. WCF-PE, characterized by its black color and lowest porosity, achieved an average light-blocking efficiency of 99.98 % across the sunlight visible wavelength range favorable for photosynthesis (400 nm-700 nm). In contrast, WCF-PP, with its highest porosity, exhibited the lower shading efficiency. Unstained JWCFs demonstrated comparable light-blocking rates to that of WCF-PE except of JWCF-1, reducing levels of sunlight effective for weed photosynthesis. The above experimental results confirmed that JWCFs not only provided efficient channels for the natural diffusion and convection of air and water vapor, but also effectively block sunlight, making them ideal soil mulching materials for controlling weed and promoting healthy plant growth. Furthermore, the varying porosities of JWCFs allowed for the selection of the materials that balance effective sunlight blocking with good water and air permeability based on specific needs.

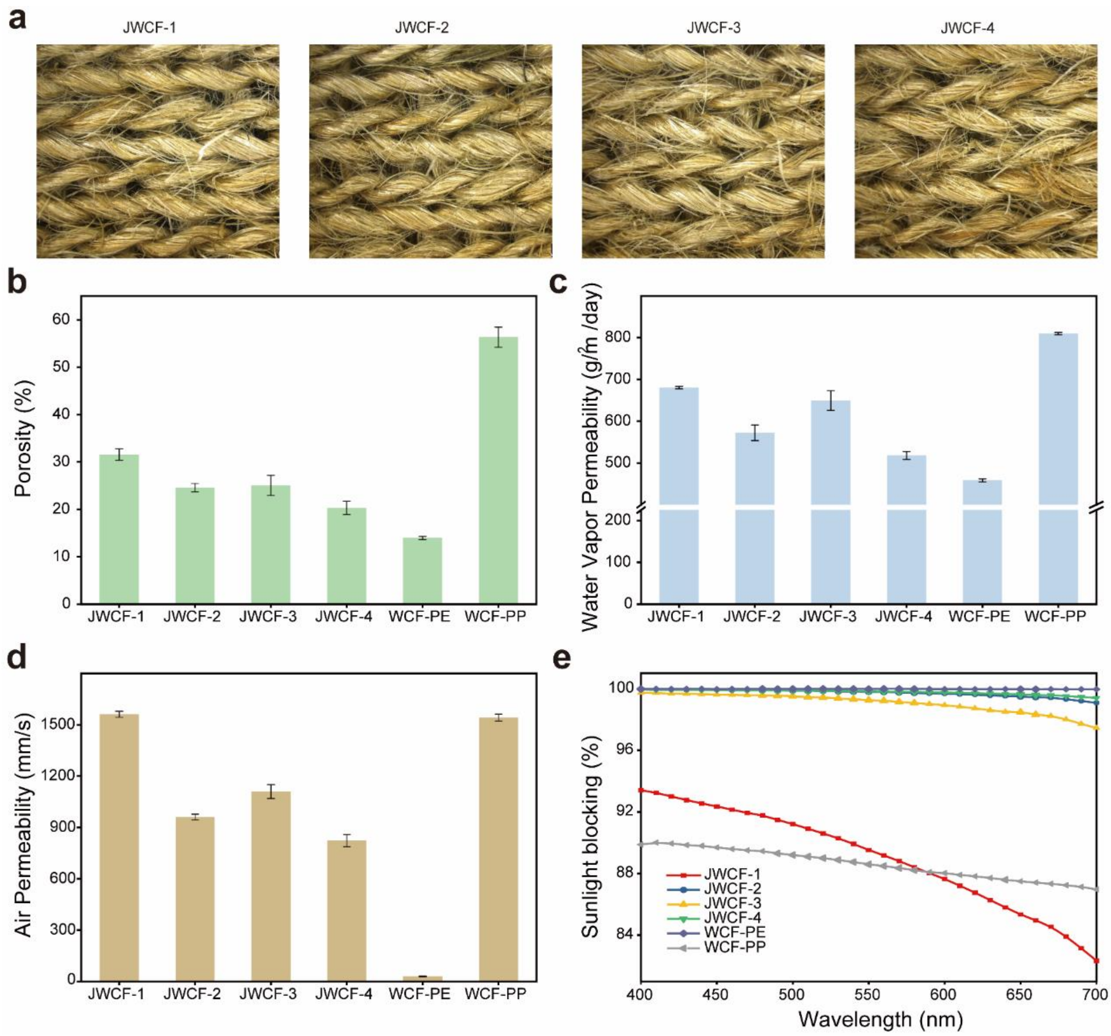

Figure 5-5 Fabrication and characterizations of JWCFs for weed control. (a) Optical microscope photographs of JWCFs. Scale bar, 2mm. (b) Porosity of JWCFs, WCF-PE and WCF-PP. Compared the (c) water vapor and (d) air permeability of different fabrics. (e) Sunlight blocking by different covering materials in the wavelength range of 400-700nm.

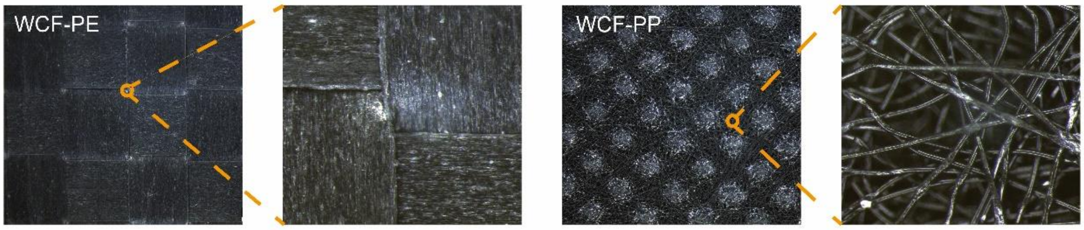

Figure 5-6 The photographs of WCF-PE and WCF-PP are shown for comparison. Scale bar, 2mm.

5.3.2 Temperature changes and water retention performance

The measured optical spectra of JWCFs, WCF-PE and WCF-PP are presented in Figure 5-7a. The WCF-PE and WCF-PP featured high absorptivity of 91.5 % and 86.5 % respectively in the entire sunlight wavelength range, while JWCFs exhibited the lowest absorptivity with the minimum absorption of 7.9 %, which effectively rejected sunlight by reflection. Thus, it was expected that JWCFs would reduce heat accumulation and water evaporation in the covered area. The temperature changes and water retention performance of JWCFs were estimated by outdoor temperature and water loss experiments. WCF-PE, WCF-PP and an uncovered case were used as controls (Figure 5-7b). Experimental analysis of the surface temperature of JWCFs and the three controls (Figure 5-7c) under weather conditions (Figure 5-8) showed results as expected for the fabric absorption property. WCF-PE, with its high solar radiation absorptivity and low air permeability, resulted in substantial heat accumulation, leading to a sharp increase in surface temperature to about 63.9 °C. The porous surface of WCF-PP enhanced heat dissipation, effectively mitigating the rise in fabric temperature, with a maximum recorded temperature of 58.2 °C. In contrast, although the surface temperature of JWCFs exposed to sunlight also increased, they were lower than those of WCF-PE and WCF-PP by about 11.2 ℃ and 5.5 ℃, respectively. It is worth noting that changes in the surface temperature have a significant effect on the soil temperature in the covered area, determined mainly by the thermal absorption properties, thickness, and the breathability and water permeability of the fabric. Analysis of the soil temperature with different covering showed basically consistent with the changes of fabric surface temperature (Figure 5-7d). JWCFs produced lower soil temperature of average 40.3 °C, which is 4.3 °C and 1.6 °C than those under the WCF-PE and WCF-PP, respectively. This indicated that JWCFs exhibited relatively thermal regulation properties, effectively maintaining soil temperature stability. In addition, the inherent thickness of JWCFs allowed them to retain heat in the covered area, resulting in soil temperatures that were 0.4~1.7 °C higher than that under no cover scenario. The slight rise in temperature could help maintain a more stable soil temperature conductive to plant growth, especially in cooler conditions. JWCFs reduced water evaporation from the soil, where JWCF-4 slowed soil moisture evaporation by 6.0 %, 38.6 % and 68.5 % compared with WCF-PE, WCF-PP and no cover, respectively (Figure 5-7e). These results together confirm that the JWCFs exhibited the best water conservation effects, crucial for supporting plant growth in dry regions.

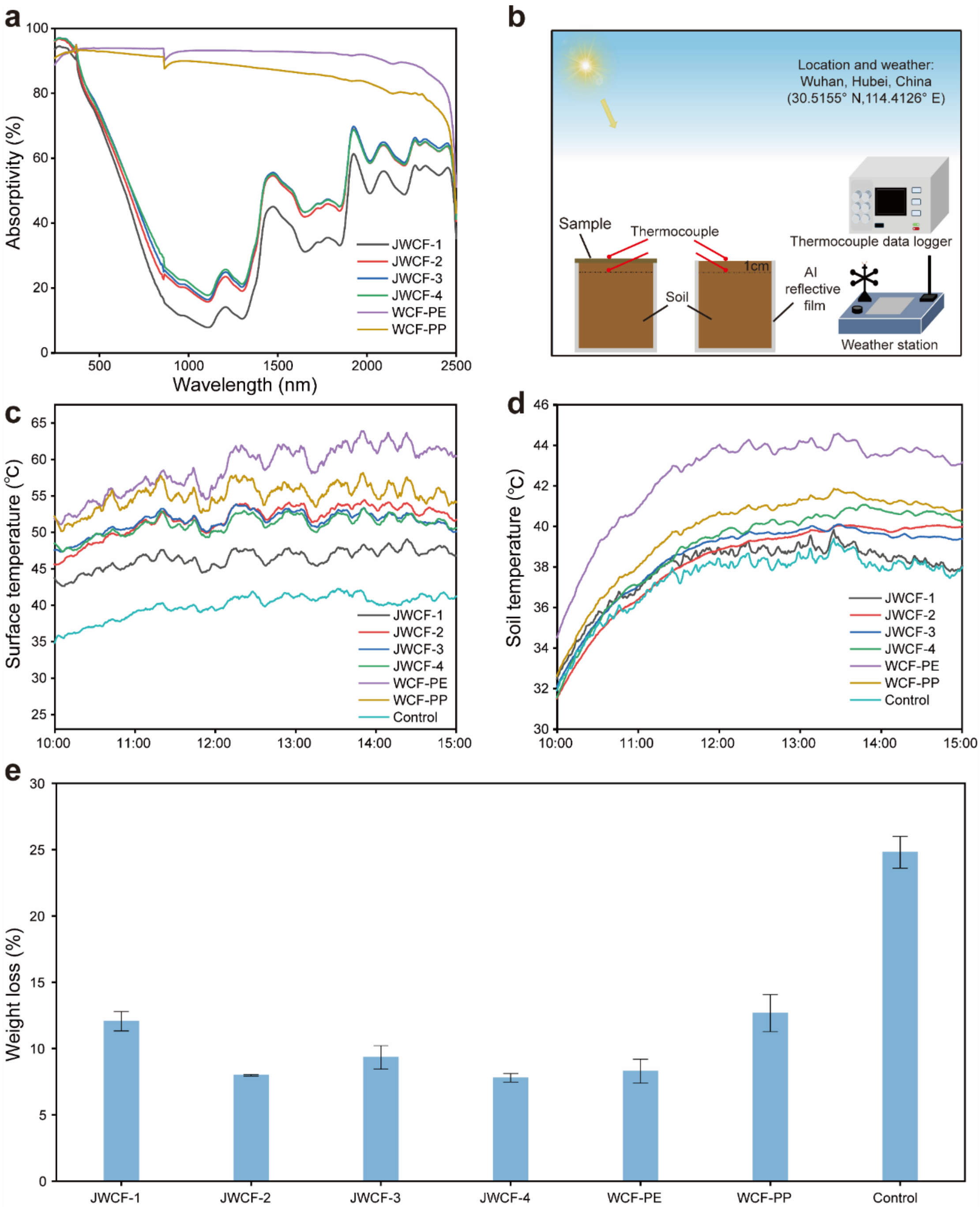

Figure 5-7 Heat accumulation reduction and water conservation performance. (a) Absorptivity of different WCFs. (b) A schematic of the custom-made device for verifying the cooling effects of the JWCFs. (c) Surface temperature and (d) soil temperature recorded under covered of the JWCF and the three controls from 10:00 to

15:00. (e) Comparison of soil water evaporation loss under the JWCF application and the three control conditions. The JWCF can reduce heat accumulation after covering and achieve water-saving effect.

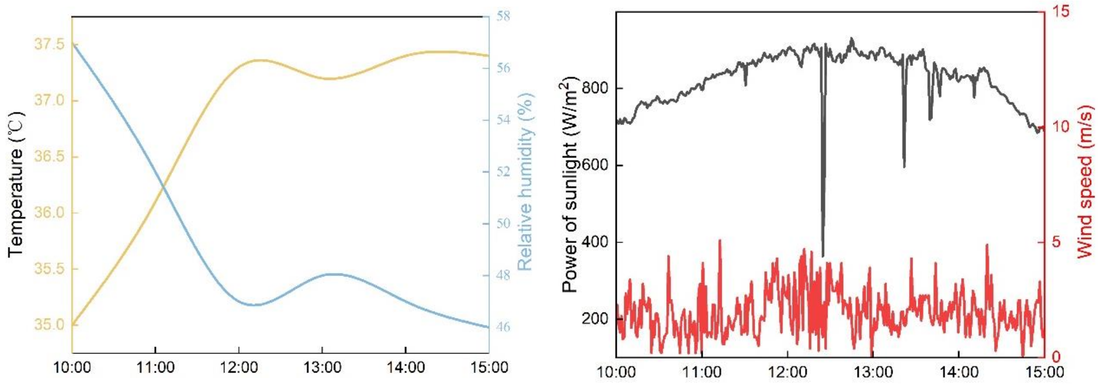

Figure 5-8 Environment conditions of the temperature and water-loss tests outdoor. Left panel: temperature and relative humidity. Right panel: power of sunlight and wind speed.

5.3.3 Weed control experiment

The weed control performance of the JWCFs was demonstrated by direct weeding measurements. JWCFs, WCF-PE and WCF-PP were mulched in outdoor grassland with dimensions of 50*50 cm and the results were compared with open field weeds as a control (Figure 5-4). The photographs in Figure 5-9a showed the physiological states of weeds grown under the JWCFs, WCF-PE, WCF-PP and no cover scenario with or without irrigation over a period of 70 days. Weeds growing under JWCFs, WCF-PE and WCF-PP showed inhibited growth compared to those in the open area, demonstrating that all fabrics had a certain level of weed control effectiveness. JWCFs (JWCF-2, JWCF-3 and JWCF-4) exhibited weed control effectiveness comparable to that of WCF-PE by blocking sunlight effective for weed photosynthesis. In contrast, the larger porosity of JWCF-1 and WCF-PP allowed certain wavelengths of visible sunlight to penetrate, resulting in inferior weed control effect in the covered area after 70 days. In addition, comparing the physiological status of weeds in the non-irrigation group, irrigation further improved the weed suppression of JWCF-1. However, it had minimal impact on the effectiveness of WCF-PP, which can be attributed to its excessive porosity, allowing more sunlight and moisture to reach the soil and thereby promoting weed growth. Weed control rate analysis based on the photographs showed in Figure 5-4a. The results demonstrated that the JWCF-4 and WCF-PE in non-irrigation group had the best weed control rate of 100 %, which was 39.0 %, 3.6 %,9.8 % and 11.1 % higher than those under the JWCF-1, JWCF-2, JWCF-3 and WCF-PP (Figure 5-9b). The weed containment effectiveness of JWCFs in the irrigation group were improved by 25.5 %, 3.7 % and 10.8 % greater than that achieved in the non-irrigation group under the JWCF-1, JWCF-2 and JWCF-3, respectively. Prolonged wet conditions with condition of sunlight lackage can lead to oxygen deprivation in shallow weed roots, further accelerating root decomposition and necrosis [314].

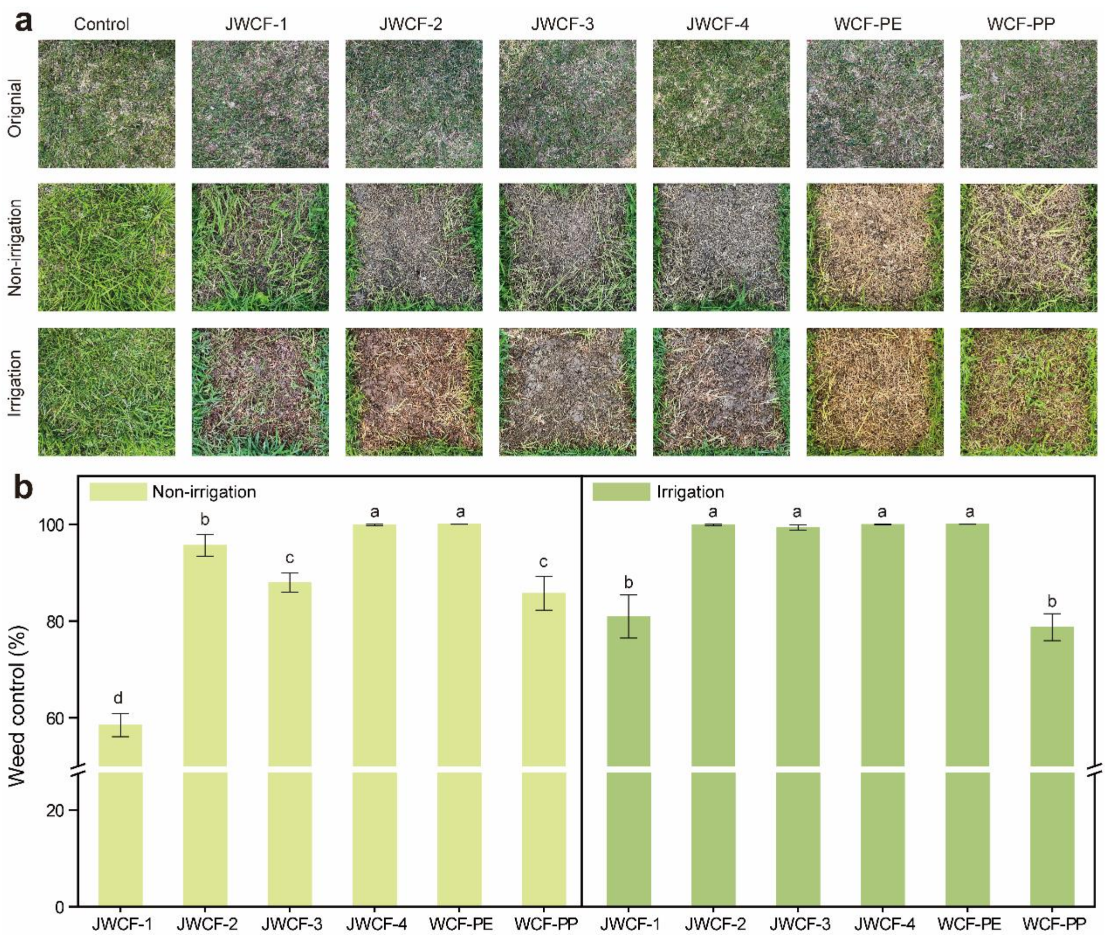

Figure 5-9 The weed control effects of the JWCFs compared with the WCF-PE, WCF-PP and bare control. (a) Photographs presenting the physiological condition of weed growth in the non-irrigation group and irrigation group after 70 days of coverage under the four conditions and (b) the weed control rate of different materials under irrigation or non-irrigation condition.

5.3.4 Soil-buried biodegradation experiment

Having demonstrated the excellent weed control and water conservation performances of JWCFs, biodegradability at the end of life is another crucial issue that should be given full consideration. The biodegradation performance of JWCF, WCF-PE and WCF-PP were measured in actual natural soil environments (Figure 5-10a). The changes in the physical appearance of fabrics were observed through photographic and optical microscope images. WCF-PE and WCF-PP exhibit notable resistance to bio-aggressive degradation, with the fabric remaining intact and showing any discernible surface alterations of degradation in the fabric (Figure 5-10b). In contrast, JWCF exhibited significant physical changes, with the degree of surface discoloration increasing over time, possibly due to the mold and mildew growth [117, 275] . The natural decomposition process, driven by microbial activity, moisture, and exposure to soil environmental conditions, resulted in the breakage of the fabric matrix, ultimately leading to the disintegration of the plant-based fibers. Experimental analysis of the weight loss after degradation revealed that JWCF experienced a significant reduction in mass, with 47.5 % weight loss after 40 days of soil buried (Figure 5-10b). Therefore, it offered a sustainable weed control method that minimized soil environmental impact by naturally degrading over time, ultimately contributing to improved soil health.

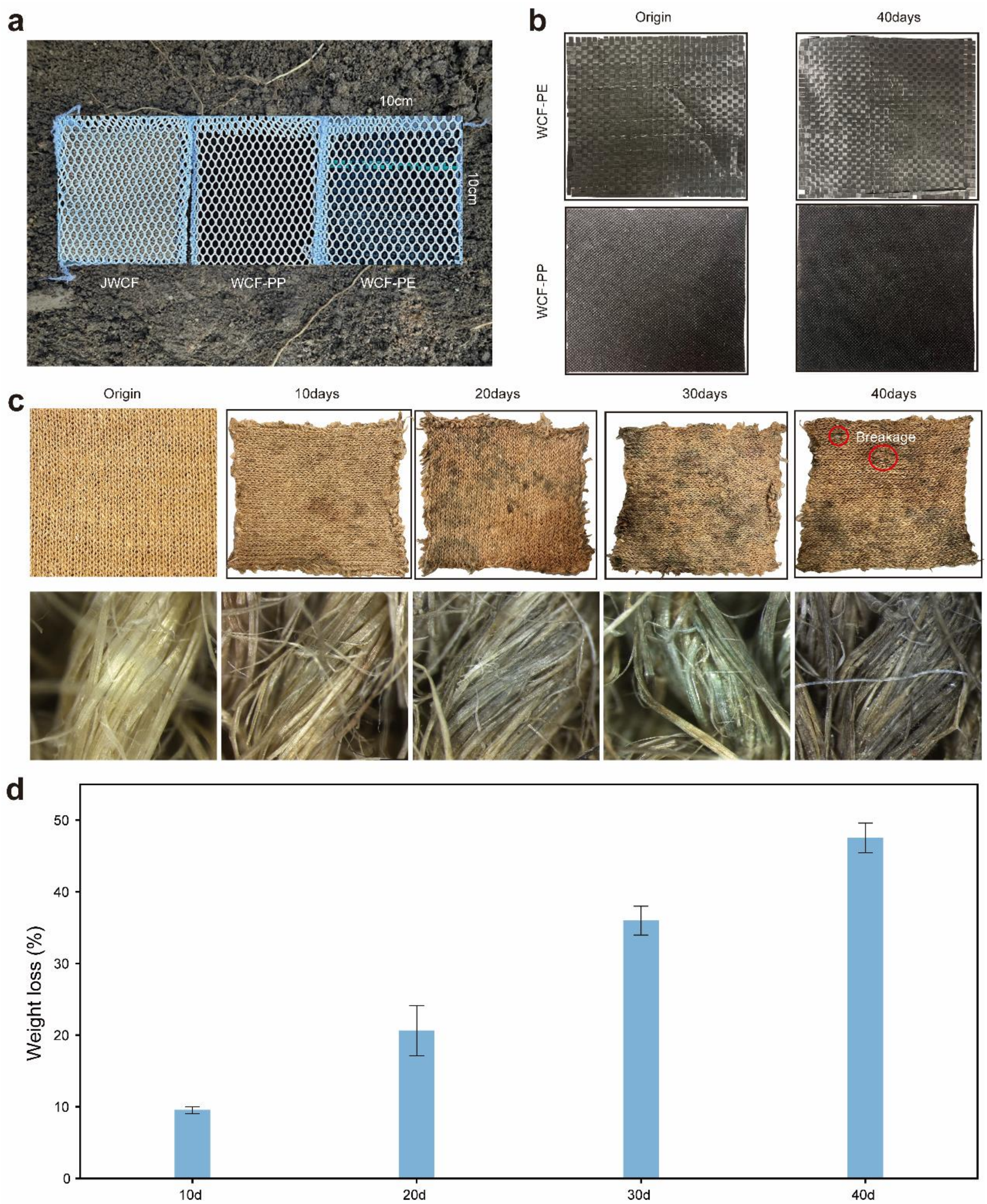

Figure 5-10 The biodegradability tests under moist soil of JWCF, WCF-PE and WCF-PP. (a) Photograph of samples prepared to test the degradation performance of different covering fabrics. The samples were placed in mesh bags (for easy sampling) and buried in soil at a depth of 20cm for natural biodegradation. (b) Photographs of the commercial

WCFs degradation after 40 days. Top panel: overall physical pictures of WCF-PE. Scar bar: 3cm. Bottom panel: overall physical pictures of WCF-PP. Scar bar: 3cm. (c) Photographs of the JWCF degradation after different burial times. Top panel: overall physical pictures of JWCF. Scar bar: 3cm. Bottom panel: Photographs of the jute yarn with discoloration or mildew. Scar bar: 500μm. (d) Weight loss of the JWCF after degradation from 10days to 40days.

5.4 Conclusion

In this work, a jute fiber-based weed control and water retention strategy was proposed for sustainable weed management while simultaneously minimizing soil environment pollution. A comprehensive investigation was conducted to analyze and evaluate their properties compared with two commercial WCFs (WCF-PE and WCF-PP). JWCFs with different porosities had excellent moisture permeability, air permeability, and effectively blocking visible sunlight required for photosynthesis. The weeding experimental results showed that JWCFs notably impeded weed growth (61 %~100 %), which approached or even exceeded the weed control rate of WCF-PE and WCF-PP. The weed control efficiency of JWCFs was improved 3.7 %~25.5 % under irrigated conditions compared with non-irrigation group. Field tests demonstrated that JWCFs reduced soil temperature (average 1.6~4.3 °C) compared to traditional mulching materials, which also decreased water evaporation (6.0~68.5 %) compared to both conventional covering materials and the uncovered scenario. Degradation tests showed a 47.5 % weight loss of the JWCF after 40 days of soil buried, indicating the biodegradability and suitability for sustainable agricultural applications. In summary, based on the superior performance achievements and the completely biodegradable advantage, the proposed JWCFs demonstrated significant potential as a promising substitute for conventional polymer-based WCFs. The sustainability implications of the

JWCFs are anticipated to be significant. By utilizing plant fiber to impede weed growth while reducing soil environmental pollution, the JWCF may advance the goal of promoting sustainable agricultural practices. Effective weed management and reduced water evaporation can conserve vital resources and diminish the dependence on chemical herbicides and water-intensive irrigation, thereby fostering the long-term development of sustainable agriculture. This impact would contribute to safeguard vulnerable ecosystems and foster the sustainability of natural resource management. Moreover, this work provides novel perspectives and innovative ideas for the application of cellulosic materials in agriculture and contributes to an important significance for expanding the application of natural fibers.

Chapter 6 Long-term Field Evaluation of JWCF Performance

6.1 Introduction

This chapter focuses on the long-term field evaluation of JWCF-4 to assess its effectiveness and durability under real agricultural conditions. The study aims to investigate its weed suppression performance, impact on soil conditions and crop yield, and biodegradation over an extended period. By conducting field experiments under actual environmental conditions, this chapter provides valuable insights into the practical applicability of JWCF-4, offering a comprehensive understanding of its long-term effects and potential for sustainable agricultural practices.

6.2 Experiment Section

6.2.1 Material

JWCF-4 used in the study was prepared as described in the above chapter. Two conventional WCFs made from polyethylene (WCF-PE) and polypropylene (WCF-PP) were purchased from Taobao commercial sources.

6.2.2 Field experiment setup

Based on the results of a small outdoor weed control experiment conducted at the Hong Kong Polytechnic University campus, JWCF-4 demonstrated 100% weed control efficiency under both irrigation and non-irrigation conditions. Therefore, it was selected for a one-year field trial in Meizhou, Guangdong, to evaluate its long-term weed suppression performance. After pomelo harvesting, the experimental area was cleaned through basic weeding, lime disinfection, and other farm maintenance tasks, followed by the installation of JWCF-4, WCF-PE, and WCF-PP under the pomelo trees to observe and compare the weed control effectiveness of different covering materials in a natural environment (Figure 6-1).The total laying area of JWCF-4, WCF-PE and WCF-PP was 80 m^2, respectively. A diverse range of weed species was identified in the field, including *Commelina communis* (L.), *Bidens alba* (L.), Setaria sp., and Arctium sp., with *Commelina communis* emerging as the dominant species.

Figure 6-1 Photographs of the actual covering of pomelo tree.

To meet the nutritional requirements of honey pomelo, multi-element water-soluble fertilizers were applied four times during the entire period of honey pomelo growth (Table 6-1). Each fertilizer application was carried out according to the specific growth stages of the honey pomelo (e.g. budding, flowering, fruit expansion).

Table 6-1 Fertilizer applications in the experimental area.

Date	Type	Fertilizer amount per tree
2023.9-2023.10	Multi-element water soluble fertilizer+ microbial agent	5kg

2024.02-2024.03		5kg
2024.05-2024.06	Multi-element water soluble fertilizer	5kg
2024.07-2024.08		5kg

6.3 Result and Discussion

6.3.1 Weather conditions

The one-year field experiment evaluated the effects of seasonal precipitation and temperature variations on soil moisture, nutrient dynamics, and plant health. Precipitation exhibited significant monthly variability (Figure 6-2a), with eight months experiencing over 15 days of rainfall, including a peak in June (29 days). Rainfall exceeding 50 mm, particularly during the rainy season (April–May 2024), significantly influenced soil moisture at 20–25 cm depth. Temperature trends ranged from 5 °C to 35 °C, with winter months (January–March 2024) frequently dropping below 10°C. These low temperature in winter months caused frost damage to pomelo trees, evident in yellowing, wilting, and defoliation, particularly affecting new shoots and buds. From spring onward, temperatures rose steadily, exceeding 35 °C in summer, which likely accelerated material degradation and affected soil moisture dynamics (Figure 6-2b). These seasonal fluctuations highlight the important relationship between environmental conditions, soil conditions, and plant health during the study period.

6.3.2 Weed control performance

JWCF-4, which demonstrated 100 % weed control efficiency under actual short-term experiment conditions, was selected for one-year field application to evaluate the long-term weed suppression performance in Meizhou, Guangdong (Figure 6-2c). JWCF-4 could consistently maintain weed management effectiveness comparable to commercial WCFs, achieving 100 % weed suppression for a long time under natural conditions (Figure 6-2d). In contrast, the control group without mulching exhibited rapid weed proliferation, particularly during rainy periods, resulting in significantly higher weed density compared to treatment groups using WCFs. These results together confirmed that the JWCFs had excellent weed control effect under any conditions.

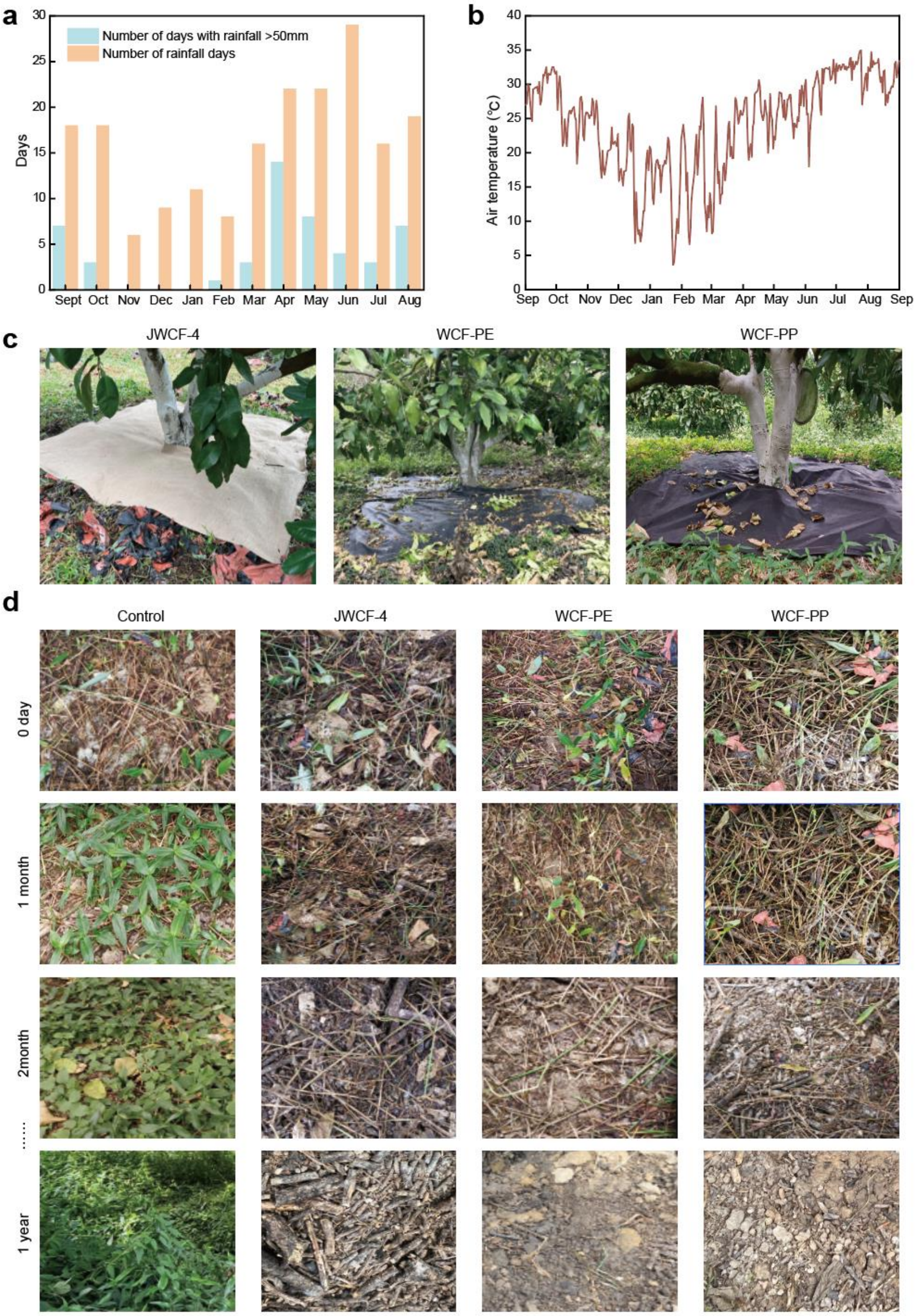

Figure 6-2 One-year (a) rainfall and (b) temperature statistics in the field experiment

area. (c) Photographs of the actual covering of pomelo tree. (d) Photographs of weeds grown under different conditions in a one-year long-term covering pomelo farm.

6.3.3 Soil conditions

The soil moisture content varied significantly across treatments, as illustrated in Figure 6-3a. JWCF-4 demonstrated superior soil moisture retention, particularly under low precipitation, by reducing evaporation and enhancing moisture regulation. Its unique water-absorbing and slow-release properties, combined with good air permeability, allowed it to prevent soil over-wetting during rainfall below 50 mm and maintain balanced moisture levels. In contrast, WCF-PE, due to poor water and air permeability, caused soil waterlogging and prolonged water stagnation under heavy rainfall, impairing root respiration and growth. WCF-PP, while highly porosity, led to rapid water penetration and evaporation, resulting in unstable soil moisture levels similar to bare soil. Overall, JWCF-4 exhibited effective moisture regulation under varying precipitation conditions, maintaining stable soil moisture and promoting healthy root growth. In contrast, WCF-PE and WCF-PP showed limitations in moisture management, with WCF-PE prone to over-wetting during periods of excessive precipitation and WCF-PP ineffective in moisture retention during drought. These findings highlight the advantages of JWCF in maintaining optimal soil moisture for long-term field applications.

Appropriate soil temperatures enhance root growth, nutrient uptake, and microbial metabolic processes. Mulching materials are commonly used to regulate surface temperature, reduce evaporation, and stabilize soil conditions. Figure 6-3b illustrates soil temperature variations at a depth of 20-25 cm under different mulches. Soil temperature fluctuations lagged ambient temperature changes due to soil's higher heat capacity, with smaller variations observed at deeper depths. During winter, ambient temperatures dropped below 10 °C, but soil temperatures in the root zone remained above 10 °C, ensuring continued nutrient uptake and metabolic activity. Notably, no significant differences in soil temperature were observed between mulched and un-mulched treatments at 20-25 cm depth, indicating that the influence of surface mulching diminished with increasing soil depth. This lack of significant variation can be attributed to strong thermal buffering capacity of soil and the moderating effect of soil moisture.

The nutrient root system of pomelo trees requires an optimal soil pH range of 5.5–6.5 for healthy growth, as the slightly acidic environment facilitates nutrient uptake and microbial activity. Figure 6-3c illustrates the variation in soil pH at this depth during the experimental period, showing stable pH values around 6, which aligns with the ideal conditions for pomelo cultivation. No significant fluctuations were observed, regardless of the mulch type (JWCF-4, WCF-PE, or WCF-PP), indicating that none of these materials significantly influenced soil acidity or alkalinity. The partial degradation of JWCF-4 primarily affected the surface soil condition, while PP and PE fabrics retained structural integrity, contributing to their minimal impact on soil pH at this depth. Additionally, the inherent buffering capacity of soil also played a key role in maintaining pH stability at deeper layers. These findings suggest that mulch type, degradation extent, and soil buffering influence stable pH conditions during the experiment.

Throughout the growth cycle of pomelo, key nutrients such as nitrogen(N), phosphorus(P), and potassium(K) at 20-25 cm nutritional root play an important role, directly affecting the health of the tree and the quality of the fruit. Therefore, maintaining appropriate levels of N, P and K throughout the year is particularly critical for the continued health of the pomelo tree and high fruit yield and quality. Figure 6-3d illustrates the changes in soil nutrient content (N, P, and K) across different experimental treatments (JWCF-4, WCF-PE, WCF-PP, and Control). The JWCF-4 covering area exhibited significantly higher nutrient levels during spring and summer, demonstrating that JWCF-4 effectively reduced nutrient losses, particularly nitrogen volatilization. By regulating water penetration, JWCF-4 minimized soil nutrient loss, especially during the rainy season. In contrast, the WCF-PE covering area consistently showed lower nutrient levels, primarily due to its poor water and air permeability. This hindered effective water and fertilizer infiltration and led to water accumulation and nutrient leaching during heavy rainfall. In addition, limited soil-air exchange and suppressed microbial activity further reduced nutrient availability. WCF-PP, due to good water and air permeability, exhibited nutrient dynamics similar to those of the bare soil control group, with rainfall significantly influence on nutrient changes. These results demonstrated the superior nutrient retention capacity of jute fabrics compared to synthetic mulches.

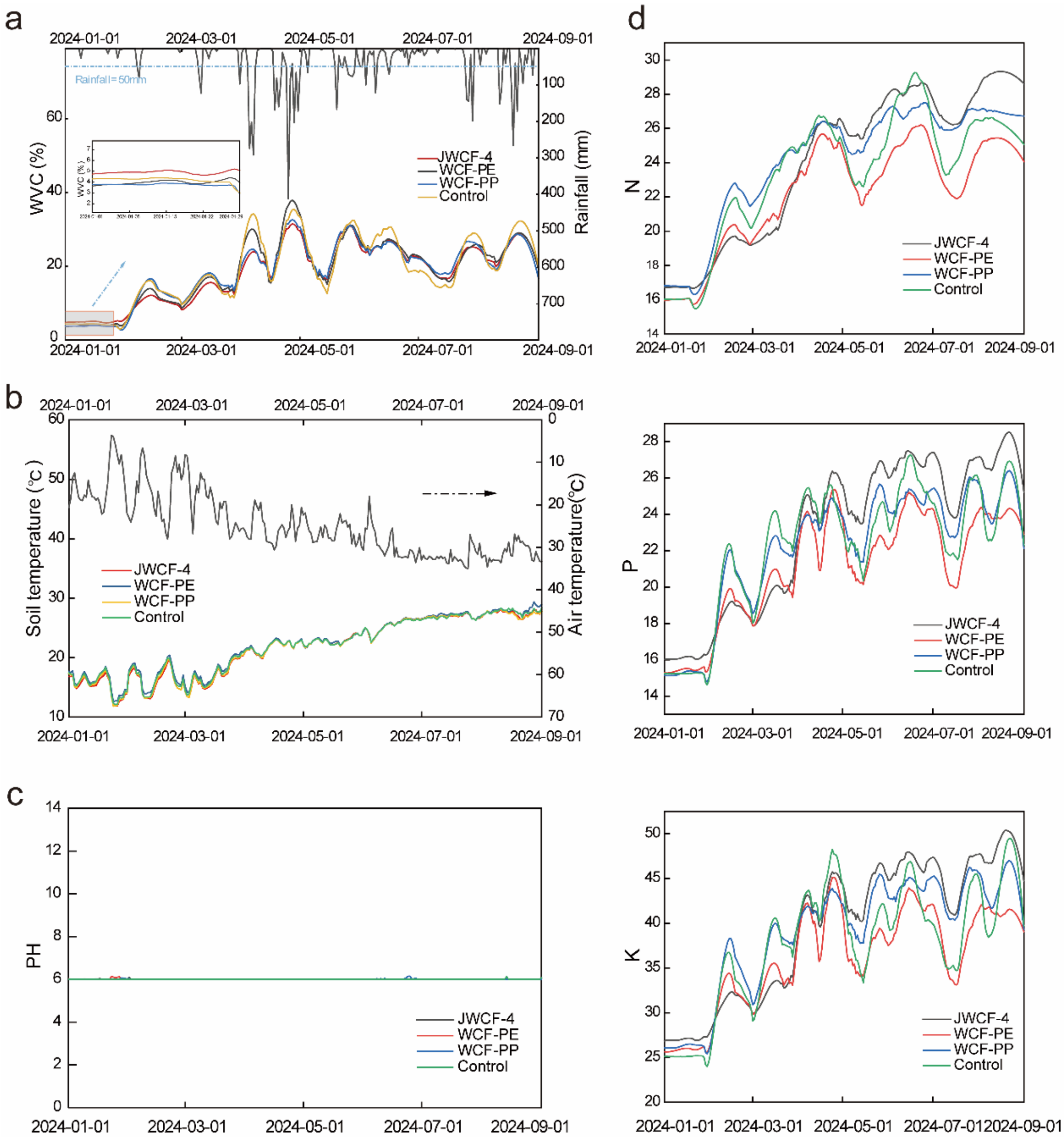

Figure 6-3 Soil conditions in honey pomelo tree area. (a) Soil moisture, (b) soil temperature, (c) soil pH and (d) soil nutrients (N, P, K) content under different fabrics mulching and uncovered area.

6.3.4 Honey pomelo yield and quality

Changes in the soil environment significantly influence fruit tree fruiting, with optimized soil moisture, nutrient availability, aeration, and biological activity playing crucial roles in enhancing fruit production. Figure 6-4a illustrates the fruiting performance of pomelo trees across different experimental treatments. The JWCF-4 treatment group demonstrated a significant improvement in fruiting capacity compared to the control group, attributed to the positive feedback between efficient water and nutrient cycling. The consistent and adequate supply of water and nutrients in the JWCF-4 zone improved photosynthetic efficiency and root vitality, thereby promoting enhanced flower bud differentiation and fruit formation. In contrast, other treatment groups exhibited unstable water and nutrient availability, leading to nutrient imbalances or water stress, which ultimately reduced fruit yield.

The honey pomelo in the test area was harvested in September 2024 after one year of laying experiments. From the statistics of yield shown as Figure 6-4b, the yield of pomelo in the test area reached 3697 kg, which was 22.2 % increase compared to the yield in 2023. The experimental area with JWCF-4 showed a significant increase in pomelo yield compared to the other experimental groups with an increase of 226 kg, which was 38.7 %, 32.6 % and 102.6 % higher compared to the WCF-PE, WCF-PP and no-mulch experimental areas, respectively (Figure 6-4c). This may be related to the advantages of jute fabric in regulating soil moisture and fertilizer retention. Additionally, pomelos in the JWCF-4 treatment group exhibited a sugar level of around 13 °Brix, representing an average increase of 1 °Brix compared to 2023, along with fuller flesh and enhanced flavor (Figure 6-4d). In contrast, the WCF-PP and WCF-PE treatment groups yielded fruit with lower quality, likely due to insufficient soil moisture retention and nutrient regulation.

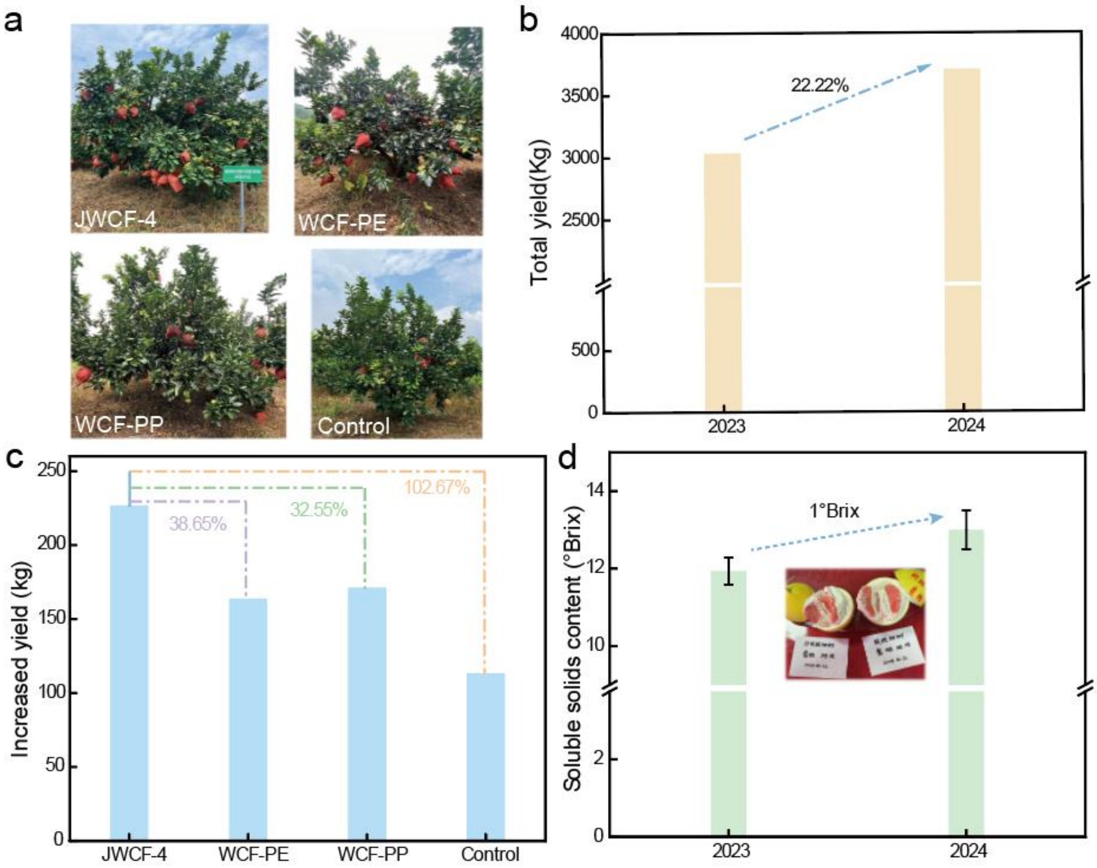

Figure 6-4 Honey pomelo yield and quality under different soil treatment. (a)Fruiting of pomelo trees in different fabric coverage areas. (b) Total and (c) increased yield of honey pomelo trees covered with different fabrics. (d) Comparison of the soluble solids content in honey pomelo treated with JWCF-4 between the years 2023 and 2024.

6.3.5 Durability and biodegradation of JWCF

During the first eight months of the experiment, JWCF-4 showed good durability, maintaining overall integrity with only slight surface discoloration, as shown in Figure 6-5(a). However, in the later stages, the harsh weather conditions (high temperatures, frequent rainfall, and occasional localized flooding) in Meizhou, Guangdong Province had a more pronounced impact on their durability. significantly accelerating the degradation process (Figure 6-5b). Prolonged exposure to moisture led to gradual decomposition and a subsequent loss of structural integrity. The results indicate that under normal climatic conditions, jute fabrics exhibit good durability, maintaining structural integrity and functionality over extended periods. However, under extreme climatic conditions such as high temperature and flooding, the degradation of jute fabrics accelerated significantly, limiting the service life to approximately one year. During this period, jute fabrics effectively suppressed weed growth and contributed to the regulation of soil health. After use, jute fabrics could be conveniently managed by plowing them into the soil instead of removal. In contact with soil moisture and indigenous microorganisms, the cellulose fabrics undergo gradual microbial attack and ultimately mineralize into harmless byproducts such as carbon dioxide, water, and humic-type organic matter [315]. This natural decomposition process has been shown to have a beneficial influence on jute-fabric residue on soil physical and biological properties according to relevant literature [316, 317].

Figure 6-5 (a) Photographs of the JWCF-4 covered after 8 months and (b) photographs of the JWCF-4 degradation after covered 1 year.

6.4 Conclusion

In this work, a one-year field experiment successfully verified the functional effectiveness of JWCFs. The covering experiment demonstrated that JWCF can maintain 100 % weed control efficiency over a long and consistent period. Soil indicators recorded by sensors in the nutrient root zone located at 25 cm showed that the jute fabric covering was effective in improving the soil environment and reducing soil nutrient loss. JWCF-4 coverings conserved 29.6 % and 82.8 % and 56.6 % more soil moisture compared to that covered under WCF-PE, WCF-PP, and uncovered scenarios, respectively. JWCF-4 proved to be notably efficient in mitigating soil nutrient depletion, maintaining soil nutrient levels consistently at their highest levels. The yield analysis indicated a 22.2 % increase in the 2024 test area compared to 2023, with a 226 kg rise observed in the JWCF-covered area, representing a 102.7 % higher yield enhancement compared to the uncovered control area. The sugar content of the honey pomelo under JWCF-4 covering also increased by approximate 1 °Brix, subsequently contributed to a higher market value of the fruit. Long-term field trials have further demonstrated the viability of JWCFs for a minimum duration of one year. Post-use, the JWCFs could be integrated into the soil during soil turnover, decomposing into carbon dioxide, water, and organic compounds, thereby augmenting soil nutrient levels.

Chapter 7 Conclusions and Suggestions for Future Research

7.1 Conclusions

Through an overview of the current developments and research progress of agricultural materials, key challenges and limitations in this field were proposed. To address these challenges, sustainable agricultural textiles with multifunctional integration were developed through the selection of materials, structural design, and preparation strategies. The properties of jute-based fabrics were thoroughly assessed to explore their viability as sustainable alternatives to conventional agricultural plastics through lab and outdoor experiments. The main conclusions are summarized as follows:

1) In chapter 3, the fundamental properties of jute yarns were systematically investigated. Alkali treatment was employed as the primary method for modifying the jute yarns. SEM analysis demonstrated that alkali treatment removed surface impurities followed by a maximum 30.6 % reduction in yarn diameter. The JY-2.0h sample exhibited a 17.1 % increase in tensile strength and a 65.2 % improvement in water absorption.

2) In chapter 4, a green jute fiber-reinforced composite (JFPC) pipe was proposed for sustainable irrigation management. The study examined the influence of PLA film porosity on the properties of JFPCs. The results showed that the combining jute fiber with PLA enhanced thermal stability and mechanical properties. The controllable seepage rate of JFPC pipes could be achieved by adjusting PLA film porosity to meet specific irrigation requirements. Life cycle and degradation tests demonstrated that JFPCs had a lower environmental impact compared to conventional plastic pipes and exhibited promising biodegradability (20.2 % weight loss after 3 months of soil burial). These findings highlight the potential of JFPC pipes as a sustainable alternative for

agricultural irrigation, providing controlled water seepage while minimizing dependence on non-renewable resources and mitigating end-of-life plastic waste.

3) In chapter 5, a jute fiber-based strategy was proposed to promote sustainable weed management and reduce soil pollution. The study demonstrated that jute-based weed control fabrics (JWCFs) either outperformed or matched the effectiveness of commercial polymer-based fabrics (WCF-PE and WCF-PP) in blocking sunlight and inhibiting weed growth (61 %–100 %). Under irrigated conditions, JWCFs showed improved weed control efficiency (3.7 %–25.5 %). Field tests indicated that JWCFs reduced soil temperature by 1.6–4.3 °C and decreased water evaporation by 6.0 %–68.5 %. Degradation tests revealed a 47.5 % weight loss after 40 days of soil burial, underscoring their biodegradability and suitability for sustainable agriculture. These findings suggest that JWCFs, with their superior performance and environmental benefits, offer a promising alternative to conventional plastic-based weed control fabrics, supporting the advancement of sustainable agricultural practices and resource conservation.

4) In chapter 6, a one-year field experiment confirmed the functional effectiveness of JWCFs in sustainable weed control and soil improvement. JWCF maintained 100 % weed control efficiency over an extended period. Soil sensor data at a 25 cm depth indicated improved soil conditions and reduced nutrient loss. JWCF-4 coverings retained 29.6 %, 82.8 %, and 56.6 % more soil moisture than WCF-PE, WCF-PP, and uncovered plots, respectively, while effectively mitigating soil nutrient depletion. Yield analysis showed a 22.2 % increase in 2024 compared to 2023, with a 226 kg gain in JWCF-covered areas—102.7 % higher than the uncovered control. Additionally, sugar content of honey pomelo increased by approximately 1 °Brix, enhancing fruit market value. Long-term trials confirmed the durability of JWCFs for at least one year, with their post-use incorporation into the soil facilitating natural decomposition.

In summary, this study developed and systematically evaluated jute fiber-based materials for multifunctional agricultural applications, effectively overcoming the limitations of traditional non-degradable materials. The results demonstrate that jute fiber-based systems hold great promise as sustainable alternatives to conventional agricultural plastics. By integrating weed suppression, water retention, and irrigation functionalities with intrinsic biodegradability, these materials offer an environmentally responsible pathway toward reducing plastic pollution, enhancing agricultural performance, and promoting soil health and resource sustainability.

7.2 Suggestions

Although this study successfully prepared multifunctional jute-based agricultural materials, there are still some limitations that need to be improved in future work. For instance:

1) Future research will focus on a systematic evaluation of their long-term effects on soil quality. This includes long-term monitoring of key soil indicators such as organic matter content, microbial biomass and their activity. These parameters will help to comprehensively understand how biodegradable jute-based fabrics influence soil fertility and ecosystem balance during and after degradation.

2) Given the current experimental limitations, future research can further optimize the composite mechanical properties to ensure their application in high-pressure conditions without compromising biodegradability. Moreover, long-term field evaluations will be conducted to fully assess the durability, environmental impact, and practical performance of JFPCs in diverse agricultural applications.

3) The scalability of the proposed forming method of composite pipe under industrial production conditions has not yet been explored. While the potential for scalable

production has been demonstrated, the current equipment remains at the laboratory scale with limited production speed. Future efforts should focus on optimizing the production process and equipment design to enhance automation, thereby establishing a foundation for large-scale manufacturing.

4) To achieve reasonable large-scale industrial production, it is necessary to explore cost-effective methods to balance performance and production efficiency. Although mass production is still in its infancy, the commercialization of multifunctional integrated natural agricultural textiles shows great potential.

References

[1] Viana CM, Freire D, Abrantes P, Rocha J, Pereira P. Agricultural land systems importance for supporting food security and sustainable development goals: A systematic review. *Science of the Total Environment*. **2022**, *806,* 150718.

[2] Denning G. Sustainable intensification of agriculture: the foundation for universal food security. *npj Sustainable Agriculture.* **2025**, *3*, 7.

[3] Guo SC, Guo HP. Development of ecological low-carbon agriculture with chinese characteristics in the new era: features, practical issues, and pathways. *Sustainability*. **2024**, *16(17),*7844.

[4] Khanna M, Atallah SS, Kar S, Sharma B, Wu LH, Yu CZ, Chowdhary G, Soman C, Guan KY. Digital transformation for a sustainable agriculture in the United States: Opportunities and challenges. *Agricultural Economics*. **2022**, *53*, 924-937.

[5] Reynolds TW, Waddington SR, Anderson CL, Chew A, True Z, Cullen A. Environmental impacts and constraints associated with the production of major food crops in Sub-Saharan Africa and South Asia. *Food Security*. **2015**, *7*, 795-822.

[6] Molotoks A, Smith P, Dawson TP. Impacts of land use, population, and climate change on global food security. *Food and Energy Security*. **2021**, *10(1),* e261.

[7] De Wrachien D, Schultz B, Goli MB. Impacts of population growth and climate change on food production and irrigation and drainage needs: A world-wide view. *Irrigation and Drainage*. **2021**, *70*, 981-995.

[8] Falcon WP, Naylor RL, Shankar ND. Rethinking Global Food Demand for 2050. *Population and Development Review*. **2022**, *48*, 921-957.

[9] Mishra H. Environmental degradation and impacts on agricultural production: a challenge to urban sustainability. sustainable urban environment and waste management: theory and practice. *Singapore: Springer Nature Singapore*, **2025**. 53-92.

[10] Numbere AO, Jude K, Chuku SB, Uzoma MC, Obanye C, Ohia P, Emoyoma U, Dick-Abbey IW, Sustainability. The impact of unsustainable development and climate change on agriculture and forestry in nigeria: predictions, solutions, and management. *Ecosystem Management: Climate Change and Sustainability.* **2024**, 541-579.

[11] Sharma N, Allardyce B, Rajkhowa R, Adholeya A, Agrawal R. A substantial role of agro-textiles in agricultural applications. *Frontiers in Plant Science*. **2022**,

*13,*895740.

[12] Dorugade V, Taye M, Qureshi SA, Agazie T, Seyoum B, Abebe B, Komarabathina S. Agrotextiles: important characteristics of fibres and their applications - a review. *Journal of Natural Fibers*. **2023**, *20(2)*,2211290.

[13] Kopitar D, Marasovic P, Jugov N, Schwarz I. Biodegradable nonwoven agrotextile and films-a review. *Polymers*. **2022**, *14(11),*2272.

[14] Levintal E, Kniffin ML, Ganot Y, Marwaha N, Murphy NP, Dahlke HE. Agricultural managed aquifer recharge (Ag-MAR)-a method for sustainable groundwater management: A review. *Critical Reviews in Environmental Science and Technology*. **2023**, *53(3)*, 291-314.

[15] Ingrao C, Strippoli R, Lagioia G, Huisingh D. Water scarcity in agriculture: An overview of causes, impacts and approaches for reducing the risks. *Heliyon*. **2023**, *9*.

[16] Begizew G, Technology F. Agricultural production system in arid and semi-arid regions. *International Journal of Agricultural Science and Food Technology.* **2021**, 234-244.

[17] Mitter H, Schmid E. Informing groundwater policies in semi-arid agricultural production regions under stochastic climate scenario impacts. *Ecological Economics*. **2021**, *180,*106908.

[18] Venot JP, Zwarteveen M, Kuper M, Boesveld H, Bossenbroek L, Van der Kooij S, Wanvoeke J, Benouniche M, Errahj M, De Fraiture C, Verma S. Beyond the promises of technology: A review of the discourses and actors who make drip irrigation. *Irrigation and Drainage*. **2014**, *63(2)*, 186-194.

[19] Yang P, Cheng MH, Wu LF, Fan JL, Li S, Wang HD, Qian L. Review on drip irrigation: impact on crop yield, quality, and water productivity in china. *Water*. **2023**, *15(9),*1733.

[20] Hoang V, Nguyen MK, Hoang TD, Ha MC, Huyen NTT, Bui VKH, Pham MT, Nguyen CM, Chang SW, Nguyen DD. Sources, environmental fate, and impacts of microplastic contamination in agricultural soils: A comprehensive review. *Science of the Total Environment*. **2024**, *950,*175276.

[21] Parven A, Meftaul IM, Venkateswarlu K, Megharaj M. Herbicides in modern sustainable agriculture: environmental fate, ecological implications, and human health concerns. *International Journal of Environmental Science and Technology*. **2025**, *22*, 1181-1202.

[22] Kubiak A, Wolna-Maruwka A, Niewiadomska A, Pilarska AA. The problem of weed infestation of agricultural plantations vs. the assumptions of the european biodiversity strategy. *Agronomy-Basel*. **2022**, *12(8),* 1808.

[23] Chauhan BS. Grand challenges in weed management. *Frontiers in Agronomy*. **2020**, *1,* 3.

[24] Clay SAJAJ. Near‐term challenges for global agriculture: Herbicide‐resistant weeds. *Agronomy Journal.* **2021**, *113(6)*, 4463-4472.

[25] Ahmad MF, Ahmad FA, Alsayegh AA, Zeyaullah M, Alshahrani AM, Muzammil K, Saati AA, Wahab S, Elbendary EY, Kambal N, Abdelrahman MH, Hussain S. Pesticides impacts on human health and the environment with their mechanisms of action and possible countermeasures. *Heliyon*. **2024**, *10*.

[26] Hjelm K, Mc Carthy R, Rytter L. Establishment strategies for poplars, including mulch and plant types, on agricultural land in Sweden. *New Forests*. **2018**, *49(6)*, 737-755.

[27] Böhlenius H, Övergaard R. Growth response of hybrid poplars to different types and levels of vegetation control. *Scandinavian Journal of Forest Research*. **2015**, *30*, 516-525.

[28] Farmer J, Zhang B, Jin XX, Zhang P, Wang JK. Long-term effect of plastic film mulching and fertilization on bacterial communities in a brown soil revealed by high through-put sequencing. *Archives of Agronomy and Soil Science*. **2017**, *63(2)*, 230-241.

[29] Iqbal R, Raza MAS, Valipour M, Saleem MF, Zaheer MS, Ahmad S, Toleikiene M, Haider I, Aslam MU, Nazar MA. Potential agricultural and environmental benefits of mulches—a review. *Bulletin of the National Research Centre***. 2020**, *44*, 1-16.

[30] Sengupta S, Debnath S, Bhowmick M. Sustainable agrotextile: jute needle-punched nonwoven preparation, properties and use in indian perspective. sustainable approaches in textiles and fashion: fibres, raw materials and product development. *Singapore: Springer Nature Singapore*. **2022**, 41-80.

[31] Basuk M, Yadav A. Eco-friendly natural fibers based sustainable agro-textiles for packaging of agro-products. *Advances in Renewable Natural Materials for Textile Sustainability*. **2025**, 37-53.

[32] Karimah A, Ridho MR, Munawar SS, Adi DS, Ismadi, Damayanti R, Subiyanto B, Fatriasari W, Fudholi A. A review on natural fibers for development of eco-friendly bio-composite: characteristics, and utilizations. *Journal of Materials Research and Technology-Jmr&T*. **2021**, *13*, 2442-2458.

[33] Ahmad J, Arbili MM, Majdi A, Althoey F, Deifalla AF, Rahmawati C. Performance of concrete reinforced with jute fibers (natural fibers): A review. *Journal of Engineered Fibers and Fabrics*. **2022**, *17,* 15589250221121871.

[34] Islam MS. Future aspects of jute fiber in terms of eco-friendly and sustainable world: a review. *Mühendislik Bilimleri.* 5.

[35] Akter N, Das SC, Grammatikos SA, Saha J, Khan MA. Development of sustainable jute geotextiles by bitumen emulsion and polyester resin: Effect of gamma radiation. *Journal of Engineered Fibers and Fabrics*. **2020**, *15,* 1558925020957969.

[36] Midha VK, Kumar SS. Influence of weft density on runoff erosion control performance of rolled erosion control systems. *Recent Trends in Traditional and Technical Textiles: Select Proceedings of ICETT 2019.* **2021**, 1-16.

[37] Lewicka K, Szymanek I, Rogacz D, Wrzalik M, Lagiewka J, Nowik-Zajac A, Zawierucha I, Coseri S, Puiu I, Falfushynska H, Rychter P. Current trends of polymer materials' application in agriculture. *Sustainability*. **2024**, *16(19).*

[38] Papadopoulos G, Arduini S, Uyar H, Psiroukis V, Kasimati A, Fountas S. Economic and environmental benefits of digital agricultural technologies in crop production: A review. *Smart Agricultural Technology*. **2024**, 100441.

[39] Thakur M, Kumar R. Mulching: Boosting crop productivity and improving soil environment in herbal plants. *Journal of Applied Research on Medicinal and Aromatic Plants*. **2021**, *20,* 100287.

[40] Xiao L, Wei X, Wang C, Zhao R. Plastic film mulching significantly boosts crop production and water use efficiency but not evapotranspiration in China. *Agricultural Water Management.* **2023**, *275*, 108023.

[41] Moreira T, Koerkamp PG, Janssen A, Stomph TJ, van der Werf W. Breaking the mould: Developing innovative crop protection strategies with reflexive interactive design. *Agricultural Systems*. **2023**, *210,* 103727.

[42] Kalogiannidis S, Kalfas D, Chatzitheodoridis F, Papaevangelou O. Role of crop-protection technologies in sustainable agricultural productivity and management. *Land*. **2022**, *11(10),* 1680.

[43] El-Beltagi HS, Basit A, Mohamed H, Ali I, Ullah S, Kamel EAR, Shalaby TA, Ramadan KMA, Alkhateeb AA, Ghazzawy HS. Mulching as a sustainable water and soil saving practice in agriculture: a review. *Agronomy-Basel*. **2022**, *12(8),*1881.

[44] Wang X, Zhang Q, Li L. Biodegradable fabric with efficient thermal-wet

management for eco-friendly weed control and water retention of soil. *Industrial Crops and Products*. **2025**, *225,* 120586.

[45] Giannoulis A, Briassoulis D, Papardaki NG, Mistriotis A. Evaluation of insect-proof agricultural nets with enhanced functionality. *Biosystems Engineering*. **2021**, *208*, 98-112.

[46] Roldán-Cañas J, Moreno-Pérez MF. Water and irrigation management in arid and semiarid zones. *Water*, **2021,** *13*(17), 2446.

[47] Abd-Elaty I, Ramadan EM, Elbagory IA, Nosair AM, Kuriqi A, Garrote L, Ahmed AA. Optimizing irrigation systems for water efficiency and groundwater sustainability in the coastal nile delta. *Agricultural Water Management*. **2024**, *304,* 109064.

[48] Haq F, Kiran M, Khan IA, Mehmood S, Aziz T, Haroon M. Exploring the pathways to sustainability: A comprehensive review of biodegradable plastics in the circular economy. *Materials Today Sustainability*. **2025**, *29,* 101067.

[49] Food and Agriculture Organization of the United Nations. assessment of agricultural plastics and their sustainability: a call for action. FAO, 2021.

[50] Chowdhury MJ, Nasrin S, Al Faruque MA. Significance of agro-textiles and future prospects in Bangladesh. *Eur. Sci. J.* **2017**, *13*.

[51] Chen H, Huang SH, Quan CQ, Chen ZN, Xu MH, Wei F, Tang DF. Effects of different colors of plastic-film mulching on soil temperature, yield, and metabolites in Platostoma palustre. *Scientific Reports*. **2024**, *14,* 5110.

[52] Arthur EK, Gikunoo E, Agyemang FO, Azeko ST, Andrews A, Twenewaa A. Material selection for water pipes by the multi-objective decision-making method: the case of alternative materials for PVC pipes. *Sci. Technol,* **2020**, *5*, 29-42.

[53] Zhu DL, Wu SJ, Guo B. On the use of low-density polyethylene as disposable drip tape for field irrigation. *Plastics Rubber and Composites*. **2018**, *47*, 133-137.

[54] Maraveas C. Environmental sustainability of greenhouse covering materials. *Sustainability*. **2019**, *11(21),*6129.

[55] Khalid N, Aqeel M, Noman A, Rizvi ZF. Impact of plastic mulching as a major source of microplastics in agroecosystems. *J Hazard Mater*. **2023**, *445,* 130455.

[56] Rillig MC, Lehmann A. Microplastic in terrestrial ecosystems. *Science,* **2020**, *368*, 1430-1431.

[57] Sun JX, Zheng HY, Xiang H, Fan JX, Jiang H. The surface degradation and release of microplastics from plastic films studied by UV radiation and mechanical abrasion. *Science of the Total Environment*. **2022**, *838,* 156369.

[58] Andrady AL, Barnes PW, Bornman JF, Gouin T, Madronich S, White CC, Zepp RG, Jansen MAK. Oxidation and fragmentation of plastics in a changing environment; from UV-radiation to biological degradation. *Science of the Total Environment*. **2022**, *851,* 158022.

[59] Zhang K, Hamidian AH, Tubic A, Zhang Y, Fang JKH, Wu CX, Lam PKS. Understanding plastic degradation and microplastic formation in the environment: a review. *Environmental Pollution*. **2021**, *274,* 116554.

[60] Uheida A, Mejia HG, Abdel-Rehim M, Hamd W, Dutta J. Visible light photocatalytic degradation of polypropylene microplastics in a continuous water flow system. *J Hazard Mater*. **2021**, *406,* 124299.

[61] Kasirajan S, Ngouajio M. Polyethylene and biodegradable mulches for agricultural applications: a review. *Agronomy for Sustainable Development*. **2012**, *32*, 501-529.

[62] Li Zhen LZ, He WenQing HW, Liu EnKe LE, Zhou JingLun ZJ, Liu Qin LQ, Yan ChangRong YC. A review on polyethylene mulch film degradation. **2019**.

[63] Fairbrother A, Hsueh HC, Kim JH, Jacobs D, Perry L, Goodwin D, White C, Watson S, Sung LP. Temperature and light intensity effects on photodegradation of high-density polyethylene. *Polymer Degradation and Stability*. **2019**, *165*, 153-160.

[64] Qi RM, Jones DL, Li Z, Liu Q, Yan CR. Behavior of microplastics and plastic film residues in the soil environment: A critical review. *Science of the Total Environment*. **2020**, *703,* 134722.

[65] Julienne F, Lagarde F, Delorme N. Influence of the crystalline structure on the fragmentation of weathered polyolefines. *Polymer Degradation and Stability*. **2019**, *170,* 109012.

[66] Albertsson A. Degradable polymers. *Journal of Macromolecular Science, Part A: Pure and Applied Chemistry.* **1993**, *30(9-10)*, 757-765.

[67] Weber R, Watson A, Forter M, Oliaei F. Persistent organic pollutants and landfills - a review of past experiences and future challenges. *Waste Management & Research*. **2011**, *29*, 107-121.

[68] He P, Chen L, Shao L, Zhang H, Lü F. Municipal solid waste (MSW) landfill: A source of microplastics?-Evidence of microplastics in landfill leachate. *Water research.*

2019, *159*, 38-45.

[69] Su YL, Zhang ZJ, Wu D, Zhan L, Shi HH, Xie B. Occurrence of microplastics in landfill systems and their fate with landfill age. *Water Research*. **2019**, *164,* 114968.

[70] Law KL. Plastics in the marine environment. *Annual review of marine science.* **2017**, *9*, 205-229.

[71] Yang H, Ma MG, Thompson JR, Flower RJ. Waste management, informal recycling, environmental pollution and public health. *Journal of Epidemiology and Community Health*. **2018**, *72*, 237-243.

[72] Wong JKH, Lee KK, Tang KHD, Yap PS. Microplastics in the freshwater and terrestrial environments: Prevalence, fates, impacts and sustainable solutions. *Science of the Total Environment*. **2020**, *719,* 137512.

[73] Pico Y, Alfarhan A, Barcelo D. Nano- and microplastic analysis: Focus on their occurrence in freshwater ecosystems and remediation technologies. *Trac-Trends in Analytical Chemistry*. **2019**, *113*, 409-425.

[74] Ouyang D, Peng YF, Li BC, Shao FL, Li KA, Cai YM, Guo T, Zhang HB. Microplastic formation and simultaneous release of phthalic acid esters from residual mulch film in soil through mechanical abrasion. *Science of the Total Environment*. **2023**, *893,* 164821.

[75] Jansen MAK, Andrady AL, Bornman JF, Aucamp PJ, Bais AF, Banaszak AT, Barnes PW, Bernhard GH, Bruckman LS, Busquets R, Häder DP, Hanson ML, Heikkilä AM, Hylander S, Lucas RM, Mackenzie R, Madronich S, Neale PJ, Neale RE, Olsen CM, Ossola R, Pandey KK, Petropavlovskikh I, Revell LE, Robinson SA, Robson TM, Rose KC, Solomon KR, Andersen MPS, Sulzberger B, Wallington TJ, Wang QW, Waengberg SA, White CC, Young AR, Zepp RG, Zhu LP. Plastics in the environment in the context of uv radiation, climate change and the montreal protocol: unep environmental effects assessment panel. *Photochemical & Photobiological Sciences*. **2024**, *23*, 629-650.

[76] Dhali SL, Parida D, Kumar B, Bala K. Recent trends in microbial and enzymatic plastic degradation: a solution for plastic pollution predicaments. *Biotechnology for Sustainable Materials.* **2024**, *1*, 11.

[77] Dogan M. Ultraviolet light accelerates the degradation of polyethylene plastics. *Microsc Res Tech*. **2021**, *84*, 2774-2783.

[78] Kuka E, Cirule D, Andersone I, Vasiljevs LO, Merna J, Sarakovskis A, Kurnosova N, Sansonetti E, Vevere L, Andersons B. A step to microplastic formation: Microcracking and associated surface transformations of recycled LDPE, LLDPE,

HDPE, and PP plastics exposed to UV radiation. *Polymer Degradation and Stability*. **2024**, *229,* 110967.

[79] Ainali NM, Bikiaris DN, Lambropoulou DA. Aging effects on low-and high-density polyethylene, polypropylene and polystyrene under UV irradiation: An insight into decomposition mechanism by Py-GC/MS for microplastic analysis. *Journal of Analytical and Applied Pyrolysis,* **2021**, *158*, 105207.

[80] Chamas A, Moon H, Zheng JJ, Qiu Y, Tabassum T, Jang JH, Abu-Omar M, Scott SL, Suh S. Degradation rates of plastics in the environment. *Acs Sustainable Chemistry & Engineering*. **2020**, *8(9)*, 3494-3511.

[81] Briassoulis D, Babou E, Hiskakis M. Degradation behaviour and field performance of experimental biodegradable drip irrigation systems. *Journal of Polymers and the Environment*. **2011**, *19*, 341-361.

[82] Wang Y, Wang F, Xiang LL, Gu CG, Redmile-Gordon M, Sheng HJ, Wang ZQ, Fu YH, Bian YR, Jiang X. Risk assessment of agricultural plastic films based on release kinetics of phthalate acid esters. *Environmental Science & Technology*. **2021**, *55*, 3676-3685.

[83] Li T, Cui LZ, Xu ZH, Liu HD, Cui XY, Fantke P. Micro- and nanoplastics in soil: Linking sources to damage on soil ecosystem services in life cycle assessment. *Science of the Total Environment*. **2023**, *904,*166925.

[84] Wen XF, Yin LS, Zhou ZY, Kang ZY, Sun QL, Zhang Y, Long YN, Nie XB, Wu ZY, Jiang CB. Microplastics can affect soil properties and chemical speciation of metals in yellow-brown soil. *Ecotoxicology and Environmental Safety*. **2022**, *243,*113958.

[85] Li BT, Huang S, Wang HM, Liu MJ, Xue S, Tang D, Cheng WL, Fan TL, Yang XM. Effects of plastic particles on germination and growth of soybean (Glycine max): A pot experiment under field condition. *Environmental Pollution*. **2021**, *272,*116418.

[86] Kong X, Jin DC, Jin SL, Wang ZG, Yin HQ, Xu MY, Deng Y. Responses of bacterial community to dibutyl phthalate pollution in a soil- vegetable ecosystem. *Journal of Hazardous Materials*. **2018**, *353*, 142-150.

[87] Wang J, Lv SH, Zhang MY, Chen GC, Zhu TB, Zhang S, Teng Y, Christie P, Luo YM. Effects of plastic film residues on occurrence of phthalates and microbial activity in soils. *Chemosphere*. **2016**, *151*, 171-177.

[88] Gao ML, Xu YL, Liu Y, Wang SL, Wang CW, Dong YM, Song ZG. Effect of polystyrene on di-butyl phthalate (DBP) bioavailability and DBP-induced phytotoxicity in lettuce. *Environmental Pollution*. **2021**, *268,*115870.

[89] Wang J, Coffin S, Sun CL, Schlenk D, Gan J. Negligible effects of microplastics on animal fitness and HOC bioaccumulation in earthworm Eisenia fetida in soil. *Environmental Pollution*. **2019**, *249*, 776-784.

[90] Boots B, Russell CW, Green DS. Effects of microplastics in soil ecosystems: above and below ground. *Environmental Science & Technology*. **2019**, *53*, 11496-11506.

[91] Liu ML, Feng JG, Shen YW, Zhu B. Microplastics effects on soil biota are dependent on their properties: A meta-analysis. *Soil Biology & Biochemistry*. **2023**, *178,*108940.

[92] Liu S, Jin R, Li T, Yang S, Shen M. Are biodegradable plastic mulch films an effective way to solve residual mulch film pollution in farmland?. *Plant and Soil.* **2024**, *494*, 85-94.

[93] Sun HF, Lei CL, Xu JH, Li RL. Foliar uptake and leaf-to-root translocation of nanoplastics with different coating charge in maize plants. *Journal of Hazardous Materials*. **2021**, *416,*125854.

[94] Li LZ, Luo YM, Li RJ, Zhou Q, Peijnenburg W, Yin N, Yang J, Tu C, Zhang YC. Effective uptake of submicrometre plastics by crop plants via a crack-entry mode. *Nature Sustainability*. **2020**, *3*, 929-937.

[95] Uwamungu JY, Wang Y, Shi G, Pan S, Wang Z, Wang L, Yang S. Microplastic contamination in soil agro-ecosystems: a review. *Environmental Advances,* **2022**, *9*, 100273.

[96] Medynska-Juraszek A, Szczepanska A. Microplastic pollution in eu farmland soils: preliminary findings from agricultural soils (Southwestern Poland). *Agriculture-Basel*. **2023**, *13(9),* 1733.

[97] Zhang GS, Liu YF. The distribution of microplastics in soil aggregate fractions in southwestern China. *Science of the Total Environment*. **2018**, *642*, 12-20.

[98] He D, Zhang Y, Gao W. Micro (nano) plastic contaminations from soils to plants: human food risks. *Current Opinion in Food Science,* **2021**, *41*, 116-121.

[99] Elfaleh I, Abbassi F, Habibi M, Ahmad F, Guedri M, Nasri M, Garnier C. A comprehensive review of natural fibers and their composites: An eco-friendly alternative to conventional materials. *Results in Engineering*. **2023**, *19,*101271.

[100] Duan J, Wu H, Fu W, Hao M. Mechanical properties of hybrid sisal/coir fibers reinforced polylactide biocomposites. *Polymer Composites,* **2018**, *39*, E188-E199.

[101] Manzato L, Takeno ML, Pessoa WAG, Mariuba LAM, Simonsen J. Optimization of cellulose extraction from jute fiber by box-behnken design. *Fibers and Polymers*. **2018**, *19*, 289-296.

[102] Osullivan AC. Cellulose: the structure slowly unravels. *Cellulose*. **1997**, *4*, 173.

[103] Poletto M, Ornaghi HL, Zattera AJ. Native cellulose: structure, characterization and thermal properties. *Materials*. **2014**, *7*, 6105.

[104] Wohlert M, Benselfelt T, Wågberg L, Furó I, Berglund LA, Wohlert J. Cellulose and the role of hydrogen bonds: not in charge of everything. *Cellulose,* **2022**, 1-23.

[105] Langan P, Nishiyama Y, Chanzy H. X-ray structure of mercerized cellulose II at 1 Å resolution. *Biomacromolecules*. **2001**, *2*, 410.

[106] DEJI W, Ramie Cellulose Chemistry and Processing[M]. Beijing: Science Press, **2001**.

[107] Thoresen PP, Lange H, Rova U, Christakopoulos P, Matsakas L. Role and importance of solvents for the fractionation of lignocellulosic biomass. *Bioresource Technology*. **2023**, *369,*128447.

[108] Molin U, Teder A. Importance of cellulose/hemicellulose-ratio for pulp strength. *Nordic Pulp & Paper Research Journal.* **2002**, *17*, 14-19a.

[109] Lara-Espinoza C, Carvajal-Millán E, Balandrán-Quintana R, López-Franco Y, Rascón-Chu A. Pectin and Pectin-Based Composite Materials: Beyond Food Texture. *Molecules*. **2018**, *23(4),* 942.

[110] Koul B, Yakoob M, Shah MP. Agricultural waste management strategies for environmental sustainability. *Environmental Research*. **2022**, *206,* 112285.

[111] Zabed H, Sahu JN, Boyce AN, Faruq G. Fuel ethanol production from lignocellulosic biomass: An overview on feedstocks and technological approaches. *Renewable & Sustainable Energy Reviews*. **2016**, *66*, 751.

[112] Jahja M, Mudatstsir A, Supu I, Arifin YI, Rauf J, Sakakibara M, Yamaguchi T, Metaragakusuma AP, Butolo I. How effective are palm-fiber-based erosion control blankets (ecb) against natural rainfall?. *Sustainability.* **2024**, *16*, 1655.

[113] Colley TA, Valerian J, Hauschild MZ, Olsen SI, Birkved M. Addressing nutrient depletion in tanzanian sisal fiber production using life cycle assessment and circular economy principles, with bioenergy co-production. *Sustainability*. **2021**, *13(16),* 8881.

[114] Xu JW, Song F, Wang ZW, Qi ZJ, Liu M, Guan S, Sun JL, Li SR, Zhao JB. Effects of different straw return methods on the soil structure, organic carbon content and maize yield of black soil farmland. *Agronomy-Basel*. **2024**, *14(9),* 2011.

[115] Islam MM, Ali MS. Economic importance of jute in Bangladesh: production, research achievements and diversification. *International Journal of Economic Theory and Application.* **2017**, *4(6)*, 45-57.

[116] Roy S, Lutfar LB. Bast fibres: jute. Handbook of natural fibres. *Woodhead Publishing.* **2012**, 39-59.

[117] Shahinur S, Sayeed MMA, Hasan M, Sayem AM, Haider J, Ura S. Current development and future perspective on natural jute fibers and their biocomposites. *Polymers*. **2022**, *14(7),* 1445.

[118] Shahinur S, Hasan M, Ahsan Q, Saha DK, Islam MS. Characterization on the properties of jute fiber at different portions. *International Journal of Polymer Science*. **2015**, *2015,* 262348.

[119] Roy TKG, Sur D, Nag D. Chemistry of jute and its applications. The Jute Genome Cham. Springer International Publishing; **2022**, 37-51.

[120] Farooq A, Islam SR, Al-Amind M, Patoary MK, Hossain MT, Khawar MT, Wang ZQ, Tian MW. From farm to function: Exploring new possibilities with jute nanocellulose applications. *Carbohydrate Polymers*. **2024**, *342,* 122423.

[121] Islam MM, Chowdhury MA, Talukder A, Hossain N, Rana MM, Khandaker MR, Khan RA. Enhancement of moisture and water resistance in chemically treated and gamma irradiated jute fibers. *Fibers and Polymers*. **2025**, 1-18.

[122] Riseh RS. Advancing agriculture through bioresource technology: The role of cellulose-based biodegradable mulches. *International Journal of Biological Macromolecules*. **2024**, *255,* 128006.

[123] Lim BKH, San Thian E. Biodegradation of polymers in managing plastic waste-A review. *Science of the Total Environment*. **2022**, *813,* 151880.

[124] Bakbolat B, Daulbayev C, Sultanov F, Beissenov R, Umirzakov A, Mereke A, Bekbaev A, Chuprakov I. Recent developments of TiO_2-based photocatalysis in the hydrogen evolution and photodegradation: a review. *Nanomaterials*. **2020**, *10(9),* 1790.

[125] Pal D, Konar D, Sumerlin BS. Poly(Vinyl Ketones): New directions in photodegradable polymers. *Macromolecular Rapid Communications*. **2023**, *44(15),*2300126.

[126] Liu P, Li H, Wu JJ, Wu XW, Shi YQ, Yang ZY, Huang KR, Guo XT, Gao SX. Polystyrene microplastics accelerated photodegradation of co-existed polypropylene via photosensitization of polymer itself and released organic compounds. *Water Research*. **2022**, *214,*118209.

[127] Yousif E, Haddad R. Photodegradation and photostabilization of polymers, especially polystyrene: review. *Springerplus*. **2013**, *2,*1-32.

[128] Guo CY, Guo HG. Progress in the degradability of biodegradable film materials for packaging. *Membranes*. **2022**, *12,*500.

[129] Azwa ZN, Yousif BF, Manalo AC, Karunasena W. A review on the degradability of polymeric composites based on natural fibres. *Materials & Design*. **2013**, *47*, 424-442.

[130] Huang BR, Wei MF, Vargo E, Qian YW, Xu T, Toste FD. Backbone-photodegradable polymers by incorporating acylsilane monomers via ring-opening metathesis polymerization. *Journal of the American Chemical Society*. **2021**, *143*, 17920-17925.

[131] Do PT, Poad BLJ, Frisch H. Programming Photodegradability into vinylic polymers via radical ring-opening polymerization. *Angewandte Chemie-International Edition*. **2023**, *62*.

[132] Chae JH, Choi M, Son S, Ko SM, Lee IH. Living cationic ring-opening polymerization of hetero diels-alder adducts to give multifactor-controlled and fast-photodegradable vinyl polymers. *Angewandte Chemie-International Edition*. **2023**, *62*.

[133] Amobonye A, Bhagwat P, Singh S, Pillai S. Plastic biodegradation: Frontline microbes and their enzymes. *Science of the Total Environment*. **2021**, *759*, 143536.

[134] Jayanth D, Kumar PS, Nayak GC, Kumar JS, Pal SK, Rajasekar R. A review on biodegradable polymeric materials striving towards the attainment of green environment. *Journal of Polymers and the Environment*. **2018**, *26*, 838-865.

[135] Engineer C, Parikh J, Raval A. Review on hydrolytic degradation behavior of biodegradable polymers from controlled drug delivery system. *Trends in biomaterials & artificial organs.* **2011**, *25*.

[136] Rai P, Mehrotra S, Priya S, Gnansounou E, Sharma SK. Recent advances in the sustainable design and applications of biodegradable polymers. *Bioresource Technology*. **2021**, *325,* 124739.

[137] Ghalia MA, Dahman Y. Synthesis and utilization of natural fiber-reinforced poly

(lactic acid) bionanocomposites. *Lignocellulosic Fibre and Biomass-Based Composite Materials*. Woodhead Publishing. **2017**, 313-345.

[138] Patidar MK, Ranawat K, Matkawala F, Nigam S, Das AK. Polylactic acid blends: an insight to their microbial production, biodegradation and applications. *Environmental Sustainability*. **2024**, 1-21.

[139] Reshma CS, Remya S, Bindu J. A review of exploring the synthesis, properties, and diverse applications of poly lactic acid with a focus on food packaging application. *International Journal of Biological Macromolecules*. **2024**, *283,*137905.

[140] Chen TY, Zhao XY, Weng YX. Self-assembled polylactic acid (PLA): Synthesis, properties and biomedical applications. *Frontiers in Chemistry*. **2023**, *10,* 1107620.

[141] Kalita NK, Damare NA, Hazarika D, Bhagabati P, Kalamdhad A, Katiyar V. Biodegradation and characterization study of compostable PLA bioplastic containing algae biomass as potential degradation accelerator. *Environmental Challenges.* **2021**, *3*, 100067.

[142] Chen J, Rong C, Lin T, Chen Y, Wu J, You J, Wang H, Li Y. Stable co-continuous PLA/PBAT blends compatibilized by interfacial stereocomplex crystallites: toward full biodegradable polymer blends with simultaneously enhanced mechanical properties and crystallization rates. *Macromolecules.* **2021**, *54*, 2852-2861.

[143] Wu N, Zhang H. Mechanical properties and phase morphology of super-tough PLA/PBAT/EMA-GMA multicomponent blends. *Materials Letters*, **2017**, *192*, 17-20.

[144] Kaing V, Guo ZY, Sok T, Kodikara D, Breider F, Yoshimura C. Photodegradation of biodegradable plastics in aquatic environments: Current understanding and challenges. *Science of the Total Environment*. **2024**, *911,* 168539.

[145] Arrington KJ, Waugh JB, Radzinski SC, Matson JB. Photo- and biodegradable thermoplastic elastomers: combining ketone-containing polybutadiene with polylactide using ring-opening polymerization and ring-opening metathesis polymerization. *Macromolecules*. **2017**, *50*, 4180-4187.

[146] Pannu AS, Singh S, Dhawan V. Composite manufacturing techniques–a review on injection, compression, pultrusion and extrusion process. *Journal of Advanced Scientific Research.* **2019**, *10*, 146-151.

[147] Pacheco A, Evangelista-Osorio A, Muchaypiña-Flores KG, Marzano-Barreda LA, Paredes-Concepción P, Palacin-Baldeón H, Dos Santos MSN, Tres MV, Zabot GL, Olivera-Montenegro L. Polymeric materials obtained by extrusion and injection molding from lignocellulosic agroindustrial biomass. *Polymers*. **2023**, *15(20),* 4046.

[148] Maiti S, Islam MR, Uddin MA, Afroj S, Eichhorn SJ, Karim N. Sustainable fiber-reinforced composites: a review. *Advanced Sustainable Systems*. **2022**, *6(11),* 2200258.

[149] Khosravani MR, Nasiri S. Injection molding manufacturing process: review of case-based reasoning applications. *Journal of Intelligent Manufacturing*. **2020**, *31*, 847-864.

[150] Fu H, Xu H, Liu Y, Yang Z, Kormakov S, Wu D, Sun J. Overview of injection molding technology for processing polymers and their composites. *ES Materials & Manufacturing.* **2020**, *8*, 3-23.

[151] Spiering T, Kohlitz S, Sundmaeker H, Herrmann C. Energy efficiency benchmarking for injection moulding processes. *Robotics and Computer-Integrated Manufacturing*. **2015**, *36*, 45-59.

[152] Dziadowiec D, Matykiewicz D, Szostak M, Andrzejewski J. Overview of the cast polyolefin film extrusion technology for multi-layer packaging applications. *Materials*. **2023**, *16(3),* 1071.

[153] Krause B, Kunz K, Kretzschmar B, Kühnert I, Pötschke PJP. Effect of filler synergy and cast film extrusion parameters on extrudability and direction-dependent conductivity of PVDF/carbon nanotube/carbon black composites. *Polymers*. **2020**, *12*, 2992.

[154] Kumar B, Hu J. Engineering of high-performance textiles. *Woodhead Publishing*, **2018**. 133-151.

[155] Patti A, Acierno D. Materials, Weaving parameters, and tensile responses of woven textiles. *Macromol*. **2023**, *3*, 665-680.

[156] Bueno M-A, Camillieri B. Structure and mechanics of knitted fabrics. *Structure and mechanics of textile fibre assemblies. Woodhead Publishing*. **2019**, 61-107.

[157] Bosson Research. The biodegradable materials market research report. **2024**. https://baijiahao.baidu.com/s?id=1814512096424263241

[158] Sintim HY, Flury M. Is biodegradable plastic mulch the solution to agriculture's plastic problem?. *ACS Publication*s; **2017,**1068-1069.

[159] Global Industy Analysts. Global Biodegradable mulch film market to reach $83.6 million by 2023. **2022**. https://www.prnewswire.com/news-releases/global-biodegradable-mulch-film-market-to-reach-83-6-million-by-2026–301526421.html

[160] Hayes DG, Anunciado MB, DeBruyn JM, Bandopadhyay S, Schaeffer S, English

M, Ghimire S, Miles C, Flury M, Sintim HY. Biodegradable plastic mulch films for sustainable specialty crop production. *Polymers for agri-food applications.* **2019**, 183-213.

[161] Serrano-Ruiz H, Martin-Closas L, Pelacho AM. Biodegradable plastic mulches: Impact on the agricultural biotic environment. *Science of the Total Environment*. **2021**, *750,* 141228.

[162] Zhang Y, Sun TY, Zhang DS, Shi ZF, Zhang XP, Li C, Wang LL, Song JJ, Lin Q. Enhanced photodegradability of PVC plastics film by codoping nano-graphite and TiO_2. *Polymer Degradation and Stability*. **2020**, *181,* 109332.

[163] Zheng CR, Guan JN, Zhang F, Zhou JR, Wang DD, Zhao YT, Zhang PY, Zhu MQ, Chen WJ, Zhu Q, He JY, Liao FT, Zhang XK, Long MC, Chen C. Stable cage for photocatalyst in plastics enables conversion of low density polyethylene to photodegradable plastics with visualizable stable stage. *Applied Catalysis B-Environment and Energy*. **2024**, *359,* 124490.

[164] Li B, Wang J, Zhang JB, Jin QD, Wang HY, Li WZ. Biobased hydrophobic liquid mulch film from soybean oil and starch for enhanced terraced field cultivation. *International Journal of Biological Macromolecules*. **2024**, *283,* 137490.

[165] Passaretti MG, Ninago MD, Villar MA, López O. Thermoplastic Starch and Mica Clay Composites as Biodegradable Mulching Films. *Journal of Polymers and the Environment*. **2022**, *30*, 4394-4405.

[166] Lu L, Han Y, Wang J, Xu J, Li Y, Sun M, Zhao F, He C, Sun Y, Wang Y. PBAT/PLA humic acid biodegradable film applied on solar greenhouse tomato plants increased lycopene and decreased total acid contents. *Science of the Total Environment.* **2023**, *871*, 162077.

[167] de Souza AG, Ferreira RR, Harada J, Rosa DS. Field performance on lettuce crops of poly (butylene adipate-co-terephthalate)/polylactic acid as alternative biodegradable composites mulching films. *Journal of Applied Polymer Science.* **2021**, *138(11)*, 50020.

[168] Giordano M, Amoroso CG, El-Nakhel C, Rouphael Y, De Pascale S, Cirillo C. An appraisal of biodegradable mulch films with respect to strawberry crop performance and fruit quality. *Horticulturae*. **2020**, *6(3),*48.

[169] Wang ZY, Li MX, Flury M, Schaeffer SM, Chang Y, Tao Z, Jia ZJ, Li ST, Ding F, Wang JK. Agronomic performance of polyethylene and biodegradable plastic film mulches in a maize cropping system in a humid continental climate. *Science of the Total Environment*. **2021**, *786,* 147460.

[170] Liang W, Zhao Y, Xiao D, Cheng J, Zhao J. A biodegradable water-triggered

chitosan/hydroxypropyl methylcellulose pesticide mulch film for sustained control of Phytophthora sojae in soybean (Glycine max L. Merr.). *Journal of Cleaner Production*. **2020**, *245*, 118943.

[171] Merino D, Salcedo MF, Mansilla AY, Casalongué CA, Alvarez VA. Development of sprayable sodium alginate-seaweed agricultural mulches with nutritional benefits for substrates and plants. *Waste and Biomass Valorization*. **2021**, *12*, 6035-6043.

[172] Jacquiod S, Bouchard E, Beguet J, Roure F, Cheviron N, Mougin C, Coffin A, Blouin M, Martin-Laurent F. Effect of plastic film and hemp canvas mulching on soil properties, microbial diversity and lettuce yield. *Plant and Soil*. **2024**, 1-19.

[173] Tan ZJ, Yi YJ, Wang HY, Zhou WL, Yang YR, Wang CY. Physical and degradable properties of mulching films prepared from natural fibers and biodegradable polymers. *Applied Sciences-Basel*. **2016**, *6(5),* 147.

[174] Tan BK, Ching YC, Gan SN, Rozali S. Biodegradable mulches based on poly (vinyl alcohol), kenaf fiber, and urea. *BioResources*. **2015**, *10*, 5532-5543.

[175] Baheti V, Militky J. Nanoindentation measurements of jute/poly lactic acid composites. *Natural Fibres: Advances in Science and Technology Towards Industrial Applications: From Science to Market. Springer Netherlands*. **2016**, 139-154.

[176] Cao HT, Ludwig K, Cobb K, Scott C, Jin Y, Knight B, Burrichter M, Shen HQ. Development and evaluation of biodegradable weed control mulch mats from end-of-use cotton waste. *Sustainability*. **2024**, *16(16),* 7083.

[177] Liu X, Chen CJ, Sun JS, Wang XH. Development of natural fiber-based degradable nonwoven mulch from recyclable mill waste. *Waste Manage (Oxford)*. **2021**, *121*, 432-440.

[178] Manna K, Kundu MC, Saha B, Ghosh GK. Effect of nonwoven jute agrotextile mulch on soil health and productivity of broccoli (&ITBrassica oleracea &ITL.) in lateritic soil. *Environmental monitoring and assessment*. **2018**, *190,*1-10.

[179] Manna K, Kundu MC, Saha B, Ghosh GK. Residual impact of nonwoven jute agro-textile mulch on soil health and productivity of maize (Zea mays L.) in lateritic soil. *Biomass Conversion and Biorefinery*. **2024**, *14*, 23667-23677.

[180] Shahid MA, Habib MA, Hossain I, Limon MGM, Islam T, Bhat G. Eco-friendly jute-based hybrid nonwoven fabric for packaging applications. *Acs Omega*. **2024**, *9*, 44639-44645.

[181] Mridha N, Nayak D, Yadav A, Mondal T, Ghosh RK, Bhowmick M, Singha A,

Ray D, Manjunatha B, Das A. Eco-friendly sustainable farming: Enhancing summer tomato (Lycopersicon esculentum mill.) yield with jute non-woven agro textile mulch. *Heliyon*. **2025**.

[182] Chattopadhyay BC, Chakravarty S. Application of jute geotextiles as facilitator in drainage. *Geotextiles and Geomembranes*. **2009**, *27*, 156-161.

[183] Behera AK, Mohanty C, Mohanty A. Development and characterization of biodegradable jute reinforced sapling pot. *Journal of Natural Fibers*. **2022**, *19*, 7738-7749.

[184] Zai SM, Wei HY, Liu XM, Wu F, Liu LB, Liu DT, Li X, Liu WY, Li ZY. Seepage rate and uniformity of the stalk composite pipe for subsurface irrigation. *Irrigation and Drainage*. **2025**, *74*, 107-116.

[185] Das D, Chingakham N, Sarma M, Basu S, Bhaladhare S. Cellulose-based biodegradable superabsorbent hydrogel: A sustainable approach for water conservation and plant growth in agriculture. *International Journal of Biological Macromolecules*. **2025**, *305,* 141176.

[186] Hiskakis M, Babou E, Briassoulis D. Experimental processing of biodegradable drip irrigation systems-possibilities and limitations. *Journal of Polymers and the Environment*. **2011**, *19*, 887-907.

[187] Paudel B, Basak JK, Madhavi BGK, Kim NE, Lee GH, Choi GM, Choi YW, Kim HT. Properties of paper-based biodegradable pots for growing seedlings. *Horticulture Environment and Biotechnology*. **2022**,*63(6)*, 793-807.

[188] Behera AK, Avancha S, Das N, Adhikari B. Mechanical and biodegradation analysis of fully biodegradable eco-friendly natural fiber reinforced sapling pot. *Polymer Composites*. **2021**, *42*, 2910-2919.

[189] Partibha, Saha S, Hariprasad P. Paddy straw-based biodegradable horticultural pots: An integrated greener approach to reduce plastic waste, valorize paddy straw and improve plant health. *Journal of Cleaner Production*. **2022**, *337,* 130588.

[190] Fuentes RA, Berthe JA, Barbosa SE, Castillo LA. Development of biodegradable pots from different agroindustrial wastes and byproducts. *Sustainable Materials and Technologies*. **2021**, *30*.

[191] Sarker RH. Botany of Jute (Corchorus Spp.). The Jute Genome. Cham: Springer International Publishing, **2022.** 17-36.

[192] Rajlakshmi, Dutta S, Saravanabhupathy S, Jayaseelan P, Anusha, Kailasam A,

Banerjee R. Jute stick-based industrial artefact towards sustainable development goals. *Industrial Crops and Products*. **2024**, *215,* 118599.

[193] Bheel N, Sohu S, Awoyera P, Kumar A, Abbasi SA, Olalusi OB. Effect of wheat straw ash on fresh and hardened concrete reinforced with jute fiber. *Advances in Civil Engineering*. **2021**, *2021(1),* 6659125.

[194] Kaysar MA, Ahmed SJ, Jamil AMK, Habib MM, Dayan MAR, Mamun Or R, Gafur MA. Impact of NaOH treatment on the chemical, structural, physico-mechanical, and thermal characteristics of jute species. *Fibers and Polymers*. **2024**, *25*, 1765-1777.

[195] Barreto ACH, Esmeraldo MA, Rosa DS, Fechine PBA, Mazzetto SE. Cardanol biocomposites reinforced with jute fiber: microstructure, biodegradability, and mechanical properties. *Polymer Composites*. **2010**, *31*, 1928-1937.

[196] Khan J, Khan M. The use of jute fibers as reinforcements in composites. Biofiber Reinforcements in composite materials. *Woodhead Publishing*, 2015. 3-34.

[197] Tesfay AG, Kahsay MB, Kumar PS. Effect of carbon and glass fillers on tensile and impact strength, water absorption, and degradation properties of sisal/polyester composites. *Journal of Natural Fibers.* **2023**, *20*(2), 2202886.

[198] Ullah A, Foisal A. A review on sustainable textile products from jute and cotton blends. *SEU J. Sci. Eng.* **2019**, *13*, 7-12.

[199] Singh H, Singh JIP, Singh S, Dhawan V, Tiwari SK. A brief review of jute fibre and its composites. *materials today: proceedings.* **2018**, 5(14), 28427-28437.

[200] Aseer JR, Sankaranarayanasamy K, Jayabalan P, Natarajan R, Dasan KP. Morphological, physical, and thermal properties of chemically treated banana fiber. *Journal of Natural Fibers*. **2013**, *10*, 365-380.

[201] Petroudy SD. Physical and mechanical properties of natural fibers. Advanced high strength natural fibre composites in construction. *Woodhead Publishing*. **2017**. 59-83.

[202] Lee CH, Khalina A, Lee SH. Importance of interfacial adhesion condition on characterization of plant-fiber-reinforced polymer composites: a review. *Polymers*. **2021**, *13(3),* 438.

[203] Gunwant D. Moisture resistance treatments of natural fiber-reinforced composites: a review. *Composite Interfaces*. **2024**, *31*, 979-1047.

[204] Raju JSN, Depoures MV, Kumaran P. Comprehensive characterization of raw and

alkali (NaOH) treated natural fibers from Symphirema involucratum stem. *International Journal of Biological Macromolecules*. **2021**, *186*, 886-896.

[205] Pokhriyal M, Rakesh PK, Rangappa SM, Siengchin S. Effect of alkali treatment on novel natural fiber extracted from Himalayacalamus falconeri culms for polymer composite applications. *Biomass Conversion and Biorefinery*. **2024**, *14*, 18481-18497.

[206] Anbupalani MS, Venkatachalam CD, Rathanasamy R. Influence of coupling agent on altering the reinforcing efficiency of natural fibre-incorporated polymers - A review. *Journal of Reinforced Plastics and Composites*. **2020**, *39*, 520-544.

[207] Pongchaiphol S, Preechakun T, Raita M, Champreda V, Laosiripojana N. Characterization of cellulose–chitosan-based materials from different lignocellulosic residues prepared by the ethanosolv process and bleaching treatment with hydrogen peroxide. *ACS omega.* **2021**, *6*, 22791-22802.

[208] Cai M, Takagi H, Nakagaito AN, Katoh M, Ueki T, Waterhouse GIN, Li Y. Influence of alkali treatment on internal microstructure and tensile properties of abaca fibers. *Industrial Crops and Products*. **2015**, *65*, 27-35.

[209] Sarker F, Karim N, Afroj S, Koncherry V, Novoselov KS, Potluri P. High-performance graphene-based natural fiber composites. *Acs Applied Materials & Interfaces*. **2018**, *10*, 34502-34512.

[210] Mukherjee A, Ganguly P, Sur D. Structural mechanics of jute: the effects of hemicellulose or lignin removal. *Journal of the Textile Institute.* **1993**, *84(3)*, 348-353.

[211] Ghosh S, Singh S, Maity S. Thermal insulation behavior of chemically treated jute fiber quilt. *Journal of Natural Fibers*. **2021**, *18*, 568-580.

[212] Tiwari YM, Sarangi SK. Characterization of raw and alkali treated cellulosic Grewia Flavescens natural fiber. *International Journal of Biological Macromolecules*. **2022**, *209*, 1933-1942.

[213] Orue A, Jauregi A, Peña-Rodriguez C, Labidi J, Eceiza A, Arbelaiz A. The effect of surface modifications on sisal fiber properties and sisal/poly (lactic acid) interface adhesion. *Composites Part B: Engineering*, **2015**, *73*, 132-138.

[214] Fernandes EM, Mano JF, Reis RL. Hybrid cork-polymer composites containing sisal fibre: Morphology, effect of the fibre treatment on the mechanical properties and tensile failure prediction. *Composite Structures*. **2013**, *105*, 153-162.

[215] Chowdhury H, Saha A, Hasan M, Haider. Effects of alkaline and carboxilated graphene oxide (cgo) treatment on mechanical, thermal, and electrical properties of jute

fiber-reinforced epoxy composites. *Journal of Composites Science.* **2025**, *9*.

[216] Wang X, Zhao FW, Cheung TW, Lee CH, Li L. Enhancing hemp fiber performance: insights into chitosan treatment and structural evolution. *Textile Research Journal*. **2024**, *94*, 2341-2350.

[217] Li C, Li M, Li ZG, Guo PR, Zhao ZJ, Lu WJ, Li JZ, Liang JY, Tang Y, Ge SB, Wang F. Cleaner production of liquefied biomass-based phenol-formaldehyde resin with improved properties via catalyzed copolymerization. *Advanced Composites and Hybrid Materials*. **2025**, *8,*101.

[218] Liu J, Wang L, Li J, Li C, Zhang S, Gao Q, Zhang W, Li J. Degradation mechanism of Acacia mangium tannin in NaOH/urea aqueous solution and application of degradation products in phenolic adhesives. *International Journal of Adhesion and Adhesives.* **2020**, *98*, 102556.

[219] da Luz J, Losekann MA, dos Santos A, de Oliveira JH, Girotto EM, Moises MP, Radovanovic E, Fávaro SL. Hydrothermal treatment of sisal fiber for composite preparation. *Journal of Composite Materials*. **2019**, *53*, 2337-2347.

[220] Kundu C, Samudrala SP, Kibria MA, Bhattacharya S. One-step peracetic acid pretreatment of hardwood and softwood biomass for platform chemicals production. *Scientific Reports*. **2021**, *11(1),* 11183.

[221] Nikonenko NA, Buslov DK, Sushko NI, Zhbankov RG. Investigation of stretching vibrations of glycosidic linkages in disaccharides and polysaccarides with use of IR spectra deconvolution. *Biopolymers*. **2000**, *57*, 257-262.

[222] Wu JY, Zhong TH, Zou YP, Li JJ, Zhao WJ, Chen H. Microstructure, chemical composition and thermal stability of alkali-treated bamboo fibers and parenchyma cells: effects of treatment time and temperature. *Cellulose*. **2023**, *30*, 1911-1925.

[223] Setswalo K, Oladijo OP, Namoshe M, Akinlabi ET, Sanjay RM, Siengchin S, Srisuk R. The water absorption and thermal properties of green pterocarpus angolensis (mukwa)-polylactide composites. *Journal of Natural Fibers*. **2023**, *20(1)*, 2124217.

[224] Qin ZH, Cheng LD, Liu L, Zhang RY, Zhao SY, Ma LJ. Combined effects of organic solvent and ultrasonic pretreatments on cellulose fiber extraction from hemp. *Industrial Crops and Products*. **2024**, *220,* 119436.

[225] Gargol M, Klepka T, Klapiszewski L, Podkoscielna B. Synthesis and thermo-mechanical study of epoxy resin-based composites with waste fibers of hemp as an eco-friendly filler. *Polymers*. **2021**, *13(4),* 503.

[226] Boumediri H, Bezazi A, Del Pino GG, Haddad A, Scarpa F, Dufresne A. Extraction and characterization of vascular bundle and fiber strand from date palm rachis as potential bio-reinforcement in composite. *Carbohydrate polymers.* **2019**, *222*, 114997.

[227] Smail YB, El Moumen A, Lmai F, Imad A. The effects of the temperature on the mechanical properties of natural yarns. MATEC Web of Conferences; **2019**: EDP Sciences.

[228] Ullah AS, Shahinur S, Haniu H. On the mechanical properties and uncertainties of jute yarns. *Materials.* **2017**, *10*, 450.

[229] Etale A, Onyianta AJ, Turner SR, Eichhorn SJ. Cellulose: a review of water interactions, applications in composites, and water treatment. *Chemical Reviews*. **2023**, *123(5)*, 2016-2048.

[230] Perez N, Singh V, Ringler C, Xie H, Zhu TJ, Sutanudjaja EH, Villholth KG. Ending groundwater overdraft without affecting food security. *Nature Sustainability*. **2024**, *7(8),* 1007-1017.

[231] Mishra BK, Kumar P, Saraswat C, Chakraborty S, Gautam A. Water security in a changing environment: concept, challenges and solutions. *Water*. **2021**, *13(4),*490.

[232] Dolan F, Lamontagne J, Link R, Hejazi M, Reed P, Edmonds J. Evaluating the economic impact of water scarcity in a changing world. *Nature Communications*. **2021**, *12(1),*1915.

[233] Baggio G, Qadir M, Smakhtin V. Freshwater availability status across countries for human and ecosystem needs. *Science of the Total Environment*. **2021**, *792,* 148230.

[234] Yang H, Wang XX, Bin P. Agriculture carbon-emission reduction and changing factors behind agricultural eco-efficiency growth in China. *Journal of Cleaner Production*. **2022**, *334,*130193.

[235] Khan S, Hanjra MA, Mu JX. Water management and crop production for food security in China: A review. *Agricultural Water Management*. **2009**, *96*, 349-360.

[236] Yao ZS, Yan GX, Wang R, Zheng XH, Liu CY, Butterbach-Bahl K. Drip irrigation or reduced N-fertilizer rate can mitigate the high annual N_2O + NO fluxes from Chinese intensive greenhouse vegetable systems. *Atmos Environ*. **2019**, *212*, 183-193.

[237] Tao R, Wakelin SA, Liang YC, Hu BW, Chu GX. Nitrous oxide emission and denitrifier communities in drip-irrigated calcareous soil as affected by chemical and organic fertilizers. *Science of the Total Environment*. **2018**, *612*, 739-749.

[238] Wu Y, Si W, Yan SC, Wu LF, Zhao WJ, Zhang JL, Zhang FC, Fan JL. Water consumption, soil nitrate-nitrogen residue and fruit yield of drip-irrigated greenhouse tomato under various irrigation levels and fertilization practices. *Agricultural Water Management*. **2023**, *277,* 108092.

[239] Grand View Research. "Drip irrigation market size, share & trends analysis report by component (valves, pumps, filters), by method (surface, subsurface), by crop (field crops, fruits & nuts), by region, and segment forecasts, 2024 – 2030 " **2023**. https://www.grandviewresearch.com/industry-analysis/drip-irrigation-market-report.

[240] Grant F, Sheline C, Sokol J, Amrose S, Brownell E, Nangia V, Winter AG. Creating a solar-powered drip irrigation optimal performance model (SDrOP) to lower the cost of drip irrigation systems for smallholder farmers. *Applied Energy*. **2022**, *323,*119563.

[241] Sheline C, Grant F, Gelmini S, Pratt S, Winter VAG. Designing a predictive optimal water and energy irrigation (POWEIr) controller for solar-powered drip irrigation systems in resource-constrained contexts. *Applied Energy*. **2025**, *377,*124107.

[242] Briassoulis D. Agricultural plastics as a potential threat to food security, health, and environment through soil pollution by microplastics: Problem definition. *Science of the Total Environment*. **2023**, *892,*164533.

[243] Vidal F, van der Marel ER, Kerr RWF, McElroy C, Schroeder N, Mitchell C, Rosetto G, Chen TTD, Bailey RM, Hepburn C, Redgwell C, Williams CK. Designing a circular carbon and plastics economy for a sustainable future. *Nature*. **2024**, *626(7997)*, 45-47.

[244] Zhang ZS, Cai SM, Li Y, Wang Z, Long Y, Yu T, Shen Y. High performances of plant fiber reinforced composites-A new insight from hierarchical microstructures. *Composites Science and Technology*. **2020**, *194,*108151.

[245] Jagadeesh P, Puttegowda M, Boonyasopon P, Rangappa SM, Khan A, Siengchin S. Recent developments and challenges in natural fiber composites: A review. *Polymer Composites*. **2022**, *43*, 2545-2561.

[246] Chatterjee A, Kumar S, Singh H. Tensile strength and thermal behavior of jute fibre reinforced polypropylene laminate composite. *Composites Communications*. **2020**, *22,*100483.

[247] Zolfakkar M, El-Tayeb N, Halawa T. Towards sustainable composites: Evaluation of mechanical properties, erosion behavior and applications of natural fiber-epoxy composites. *Journal of Composite Materials*. **2024**, *58*, 2151-2168.

[248] You Z, Wang H, Zhang F, Zhang H, Zou C, Zhou Z, Wang Y, Xiao Z, Liang D,

Wang Q. High - strength, thermally stable, and processable wood fiber/polyamide composites for engineering structural components. *Advanced Science.* **2025**, *12*, 2408708.

[249] Dehury J, Mohanty JR, Nayak S, Dehury S. Development of natural fiber reinforced polymer composites with enhanced mechanical and thermal properties for automotive industry application. *Polymer Composites*. **2022**, *43*, 4756-4765.

[250] Patel RV, Yadav A, Winczek J. Physical, mechanical, and thermal properties of natural fiber-reinforced epoxy composites for construction and automotive applications. *Applied Sciences-Basel*. **2023**, *13(8),*5126.

[251] Zhao XH, Copenhaver K, Wang L, Korey M, Gardner DJ, Li K, Lamm ME, Kishore V, Bhagia S, Tajvidi M, Tekinalp H, Oyedeji O, Wasti S, Webb E, Ragauskas AJ, Zhu HL, Peter WH, Ozcan S. Recycling of natural fiber composites: Challenges and opportunities. *Resources Conservation and Recycling*. **2022**, *177,* 105962.

[252] Ramesh M, Deepa C. Processing and properties of jute (Corchorus olitorius L.) fibres and their sustainable composite materials: a review. *Journal of Materials Chemistry A*. **2024**, *12*, 1923-1997.

[253] Murali B, Yogesh P, Karthickeyan NK, Chandramohan D. Multi-potency of bast fibers (flax, hemp and jute) as composite materials and their mechanical properties: A review. *Materials Today: Proceedings.* **2022,** *62*, 1839-1843.

[254] Shah SS, Shaikh MN, Khan MY, Alfasane MA, Rahman MM, Aziz MA. Present status and future prospects of jute in nanotechnology: A review. *Chemical Record*. **2021**, *21*, 1631-1665.

[255] Taib N, Rahman MR, Huda D, Kuok KK, Hamdan S, Bin Bakri MK, Bin Julaihi MRM, Khan A. A review on poly lactic acid (PLA) as a biodegradable polymer. *Polymer Bulletin*. **2023**, *80*, 1179-1213.

[256] Vishwakarma DK, Kumar R, Kumar A, Kushwaha NL, Kushwaha KS, Elbeltagi A. Evaluation and development of empirical models for wetted soil fronts under drip irrigation in high-density apple crop from a point source. *Irrigation Science*. **2023**, *41*, 663-686.

[257] Vishwakarma DK, Kumar R, Abed SA, Al-Ansari N, Kumar A, Kushwaha NL, Yadav D, Kumawat A, Kuriqi A, Alataway A, Dewidar AZ, Mattar MA. Modeling of soil moisture movement and wetting behavior under point-source trickle irrigation. *Scientific Reports*. **2023**, *13(1),* 14981.

[258] Roy A. Removal of color from real textile dyeing effluent utilizing tannin

immobilized jute fiber as biosorbent: optimization with response surface methodology. *Environmental Science and Pollution Research*. **2021**, *28*, 12011-12025.

[259] Ahmed MS, Maniruzzaman M, Al-Mamun MR, Ali MA, Badal MMR, Aziz MA, Mazumder MAJ, Hakeem AS, Yousuf MA. Jute stick-derived cellulose-based hydrogel: synthesis, characterization, and methylene blue removal from aqueous solution. *Acs Omega*. **2023**, *8*, 47856-47873.

[260] Yang SL, Chen RY, Zhang PH, Yuan MW, Li HL, Jiang DB. Fabrication and characterization of poly(lactic acid-trimethylene carbonate) based biodegradable composite films. *International Journal of Biological Macromolecules*. **2024**, *262,* 130148.

[261] Vârban R, Crisan I, Vârban D, Ona A, Olar L, Stoie A, Stefan R. Comparative FTIR prospecting for cellulose in stems of some fiber plants: flax, velvet leaf, hemp and jute. *Applied Sciences-Basel*. **2021**, *11(18),* 8570.

[262] Varsavas SD, Kaynak C. Weathering degradation performance of PLA and its glass fiber reinforced composite. *Materials Today Communications*. **2018**, *15*, 344-353.

[263] Moldovan A, Cuc S, Prodan D, Rusu M, Popa D, Taut AC, Petean I, Bombos D, Doukeh R, Nemes O. Development and characterization of polylactic acid (pla)-based nanocomposites used for food packaging. *Polymers*. **2023**, *15(13),* 2855.

[264] Thomason JL, Rudeiros-Fernández JL. Thermal degradation behaviour of natural fibres at thermoplastic composite processing temperatures. *Polymer Degradation and Stability*. **2021**, *188,* 109594.

[265] Ruz-Cruz MA, Herrera-Franco PJ, Flores-Johnson EA, Moreno-Chulim MV, Galera-Manzano LM, Valadez-González A. Thermal and mechanical properties of PLA-based multiscale cellulosic biocomposites. *Journal of Materials Research and Technology-Jmr&T*. **2022**, *18*, 485-495.

[266] Ji SG, Hwang JH, Cho D, Kim HJ, technology. Influence of electron beam treatment of jute on the thermal properties of random and two-directional jute/poly (lactic acid) green composites. *Journal of adhesion science and technology.* **2013**, *27*, 1359-1373.

[267] Wang H, Hassan EAM, Memon H, Elagib THH, AllaIdris FA. Characterization of natural composites fabricated from abutilon-fiber-reinforced poly (lactic acid). *Processes*. **2019**, *7(9),* 583.

[268] Gil-Castell O, Badia JD, Kittikorn T, Strömberg E, Martínez-Felipe A, Ek M, Karlsson S, Ribes-Greus A. Hydrothermal ageing of polylactide/sisal biocomposites. studies of water absorption behaviour and physico-chemical performance. *Polymer*

Degradation and Stability. **2014**, *108*, 212-222.

[269] Niu MJ, Zhang ZZ, Wei ZZ, Wang WJ. Effect of a novel flame retardant on the mechanical, thermal and combustion properties of Poly(Lactic Acid). *Polymers*. **2020**, *12,* 2407.

[270] Fehri S, Cinelli P, Coltelli MB, Anguillesi I, Lazzeri A. Thermal properties of plasticized poly (lactic acid)(PLA) containing nucleating agent. *International Journal of Chemical Engineering and Applications.* **2016**, *7*, 85-88.

[271] Tao YB, Li P, Zhang JF, Wang SJ, Shi SQ, Kong FG. A review of fused filament fabrication of continuous natural fiber reinforced thermoplastic composites: Techniques and materials. *Polymer Composites*. **2023**, *44*, 8200-8222.

[272] Gholampour A, Ozbakkaloglu T. A review of natural fiber composites: properties, modification and processing techniques, characterization, applications. *Journal of Materials Science*. **2020**, *55*, 829-892.

[273] Vink ETH, Rábago KR, Glassner DA, Gruber PR. Applications of life cycle assessment to NatureWorks™ polylactide (PLA) production. *Polymer Degradation and Stability*. **2003**, *80*, 403-419.

[274] Rajeshkumar G, Seshadri SA, Devnani GL, Sanjay MR, Siengchin S, Maran JP, Al-Dhabi NA, Karuppiah P, Mariadhas VA, Sivarajasekar N, Anuf AR. Environment friendly, renewable and sustainable poly lactic acid (PLA) based natural fiber reinforced composites-A comprehensive review. *Journal of Cleaner Production*. **2021**, *310,* 127483.

[275] Rajeshkumar L, Kumar PS, Ramesh M, Sanjay MR, Siengchin S. Assessment of biodegradation of lignocellulosic fiber-based composites - A systematic review. *International Journal of Biological Macromolecules*. **2023**, *253,* 127237.

[276] Puniya R, Bazaya BR, Kumar A, Sharma BC, Nesar NA, Bochalya RS, Dwivedi MC, Sharma N, Kumar R, Sharma J, Sharma A, Mehta S. Effect of residue and weed management practices on weed flora, yield, energetics, carbon footprint, economics and soil quality of zero tillage wheat. *Scientific Reports*. **2023**, *13(1),* 19311.

[277] Fontanelli M, Martelloni L, Raffaelli M, Frasconi C, Ginanni M, Peruzzi A. Weed management in autumn fresh market spinach: a nonchemical alternative. *Horttechnology*. **2015**, *25*, 177-184.

[278] Karnas Z, Isik D, Tursun N, Jabran K. Critical period for weed control in sesame production. *Weed Biology and Management*. **2019**, *19*, 121-128.

[279] Guo LB, Qiu J, Ye CY, Jin GL, Mao LF, Zhang HQ, Yang XF, Peng Q, Wang YY, Jia L, Lin ZX, Li GM, Fu F, Liu C, Chen L, Shen EH, Wang WD, Chu QJ, Wu DY, Wu SL, Xia CY, Zhang YF, Zhou XM, Zhou XF, Wu LM, Song WJ, Wang YF, Shu QY, Aoki D, Yumoto E, Yokota T, Miyamoto K, Okada K, Kim DS, Cai DG, Zhang CL, Lou YG, Qian Q, Yamaguchi H, Yamane H, Kong CH, Timko MP, Bai LY, Fan LJ. Echinochloa crus-galli genome analysis provides insight into its adaptation and invasiveness as a weed. *Nature Communications*. **2017**, *8(1),* 1031.

[280] Monteiro A, Santos S. Sustainable approach to weed management: the role of precision weed management. *Agronomy-Basel*. **2022**, *12(1),* 118.

[281] Mir MS, Singh P, Kanth RH, Shah ZA, Dar EA, Bhat JA, Nazir A, Amin Z, Lone AH, Nain MS, Yousuf D, Alie BA, Ahngar TA, Abd-ElGawad AM, Mattar MA. Influence of sowing dates and weed management practices on weed dynamics, productivity and profitability of direct seeded rice. *Scientific Reports*. **2024**, *14(1),* 18877.

[282] Liu C, Yang KQ, Chen Y, Gong H, Feng X, Tang ZY, Fu DB, Qi L. Benefits of mechanical weeding for weed control, rice growth characteristics and yield in paddy fields. *Field Crops Research*. **2023**, *293,* 108852.

[283] Pannacci E, Farneselli M, Guiducci M, Tei F. Mechanical weed control in onion seed production. *Crop protection.* **2020**, *135*, 105221.

[284] Machleb J, Peteinatos GG, Kollenda BL, Andújar D, Gerhards R. Sensor-based mechanical weed control: Present state and prospects. *Computers and Electronics in Agriculture*. **2020**, *176,* 105638.

[285] Schaffner U, Steinbach S, Sun Y, Skjoth CA, de Weger LA, Lommen ST, Augustinus BA, Bonini M, Karrer G, Sikoparija B, Thibaudon M, Müller-Schärer H. Biological weed control to relieve millions from Ambrosia allergies in Europe. *Nature Communications*. **2020**, *11(1),* 1745.

[286] Morin L. Progress in biological control of weeds with plant pathogens. *Annual Review of Phytopathology*, **2020**, *58(1),* 201-223.

[287] Harms NE, Cronin JT, Diaz R, Winston RL. A review of the causes and consequences of geographical variability in weed biological control successes. *Biological Control*. **2020**, *151,* 104398.

[288] MacLaren C, Storkey J, Menegat A, Metcalfe H, Dehnen-Schmutz K. An ecological future for weed science to sustain crop production and the environment. A review. *Agronomy for Sustainable Development*. **2020**, *40,* 1-29.

[289] Menalled UD, Smith RG, Cordeau S, DiTommaso A, Pethybridge SJ, Ryan MR.

Phylogenetic relatedness can influence cover crop-based weed suppression. *Scientific Reports*. **2023**, *13(1),* 17323.

[290] Paul SK, Xi YF, Sanderson P, Naidu R. Controlled release herbicide formulation for effective weed control efficacy. *Scientific Reports*. **2024**, *14(1),*4216.

[291] Behrens MR, Mutlu N, Chakraborty S, Dumitru R, Jiang WZ, LaVallee BJ, Herman PL, Clemente TE, Weeks DP. Dicamba resistance: Enlarging and preserving biotechnology-based weed management strategies. *Science*. **2007**, *316(5828)*, 1185-1188.

[292] Vázquez-García JG, Rojano-Delgado AM, Alcántara-de la Cruz R, Torra J, Dellaferrera I, Portugal J, De Prado R. Distribution of glyphosate-resistance in echinochloa crus-galli across agriculture areas in the iberian peninsula. *Frontiers in Plant Science*. **2021**, *12,* 617040.

[293] Adeux G, Vieren E, Carlesi S, Bàrberi P, Munier-Jolain N, Cordeau S. Mitigating crop yield losses through weed diversity. *Nature Sustainability*. **2019**, *2*, 1018-1026.

[294] Lauenroth D, Gokhale CS. Theoretical assessment of persistence and adaptation in weeds with complex life cycles. *Nature Plants*. **2023**, *9*, 1267-1279.

[295] Azimi S, Amini R, Hosseingolizadeh M. Suppression of weed and insect populations by living and straw mulches in sesame (Sesamum indicum L.). *Scientific Reports*. **2023**, *13(1),* 21586.

[296] Bruce D, Silva EM, Dawson JC. Suppression of weed and insect populations by living cover crop mulches in organic squash production. *Frontiers in Sustainable Food Systems*. **2022**, *6,* 995224.

[297] Zhang H, Miles C, Gerdeman B, LaHue DG, DeVetter L. Plastic mulch use in perennial fruit cropping systems - A review. *Scientia Horticulturae*. **2021**, *281,* 109975.

[298] Steinmetz Z, Wollmann C, Schaefer M, Buchmann C, David J, Tröger J, Muñoz K, Frör O, Schaumann GE. Plastic mulching in agriculture. Trading short-term agronomic benefits for long-term soil degradation?. *Science of the total environment* **2016**, *550*, 690-705.

[299] Somanathan H, Sathasivam R, Sivaram S, Kumaresan SM, Muthuraman MS, Park SU. An update on polyethylene and biodegradable plastic mulch films and their impact on the environment. *Chemosphere*. **2022**, *307*, 135839.

[300] Khamare Y, Marble SC. Mulching as a weed management tool in container plant production - review. *Frontiers in Agronomy*. **2023**, *5,* 1235196.

[301] Shah ST, Ullah I, Basit A, Sajid M, Arif M, Mohamad HI. Mulching is a mechanism to reduce environmental stresses in plants. Mulching in agroecosystems: Plants, soil & environment. Springer Nature Singapore. **2022**, 353-376.

[302] Gabrys T, Fryczkowska B, Grzybowska-Pietras J, Binias D. Modification and properties of cellulose nonwoven fabric-multifunctional mulching material for agricultural applications. *Materials*. **2021**, *14(15),* 4335.

[303] Tang M, Liu R, Li HC, Gao XD, Wu PT, Zhang C. Optimizing soil moisture conservation and temperature regulation in rainfed jujube orchards of china's loess hilly areas using straw and branch mulching. *Agronomy-Basel*. **2023**, *13(8),* 2121.

[304] Cheng C, Qiu YM, Tang SM, Lin BY, Guo MZ, Gao BB, He BF. Artificial spider silk based programmable woven textile for efficient wound management. *Advanced Functional Materials*. **2022**, *32,* 2107707.

[305] Jin Z, Li JY, Wang QQ, Su WB, Duan XF, Tang ZQ. Characterization of multifunctional panels from jute fibers for interior wall covering. *Industrial Crops and Products*. **2021**, *167,* 113530.

[306] Rajesh M, Jayakrishna K, Sultan MTH, Manikandan M, Mugeshkannan V, Shah AUM, Safri SNA. The hydroscopic effect on dynamic and thermal properties of woven jute, banana, and intra-ply hybrid natural fiber composites. *Journal of Materials Research and Technology-Jmr&T*. **2020**, *9*, 10305-10315.

[307] Li HR, Yan Z, Li Y, Hong WP. Latest development in salt removal from solar-driven interfacial saline water evaporators: Advanced strategies and challenges. *Water Research*. **2020**, *177,*115770.

[308] Fan Q, Wu L, Liang Y, Xu ZC, Li YG, Wang J, Lund PD, Zeng MY, Wang W. The role of micro-nano pores in interfacial solar evaporation systems - A review. *Applied Energy*. **2021**, *292,*116871.

[309] Cubric IS, Matkovic VMP, Pavlovic Z, Cuden AP. Material and structural functionalization of knitted fabrics for sportswear. *Materials*. **2022**, *15,*3306.

[310] Uddin MB, Begum HA, Uddin AJ. Elastic jute yarn suitable for stretch-denim. *Cellulose*. **2024**, *31*, 7031-7051.

[311] Tong L, Hu DY, Chao L, Liu XL, Wang CH, Yi XS. Development of hybrid breathing materials for sustainable composite manufacturing. *Journal of Cleaner Production*. **2021**, *321,*129028.

[312] Shahid A, Miah S, Rahim A. Thermal and breathability management of

microencapsulated phase change material (MPCM) incorporated jute fabric. *Journal of Engineered Fibers and Fabrics*. **2021**, *16, 15589250211029564*.

[313] Dolez PI, Marsha S, McQueen RH. Fibers and textiles for personal protective equipment: review of recent progress and perspectives on future developments. *Textiles*. **2022**, *2*, 349-381.

[314] Habibi F, Liu T, Shahid MA, Schaffer B, Sarkhosh A. Physiological, biochemical, and molecular responses of fruit trees to root zone hypoxia. *Environmental and Experimental Botany*. **2023**, *206,* 105179.

[315] Brunšek, R., Marolt Gomišček, J., Fekonja, M. Biodegradation properties of cellulose fibers and PLA biopolymer: Hemp, jute and sisal fibers in burial tests. *Polymers*. **2023**, *15(17),* 3532.

[316] Kopitar, D., Marasovic, P. Degradation of biodegradable nonwoven mulches in the field: Natural and synthetic fibres under accelerated weathering conditions. *Polymers*. **2024**, *16(16),* 2279.

[317] Ishak, M. I. S., Al Manasir, Y., Nor Ashikin, N. S. S., Md Yusuff, M. S., Zuknik, M., and Abdul Khalil, H. P. S.. Application of cellulosic fiber in soil erosion mitigation: Prospect and challenges. *BioResources*. **2021**, *16(2)*, 4474-4522.